ASSESSMENT OF NEXRAD P3 DATA ON STREAMFLOW SIMULATION USING SWAT FOR NORTH FORK NINNESCAH WATERSHED, KANSAS

by

ROHITH KUMAR GALI

B.Tech, Acharya N.G. Ranga Agricultural University, 2007

A THESIS

submitted in partial fulfillment of the requirements for the degree

MASTER OF SCIENCE

Department of Biological & Agricultural Engineering
College of Engineering

KANSAS STATE UNIVERSITY
Manhattan, Kansas

2010

Approved by:

Major Professor
Dr. Kyle R. Douglas-Mankin

Abstract

Radar-derived P3 data from Next Generation Radar (NEXRAD) of the National Weather Service (NWS) offer higher spatial resolution than precipitation gauge data, which might improve the accuracy of streamflow simulations using watershed models. The objective of this study was to evaluate the performance of spatially-averaged subwatershed-specific NEXRAD P3 data on streamflow simulations using Soil and Water Assessment Tool (SWAT) model. The SWAT hydrologic model was chosen for this study to simulate the hydrologic processes in North Fork Ninnescah Watershed located in south-central Kansas. A precipitation gauge station for each subwatershed was created using an area-weighted average of NEXRAD P3 precipitation estimates for all HRAP grid cells covering the subwatershed. The SWAT model was calibrated with both NEXRAD P3 data and NCDC precipitation gauge (PG) data from 1 January 2002 to 31 December 2008. The P3-calibrated model was validated using PG data for the same simulation period (2002-2008), and vice versa. The PG-calibrated model yielded slightly higher daily Nash-Sutcliffe efficiency (E_{NS} = 0.40) than P3 calibrated model (E_{NS} = 0.35), but the yearly E_{NS} and PBIAS for P3 calibrated model (E_{NS} = 0.80) was much better than PG-calibrated model (E_{NS} = 0.43). The P3-validated model (PG calibration) had yearly E_{NS} = of 0.70, whereas the PG-calibrated model had E_{NS} = 0.43. The daily PBIAS value for P3-calibrated model in 2007 (wet year) was -14.13 and for the P3-calibrated model was -32.83; PG data overestimated the streamflow compared to P3 data in 2007. The P3 data has better agreement with PG data from 2002-2008 period than for 1996-2001 period. The streamflow estimation was better with NEXRAD P3 precipitation data in both calibration and validation runs. Even though the model was calibrated with PG data, the validated model with P3 data has comparatively high E_{NS}. The spatial variation of streamflow response within the watershed was greater compared to the temporal variation in both the calibrated models. The spatial representation of precipitation data by NEXRAD P3 has improved the modeling performance compared to PG data; it is evident that NEXRAD data is an alternative to precipitation gauge measurements.

Table of Contents

List of Figures

List of Tables

Acknowledgements

First a very special thank you to my advisor, Professor Dr Kyle R. Douglas-Mankin. I offer my sincere gratitude to Dr. Mankin, who has supported me throughout this research and thesis-writing period with his patience, enthusiasm in research and immense knowledge. The experience I have gained through this work has been invaluable. In addition, I would like to thank my graduate committee, Dr. James K. Koelliker, and Dr. Xingong Li for their encouragement, and valuable comments.

Financial support for this project was provided, in part, by the Kansas Department of Health and Environment, Bureau of Water, using EPA 319 and Kansas Water Plan funds.

I would also like to gratefully acknowledge some individuals for their support in completing this research with out any trouble. Dr. Xingong Li and Tingting Xu, for providing NEXRAD precipitation data in the format required by SWAT and for assisting with my questions at any time. Dr. Aleksey Sheshukov, for his extensive discussions, detailed comments and interesting explorations in SWAT calibration have been very helpful for this study. Dr. Pouyan Nejadhashemi, who gave me important guidance during my first steps in learning GIS.

My warm thanks to Dr. Philip L. Barnes for his expert inputs on management practices in North Fork Ninnescah Watershed during this study. I would like to thank Dr. Dan Devlin, Dr. Prem Parajuli, and Cheney Lake Watershed, Inc. people for their support in providing terraces & tillage practices data implemented in Cheney Lake Watershed. I also wish to thank Ms. Mary Knapp, State Climatologist, Kansas State University for providing me the weather data for SWAT model.

I thank my fellow graduate students in Watershed Modeling Laboratory, BAE, Kansas State University: Naga Prasad Daggupati, Naga Raghuveer Modala, Seth Perkins, Chris Siebenmorgen, for stimulating discussions and make my time in the Master's program fun and interesting.

Above all, I thank my parents, who stood beside me and encouraged me constantly, my thanks to my sister for giving me happiness and joy.

Lastly, I offer my regards to all those who supported me in any aspect during the completion of this project.

Abbreviations and Symbols

(used outside Chapter 2 – Literature Review)

β	filter parameter
γ	The psychrometric constant, kPa/^{o}C
Δ	Slope of saturation vapor pressure curve at air temperature, kPa/ºC
α_{gw}	The base flow recession constant
a	area of subwatershed piece, m^2
A	The cross-sectional area of flow in the channel, m^2
ABRFC	Arkansas Red Basin River Forecast Center
AGNPS	Agricultural Nonpoint Source Pollution Model
AGRR	Agricultural Row Crops
ALPHA_BF	Base flow Recession Constant
AnnAGNPS	Annualized Agricultural Nonpoint Source Pollution Model
ANSWERS	Areal Nonpoint Source Watershed Environment Response Simulation
AWIPS	Advanced Weather Interactive Processing System
b_t	Base flow at time step, t
BASINS	Better Assessment Science Integrating Point and Nonpoint Source
BFD	The number of base flow days
BMP	Best Management Practice
Ch_K2	Channel Hydraulic Conductivity
CH_N2	Channel Roughness Coefficient
CN	Curve Number
CN I, II, III	Curve Number at Antecedent Moisture Content I, II, III
CORN	Corn
CT	Conventional Till
d	distance between the predicted and measured gauging stations, m
e_s	saturation vapor pressure at air temperature, kPa
e_a	actual vapor pressure of air, kPa
E_{NS}	Nash-Sutcliffe Efficiency

EPA	Environmental Protection Agency
EPCO	Plant Uptake Compensation Factor
ESCO	Soil Evaporation Compensation Factor
ET	Evapotranspiration
ET_0	reference evapotranspiration, mm d^{-1}
ETM	Enhanced Thematic Mapper
G	Soil heat flux density, $MJ/m^2/d$
GOES	Geostationary Operational Environment Satellite
GIS	Geographic Information System
GRSG	Grain Sorghum
GW_DELAY	Groundwater Delay time, days
GW_Revap	Groundwater Revaporation Coefficient
ha	Hectare
HAS	Hydrometeorological Analysis and Support
HDP	Hourly Digital Precipitation
HEC-HMS	Hydrologic Engineering Centers Hydrologic Modeling System
HSPF	Hydrological Simulation Program-Fortran
HRAP	Hydrologic Rainfall Analysis Project
HRU	Hydrologic Response Unit
HUC	Hydrologic Unit Code
IDW	Inverse Distance Weighted
k	weight known as the friction distance
KS	Kansas
km	kilometer
km^2	Square kilometer
mm	millimeter
m	meter
m^2	Square meter
m^3/s	Cubic meters per second
MPE	Multi-sensor Precipitation Estimate
n	Manning's roughness coefficient for the channel

n	number of observations
NAD 83	North American Datum of 1983
NASS	National Agricultural Statistics Survey
NCDC	National Climatic Data Center
NCGC	National Cartography and Geospatial Center
NEXRAD	Next Generation Radar
NF	North Fork
NOAA	National Oceanographic Atmospheric Administration
NRCS	Natural Resources Conservation Service
NT	No Till
NWS	National Weather Service
O_i	Observed daily value, m^3/s
$\overline{O}$	Median of observed daily value, m^3/s
P	Practice Factor
P	Precipitation data of NEXRAD grid cell
P1	Process 1
P3	Process 3
P_c	Rainfall for the gauging station to be predicted, mm
P_i	Rainfall data from one of the neighboring gauge station, mm
P_i	Predicted daily value, m^3/s
PBIAS	Percent bias, %
PG	Precipitation gauge
PRMS	Precipitation-Runoff Modeling System
q_t	filtered surface runoff at the time step t
Q	The rate of flow in the channel, m^3/s
Q_{surf}	Surface Runoff Depth, mm
Q_t	The original streamflow, m^3/s
r	The hydraulic radius for a given depth of flow, m
r^2	Coefficient of determination
R	Reflectivity
R	Total rainfall depth, mm

R_n	net radiation, $MJ/m^2/d$
REVAPMN	Threshold depth of water in the shallow aquifer for revaporation to occur
RFC	River Forecast Center
RMSE	Root Mean Square Error
RSR	ratio of the root mean square error to the standard deviation of measured data
s	The slope of the channel length, m/m
S	Retention Parameter
SHALLST	Initial depth of Shallow Aquifer, mm
SMTMP	Snow Melt Base Temperature, ºC
Sol_AWC	Soil Available Water Content
Sol_K	Saturated Hydraulic Conductivity
SOYB	Soybean
SSURGO	Soil Survey Geographic Database
SURLAG	Surface Runoff Lag Coefficient
SWAT	Soil and Water Assessment Tool
SWM	Stanford Watershed Model
SWMM	Storm Water Management Model
T	Air temperature, ºC
TIN	Triangular Irregular Network
TM	Thematic Mapper
TMDL	Total Maximum Daily Load
TR-55	Technical Release 55
u_2	wind speed at 2 m height, m/s
USBOR	United States Bureau of Reclamation
USDA-ARS	United States Department of Agriculture-Agricultural Research Service
USDA-SCS	United States Department of Agriculture-Soil Conservation Service
USGS	United States Geological Survey
USGS-NED	United States Geological Survey-National Elevation Data
USLE	Universal Soil Loss Equation
UTM-14	Universal Transverse Mercator 14
V	The velocity of flow in the channel, m/s

WSR-88D	Weather Surveillance Radar 1988 Doppler
WWHT	Winter Wheat
Y_i^{obs}	Observed value for event i, m^3/s
Y_i^{sim}	Predicted value for event i, m^3/s
Y^{mean}	Mean of observed values, m^3/s
Z	Rainfall, mm

CHAPTER 1 - Introduction

1.1 General Background

Water is one of the most important natural resources on earth, covering 71% of the earth's surface. Water exists on earth as solid (ice), liquid or gas (water vapor), frequently changing its form of existence. Water moves constantly in atmosphere through the processes of evaporation, condensation, precipitation, surface runoff and underground flow (fig. 1.1), but the total amount of earth's water does not change. The scientific study of water and its properties, distribution and effects on earth's surface, subsurface, soil, and atmosphere is hydrology (McCuen, 1998). Hydrology is mainly concerned with part of the cycle after the precipitation onto lands and before its return to oceans. Hydrology includes the study about the amount and intensity of precipitation, the amount of water stored, and the amount of flow in streams and groundwater. The movement and recycling of water between the atmosphere, the land surface and underground is hydrologic cycle or water cycle. This cycle is driven by the energy of the sun and by the earth's gravity, supplying all the water needs to support life on earth.

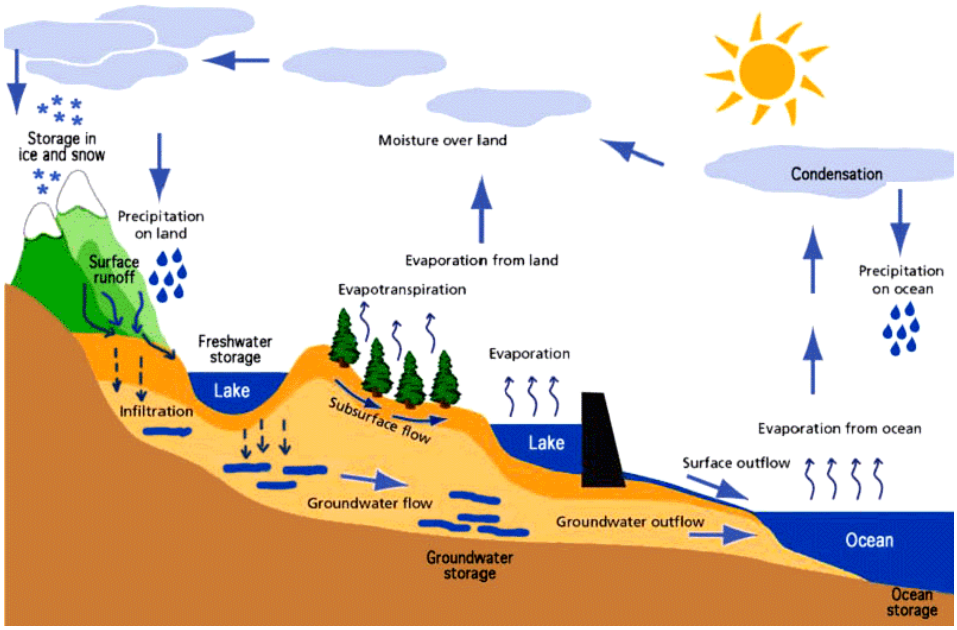

Figure 1.1 Hydrologic Cycle (www.dardel.info)

Hydrologic cycle consists of movement of water from the oceans into the atmosphere by evaporation, and then onto lands, over and under the earth's surface as runoff and infiltration, and back to the oceans. Hydrologic cycle is a continuous process and includes evaporation,

condensation, precipitation, evapotranspiration, runoff and underground flow (base flow) to lakes, streams, rivers and finally oceans. The first step in hydrologic cycle is evaporation of water from surface to atmosphere, where the water changes from liquid to gas state. Approximately 80% of all evaporation is from the oceans, with 20% from inland water and vegetation. Winds play a major role in transporting evaporated water vapor (clouds) around the globe influencing humidity around the world. Condensation is the change of water from its gaseous state to liquid water. Condensation occurs when warm air rises, cools and loses its capacity to hold water vapor. As a result water vapor condenses to form cloud droplets which eventually send water back to the earth's surface in different forms depending on the atmospheric conditions, mainly temperature.

Precipitation is the transfer of water from atmosphere to the surface of earth. There are several forms of precipitation, including rain, snow, hail, sleet and freezing rain. Precipitation that falls on the land surface follows various routes. Part of precipitation evaporates back to atmosphere, and most of the remainder either runs off or infiltrates into the ground.

Runoff is the flow of water on the surface, where the soil pores are completely saturated (excess rainfall that is not absorbed by soil). Runoff is an important component in hydrologic cycle, because it not only replenishes the lakes and rivers, but it also changes landscapes by eroding soils. Several factors that affect runoff are amount and intensity of precipitation, landuse, soils, slope, vegetation, and topography. Runoff is a major source of water pollution; various pollutants that are deposited on the surface by human activities are washed off by storms and are drained directly into streams and lakes, thereby degrading the quality of water sources.

1.1.1 Watershed Models

A watershed is defined as an area of land that drains down slope to a single point. Watershed models are computer programs used to simulate hydrological processes within the watershed and are often used to estimate the impact of human activities on these processes. Simulation of these processes can be done to address a range of water resources, environmental and agricultural productivity problems. Watershed models are helpful not only in making predictions of future flow conditions, but also in assessment of hydrologic impacts of changes in management scenarios, land cover and climate (Kalin and Hantush, 2006). Watershed models are used to estimate the water quantity and quality for the past, present and future conditions in

streams and also to evaluate the impacts of best management practices (BMPs) in achieving total maximum daily loads (TMDLs).

Many watershed-scale models have been developed over the last few decades. Watershed models advanced from field-scale models to watershed-scale and river-basin-scale distributed models with digital revolution in computers, geographical information systems (GIS) and remote sensing technology. With advancement in GIS, processing, analyzing and interpreting hydrologic data have become much more efficient.

The earliest watershed model is the Stanford Watershed Model (SWM) developed by Crawford and Linsley in 1966 (Singh and Frevert, 2006). The SWM attempted to simulate the entire hydrologic cycle. In past few decades, many other watershed models have been developed with advancement in computer capabilities. Some of the watershed hydrology models are Storm Water Management Model (SWMM) (Metcalf and Eddy, 1971), Precipitation-Runoff Modeling System (PRMS) (Leavesley et al., 1983), EPA-sponsored Agricultural Runoff Management (ARM) and SWM is now transformed into Hydrological Simulation Program-Fortran (HSPF) (Bicknell et al., 1993). Hydrologic Engineering Center's Hydrologic Modeling System (HEC-HMS) is considered to be a standard model in design of drainage systems. BASINS (Better Assessment Science Integrating Point and Nonpoint Source) developed by the EPA in 1994, consists of environmental databases and assessment tools, and performs watershed and water-quality analyses. ANSWERS (Areal Nonpoint Source Watershed Environment Response Simulation) (Beasley et al., 1980) model was developed to provide information about the effects of landuses, management and conservation practices on the quality and quantity of water from both agricultural and non-agricultural watersheds. ANSWERS is a distributed-parameter and event-based model, and consists of hydrologic and erosion models which have been interfaced to simulate hydrologic and erosion responses from a given area. AGNPS (Agricultural Non Point Source Pollution Model) a single-event based model was developed by the U.S. Department of Agriculture to evaluate diffuse source pollution and to assist with management of runoff, erosion and nutrient movement in watersheds. AnnAGNPS is a distributed-parameter, continuous-simulation, watershed-scale model developed jointly by USDA-ARS and NRCS (Bosch et al., 1998) to aid land management and decision making. AnnAGNPS uses Soil Conservation Service Curve Number Method (USDA-SCS, 1972) to calculate overland runoff and Technical Release-55 (TR-55) Method (USDA-SCS, 1986) to calculate peak flow.

Soil and Water Assessment Tool (SWAT) developed by U.S. Department of Agriculture-Agricultural Research Service (USDA-ARS), is a physically-based, river-basin-scale, distributed, deterministic, continuous-hydrologic-simulation model that operates on a daily time step (Arnold et al., 1998). After the initiation of SWAT, it has undergone several revisions; each revision has enhanced its capability to simulate hydrologic processes in a watershed. Hydrologic models should be able to replicate the actual conditions in the watershed and more user-friendly models must be developed with increased capabilities and fewer limitations.

Many of these models are physically-based, distributed in space and time, quite comprehensive, and can be used to model a multitude of environmental and ecosystem problems (Singh and Frevet, 2006). Watershed models require hydrologic, agricultural, pedologic, hydraulic and geomorphologic data for the analysis. Most of the models are limited by large data requirements to capture climatic patterns and hydrologic processes that vary with location. No single model can replicate the actual conditions of the watersheds, whether it might be due to failure in spatial integration of input data or the processes in the model. Prediction accuracy of hydrologic-simulation models largely depends on how well they represent the real world in terms of precipitation, topography, soils, landuse/landcover, land management, etc., which involves the quality of input data and the model complexity (Van Rompaey and Govers, 2002). The accuracy of model results depends heavily on the accuracy of model inputs, especially precipitation, which is the driving function in the hydrologic process (Moon et al., 2004). Studies reported that among all the inputs to the hydrologic models, precipitation is, by far, the largest source of uncertainty (Srinivasan, 2005). Failure to collect the precipitation data accurately leads to inadequate soil-moisture values and subsequent inaccuracy in the runoff estimation.

1.1.2 Precipitation

In meteorology, precipitation is defined as the deposition of moisture from atmosphere onto the earth's surface. Rainfall is the major component of precipitation in activating various processes, such as distribution, movement, quantity and quality of water, and influences soil moisture and plant growth. Representing precipitation spatially and temporally is very important for water balance analysis. Accurate estimates of precipitation are invaluable to hydrologists in calculating runoff estimates.

Traditionally, precipitation is measured by precipitation gauges. Precipitation gauges are instruments used by meteorologists and hydrologists in measuring the amount of precipitation at a specific point for a particular period of time. Precipitation is usually measured in millimeters or inches over a 24-hour period, although automated data-collection systems can achieve hourly or finer time-scale resolutions. Several types of precipitation gauges are available to collect precipitation, but standard precipitation gauge and tipping-bucket precipitation gauge are prominently in use. Gauges measure precipitation at a point, which is a significant drawback in interpreting spatial representation of precipitation; interpolation techniques must be used to represent it spatially over an area. However, interpolation cannot capture the spatial distribution of a storm event between precipitation gauges. With advancement in radar technology, not only finer spatial distribution but also finer temporal distribution of precipitation data can be measured over large areas.

Radar systems emit electromagnetic waves and detect the signal that is returned after scattering and reflection from objects within range of the system. NEXRAD (Next Generation Radar) also known as Weather Surveillance Radar-1988 Doppler (WSR-88D), is operated by the National Weather Service (NWS) of the National Oceanic and Atmospheric Administration (NOAA). This system is a joint effort of Departments of Commerce, Defense, and Transportation. The number of NEXRAD WSR-88D network sites deployed across the United States and selected overseas locations has increased from 107 in 1995 to 169 sites currently. NEXRAD systems were deployed to provide significant improvements in weather forecasting, military operations and emergency management over the previous radar-based system. Reflectivity observations from NEXRAD provides information about estimates of precipitation and all types of weather which include thunderstorm, hails, tornadoes, hurricanes, flash floods, snow and freezing precipitation.

NEXRAD systems consist of a centered parabolic dish, which continuously revolves and scans the atmosphere. It collects the data by sending microwave signals (long wavelengths that are not susceptible to atmospheric scatterings and can easily pass through clouds) into the atmosphere. The signals get scattered when they collide with target (water droplets in clouds), and the radar receptor collects the bounced signals. Radar works on the Doppler Effect, which helps in tracking and movement of the storm. The returned signals convey three important parameters: the location of storm, intensity of storm and the direction of storm travel. A

reflectivity-rainfall relationship (also known as Z-R relationship), $Z = a R^b$ (Harrison et al., 2000), is used to calculate the rainfall (Z) using the reflectivity (R) of returned signals. The maximum range of NEXRAD radar is 250 nautical miles (463 km), but the maximum range for the precipitation products is 124 nautical miles (230 km). The raw radar products undergo processing and bias corrections made by Hydrometeorological Analysis and Support (HAS) forecaster at the River Forecast Center (RFC) (Johnson et al., 1999). NWS has divided United States into 13 river forecasting centers. The data is stored in XMRG format, which contains precipitation data in form of grid cells of approximately 16-km^2 resolution.

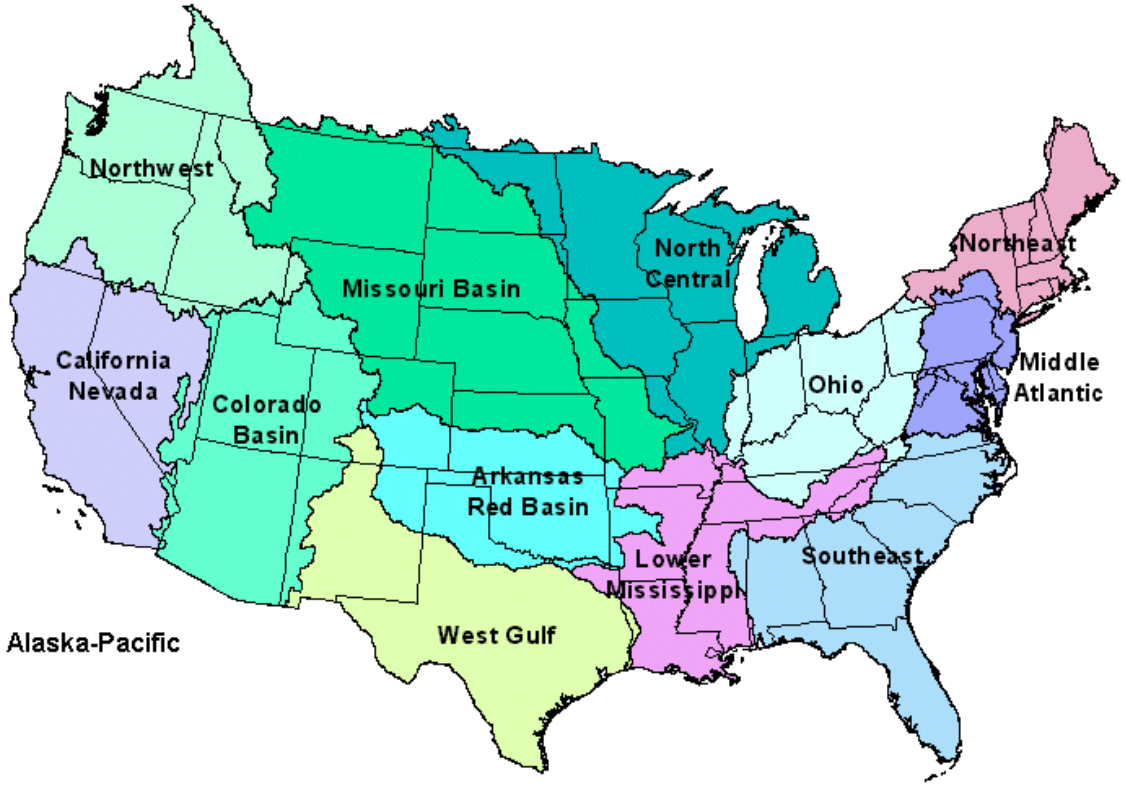

Figure 1.2 River Forecasting Centers (RFC) in US (www.noaa.gov)

NEXRAD works in two modes: clean air mode and precipitation mode. In clean air mode the radar rotates slowly; this is the most sensitive mode that can detect objects ranging from dust, pollen, and smoke released by jet planes to birds. Ornithologists use NEXRAD to study the migration of birds. In precipitation mode the radar rotates rapidly, since the meteorologists want the see the vertical structure of the storm. The radar is operated at several elevation angles up to 19.5°. In precipitation mode, the volume scan is produced every 6 minutes, whereas in clean air mode the volume scan is produced every 10 minutes. NEXRAD can also provide information

about all types of weather thunderstorms, hails, tornadoes, hurricanes, flashfloods, snow and freezing precipitation.

NEXRAD precipitation products were classified into four stages depending on the extent of preprocessing techniques and bias adjustments made to the data. Stage I data reflect the application of a generalized Z-R relationship to the direct reflectivity measurements obtained through WSR-88D (Fulton et al., 1998) in 4 km × 4 km Hydrologic Rainfall Analysis Project (HRAP) grid format. Stage I data are not associated with any bias adjustments. A raingauge bias adjustment factor is estimated by using available one-hour raingauge measurements for each radar site. The bias adjustment factor is applied to Stage I rainfall estimates for each individual WSR-88D site to generate Stage II data (Jayakrishnan et al., 2004). Finally, Stage III data is obtained by distance-weighted averaging of Stage II rainfall estimates for areas having overlapping fields from multiple adjacent radars. The Stage III process generates a single product covering an entire River Forecasting Center (RFC).

NWS Office of Hydrology developed further refinements to the adjustment process called the Multisensor Precipitation Estimate (MPE) in March 2000 and started applying MPE to RFCs in 2002 (Wang et al., 2008). Precipitation estimates from precipitation gauges, NEXRAD and Geostationary Operational Environmental Satellite (GOES) were merged to obtain MPE. Rainfall estimates from GOES were used to fill areas that were not covered by radars or raingauges. With respect to Stage III, MPE data has improved mean-field bias correction, delineation of effective coverage of radar and new local bias correction algorithm (Seo, 2003), the improvements in MPE data removed biases present in Stage III data.

Most of the RFCs in U.S. have adopted the MPE technique to estimate spatial precipitation data, but the Arkansas Red Basin River Forecast Center (ABRFC) has developed its own method for radar precipitation data processing in cooperation with Corps of Engineers, Tulsa District, called Process 1 (P1) (NWS-ABRFC, 2010). Instead of using single bias value for an entire radar coverage region, as used in Stage III and MPE precipitation processing, P1 calculates bias for each HRAP grid cell. All the Hourly Digital Precipitation (HDP) products from the radars in entire ABRFC basin were combined into one product to develop a mosaic. Hourly precipitation amounts collected by the ground-based raingauge stations were used to create a triangular irregular network (TIN). The radar mosaic and TIN were overlaid to calculate the bias based on the difference between radar estimated amount and gauge collected amount. If

the gauging stations were not available for a region, bias was calculated by using the distance between the TIN and the nearest gauging station, and this bias was used to calculate the final radar precipitation product. The current version of this radar rainfall product is P3, which has an improved interface to make manipulation and viewing of the data easier; but the process of applying the bias adjustment to the radar data has not changed since P1 was initiated in 1996 (Bill Lawrence, personal communication, 2010).

The NWS uses Advanced Weather Interactive Processing System (AWIPS), a computer-based interactive system, to process and display all meteorological and hydrological data. The AWIPS Release 7.1 includes an MPE editor to process radar, satellite, and ground raingauge data into hourly, gridded, multi-sensor precipitation estimates on the HRAP grid (NWS, 2006). For Release 7.1, NWS has adapted the local bias correction procedure from the P3 application used by the ABRFC since 1996. Thus, MPE data processed at all RFCs since the implementation of Release 7.1 in 2006 has used the P3 bias adjustment procedure.

Precipitation estimates from NEXRAD offers the advantage of providing spatial as well as temporal variability associated for precipitation. The use of improved spatial precipitation resolution from NEXRAD data should improve hydrologic modeling relative to the use of point precipitation gauge data, as long as precipitation estimation accuracy is not compromised. However, it is unclear how hydrologic models will respond to the increased spatial resolution of precipitation data, and if the model algorithms can take advantage of these data to produce more realistic hydrologic results.

CHAPTER 2 - Literature Review

Precipitation is the driving force behind all the hydrologic processes in a watershed and therefore the driving force in hydrologic modeling (Moon et al., 2004). Many studies have used rainfall measurements at raingauge stations to estimate surface runoff by using NRCS curve number (CN) method (USDA-SCS, 1972). The model estimates runoff based on rainfall depths and a CN parameter. This method is widely used in watershed modeling, and has been incorporated into various computer models. Although this is a widely used method for streamflow/runoff estimation, studies have shown that this method should be evaluated before it is used in regional agro-climatic conditions.

Gilley et al. (1986) emphasizes that land cover has a great impact on runoff volume, and their study showed that runoff decreased from 56.9 mm for plots with no residue to 0 mm for plots with 13.45 Mg/ha residue. Shirmohammadi et al. (1997) evaluated the effect of CN procedures in predicting runoff volumes using CREAMS and GLEAMS hydrologic models and found that both the models under predicted runoff because of the internal conversion of CN_{II} (representing average antecedent soil moisture conditions at the time runoff occurred) to CN_I (representing dry conditions). Curve number parameter may vary from event to event, thus selecting an appropriate CN value to reflect the effect of surface cover, management, landuse, and antecedent moisture condition in estimating storm runoff volume is a crucial task.

2.1 Watershed models

Watershed models have been developed to evaluate the effect of management practices that can be used over various time periods and to simulate runoff from a watershed. Bingner (1996) estimated runoff using SWAT, a continuous hydrologic model, in Goodwin Creek Watershed, northern Mississippi, with individual rainfall measurements for each subwatershed. Results showed very good runoff prediction on a daily and annual basis, with r^2 values for most of the subbasins at 0.90 and above, except for a completely wooded subbasin. The study showed that with adequate rainfall measurement density, SWAT has the capability to represent the spatial and temporal variations in watershed to simulate runoff. Saleh et al. (2000) assessed the effect of dairy production on water quality in Upper North Bosque River Watershed, north central Texas using SWAT, a river-basin model. A total of 94 dairies were included within the

study area of 93,250-ha at the time of study. SWAT was simulated from 1988 through 1996 and validated at 11 stream sites for the period of October 1993 to July 1995. Model output was compared to observed streamflow data and the Nash-Sutcliffe model efficiency (E_{NS}) ranged from 0.65 to 0.99 for monthly average streamflow over the validation period. The manure application fields were replaced by grasslands in the SWAT model and observed a reduction of about 33% in total-N and 79% in total-P in the watershed. This study demonstrated the advantages of using SWAT in simulating streamflow and dairy loadings.

Many watershed scale models have been developed over the last few decades including AGNPS, SWAT, ANSWERS, HEC-HMS, and HSPF. Heathman et al. (2008) evaluated the performance of SWAT and AnnAGNPS watershed models in Cedar Creek Watershed, Indiana to estimate the streamflow and atrazine losses. The watershed covers an area of 708 km^2, with 44% of the watershed being agriculture, 36% pasture, 12% forested lands and 2% urban landuse. Results of this study indicated that performance of SWAT was better compared to AnnAGNPS in estimating streamflow, with E_{NS} values ranging from 0.66 to 0.25, and E_{NS} values for AnnAGNPS ranged from 0.13 to -2.06. Both the uncalibrated models were unable to adequately predict the atrazine losses. Singh et al. (2005) compared the performance of HSPF and SWAT in simulating hydrology of Iroquois River Watershed in Illinois and Indiana. The models were calibrated, and the simulated flows from both models were mostly similar except for the low flows. SWAT predicted low flows comparatively better because of its estimation of potential evapotranspiration.

Accuracy of watershed models used to simulate hydrologic processes depends greatly on the resolution and accuracy of the input data to the models. Di Luzio et al. (2005) emphasized the importance of input GIS data quality on SWAT model simulations in Goodwin Creek Watershed, Mississippi. The primary GIS data used in the model was DEM (30 m and 90 m), landuse (LNSL, LNLCD and LULC) and soils (SNSL and STATSGO) data. A total of 12 combinations of input data were used in this study. They concluded that DEM data were critical in representing the watershed and topographic input, landuse data had a significant effect on runoff and sediment loads, and soils data had a less influence on the model results. Cotter et al. (2003) also evaluated the performance of varying spatial resolutions of DEM, landuse, and soil data (30×30 m, 100×100 m, 150×150 m, 200×200 m, 300×300 m, 500×500 m, and 1000×1000 m) on SWAT simulations in Moores Creek Watershed, Arkansas. They observed that SWAT

model outputs was most affected by input DEM data resolution, with coarser DEM data resulting in decreased watershed area and slopes which significantly affects the streamflow response. They recommended that for flow, sediment, NO_3-N, and TP simulations, minimum DEM data resolution should range from 30 to 300 m and for landuse and soils data input resolution should range from 30 to 500 m. Daggupati et al. (2009) evaluated the impacts of spatial input data in targeting sediment producing fields simulated by SWAT. A tool was developed to post-process the SWAT HRU output and calculate the sediment, nitrogen and phosphorus yields for individual fields in the Black Kettle Creek Watershed. DEM data of 10 m and 30 m, STATSGO and SSURGO soils data, NLCD, NASS, field reconnaissance survey data were used in SWAT to evaluate the different spatial resolution scales in targeting fields. Landuse data influenced the SWAT output (sediment producing fields) greatly compared to topographic and soils data, and they recommended not to use NASS landuse data in field targeting.

2.2 Watershed model response to precipitation

SWAT model output depends on accuracy of the model inputs, whether it be GIS data or weather data. Rainfall is by far the largest source of uncertainty in watershed modeling (Srinivasan, 2005), and failure to collect the rainfall data accurately leads to inadequate soil moisture measures and subsequent inaccuracy of runoff estimates. In this regard, a variety of studies have been conducted to evaluate the performance of different rainfall data products in watershed modeling.

Chaubey et al. (1999) assessed the uncertainty in output of the AGNPS model due to uncertainty in rainfall input over a 159-km^2 Cement Watershed in southwest Oklahoma using a network of 17 raingauges. The model was run for each rainfall event using each raingauge one at a time assuming homogenous spatial rainfall. They observed a bias of up to 40% in model predicted runoff, sediment, and sediment-attached N and P.

Faures et al. (1995) studied the runoff response due to rainfall spatial variability on a 4.4-ha semiarid Lucky Hills Watershed in the USDA-ARS Walnut Gulch Experimental Watershed near Tombstone, Arizona. A distributed, event-based rainfall-runoff model-KINEROSR with a dense network of 5 raingauges was used for this study. Five model runs were conducted using one raingauge at a time, the simulated runoff volumes ranged from 2 to 65% over eight storm

events. They found that even at very small scale watersheds, spatial variability of rainfall can have substantial impacts on simulated runoff.

Hernandez et al. (2000) evaluated the runoff response due to spatial variability in rainfall using KINEROS and SWAT hydrologic models on an 8.23 km^2 subwatershed in Walnut Gulch Experimental Watershed in southeastern Arizona. They found that prediction of runoff depth using KINEROS improved as the number of raingauges increased from a single raingauge to 10 gauges, with r^2 increasing from 0.60 to 0.90, similarly with SWAT, r^2 increased from 0.33 to 0.57.

Bingner et al. (1997) evaluated the effect of subwatershed size on SWAT simulated annual runoff and sediment yield in Goodwin Creek Watershed. Topographic Parameterization (TOPAZ) was used to create 10 different subwatershed sizes based on critical source area (CSA) and the minimum source channel length. The number of subwatersheds delineated ranged from 47 to 986. The average subwatershed slope increased as the number of subwatersheds increased from 47 to 986. They found that simulated annual runoff varied by less than 5% with different subwatershed scale. The annual sediment yield varied significantly for watershed delineation ranging from 47 to 125 subwatersheds, but has little variation for 300 to 986 subwatershed delineations.

2.3 NEXRAD rainfall estimation

Precipitation gauges are not able to capture the spatial and temporal variations of rainfall. With improvements in radar technology, radar data may be helpful to the advancement of watershed modeling in terms of distinguishing the spatial and temporal variability of rainfall.

Young and Brunsell (2008) evaluated NEXRAD Stage III and Multisensor Precipitation Estimator (MPE) data using NWS raingauge data over the Missouri River Basin River Forecast Center and observed the improvements in NEXRAD data over time. They used mean bias, correlation, and rain detection parameters to evaluate NEXRAD data and reported NEXRAD data performed better in the southeastern half of the Missouri River Basin than in the central and mountainous areas. NEXRAD data in warm season were better than cold season estimates, and the NEXRAD data improved over a period of 1998-2004 with rain detection increasing from 68 to 84%.

Xie et al. (2006) evaluated NEXRAD Stage III data with a network of gauge precipitation estimates over a semi arid region in central New Mexico during 1995 to 2001 period. They selected Stage III data that did not incorporate the raingauge data, which are best for evaluating the quality of Stage III products. Overall, Stage III data overestimated rainfall data in monsoon seasons and underestimated rainfall data in nonmonsoon seasons. Stage III data either overestimated by 28.2% or underestimated by 11.9% the annual rainfall during the study period. They indicated that the cause of both underestimation and overestimation of radar rainfall was due to truncation error.

Wang et al. (2008) validated the performance of NEXRAD MPE and Stage III data using a high-density raingauge network over the Upper Guadalupe River Basin of the Texas Hill Country. Only uniform rainfall events which lasted for an hour or a day were used to evaluate NEXRAD data using coefficient of variation (CV), Pearson correlation coefficient, and probability of rain detection (POD) as parameters. There were some cases where gauge data predicted more rainfall than radar because rainfall collected by gauge may not have represented the areal average rainfall within a NEXRAD grid cell. They observed that MPE data had linear correlation with gauge rainfall data for uniform rainfall events. MPE data had much higher capability of rain detection than Stage III; whereas Stage III tended to overestimate raingauge estimates by 20%, MPE tended to underestimate raingauge estimates by 7%. Better correlation with gauge data and higher probability of rain detection than Stage III made MPE data a better representation of spatial rainfall.

2.4 Watershed modeling using NEXRAD

Improved spatial and temporal resolution from radar precipitation estimates should improve watershed modeling accuracy. However, only a limited number of studies have assessed the impact of radar rainfall data on watershed modeling output.

Johnson et al. (1999) compared mean areal estimates of precipitation from NEXRAD Stage III and raingauge networks over eight basins in the southern plains region located mainly on the Oklahoma-Arkansas-Missouri border for the period from 1993-1996. They also investigated the impacts of these areal estimates on streamflow estimation using Sacramento Soil Moisture Accounting (SAC-SMA) model. On a whole, the mean areal rainfall estimates from NEXRAD were 5-10% less than the estimates from raingauge networks. NEXRAD data

produced much more runoff than raingauge data with an uncalibrated hydrologic model. Even though discharge simulated with NEXRAD data was higher, the efficiency of NEXRAD simulation was better than raingauge simulation. They also found NEXRAD data in ABRFC region produced better estimates of precipitation for some events.

Guo et al. (2004) investigated the impacts of different precipitation products on runoff, evapotranspiration and soil moisture over the Illinois River Watershed (1,645 km^2) at Watts, Oklahoma, simulated by Three-Layer Variable Infiltration Capacity (VIC-3L) land surface model. NEXRAD Stage III hourly data from May 1993 to December 1998 was aggregated in space and time to daily in order to correspond with the University of Washington (UW) daily precipitation data obtained from a raingauge network. NEXRAD data captured spatial distribution of rainfall data better than UW data. Daily runoff and evapotranspiration results were more sensitive to the temporal and spatial distributions of rainfall. Moreover, runoff and evapotranspiration obtained from simulations using NEXRAD data showed more spatial variability than those obtained by UW precipitation data.

Tuppad et al. (2010) evaluated the uncertainties in streamflow estimation at 5 stream gauge stations in the Smoky Hill River/Kanopolis Lake Watershed (6,316 km^2) in central Kansas due to spatial aggregation of NEXRAD data. NEXRAD rainfall data for a subwatershed was derived from the nearest NEXRAD HRAP grid cell. NEXRAD Stage III grid cells (approximately 4×4 km^2) were aggregated incrementally to 8, 16, 32, 64, 128, and 256 km resolutions for the period of 1995 to 2002, and streamflow was simulated using the SWAT model. The best model performance ($E_{NS,\,med} \geq 0.50$) was observed for aggregated resolutions of 32, 64, and 128 km, whereas the finest resolution (4 km) showed poorer performance. They observed NEXRAD data overestimated streamflow in low flow events and underestimated streamflow in high flow events. Overall, they observed greater variability in SWAT streamflow simulations among the stream gauge stations than in response to input spatial rainfall resolutions.

Moon et al. (2004) evaluated different rainfall inputs using spatially distributed rainfall data and traditional raingauge data for the 1999 to 2001 time period as input to the hydrologic model on 2,608-km^2 Cedar Creek Watershed in the Trinity River Basin, Texas. NEXRAD rainfall data for a subwatershed was derived from the area-weighted average of the NEXRAD grid cells covering the subwatershed. The SWAT simulated streamflow was compared to the observed streamflow at Cedar Creek Reservoir. The E_{NS} values of the SWAT-raingauge

simulations ranged from 0.48 to 0.78 and E_{NS} values for SWAT-NEXRAD simulations ranged from 0.57 to 0.82. Both NEXRAD and raingauge simulations had similar r^2 values, but the slope of NEXRAD simulations was close to 1, indicating NEXRAD was a good alternative to raingauge data.

Kalin and Hantush (2006) used NEXRAD MPE data in hydrologic modeling as an alternative source of rainfall data to surface raingauges over Pocono Creek Watershed (120 km^2), Pennsylvania. The SWAT model was calibrated with CN and ESCO parameters for monthly streamflow, base flow and surface runoff, with calibration period from July-2002 to May-2004 and validation period from June-2004 to April-2005. NEXRAD rainfall data for a subwatershed was derived from the nearest centroid of HRAP grid cell. Hydrographs generated from gauge and NEXRAD simulations matched well with observed flow hydrographs. The E_{NS} for monthly streamflow SWAT-raingauge simulations was 0.66 and for E_{NS} for SWAT-NEXRAD simulations was 0.75. The E_{NS} for daily streamflow SWAT-raingauge simulations was 0.64 and for SWAT-NEXRAD was 0.62. The model efficiency was better in monthly simulations when compared to daily simulations. They observed several underestimations in April and overestimations in June for streamflow. They concluded that the efficiency of NEXRAD data can be better understood when simulations are performed at the subwatershed scale.

Tobin and Bennet (2009) evaluated the performance of raingauges, NEXRAD and Tropical Rainfall Measurement Mission (TRMM) satellite rainfall data for the hydrologic modeling of two river basins in Texas and Mexico. The areas of the two watersheds were 7,720 km^2 and 8,905 km^2, each divided into 25 subwatersheds and the rainfall data from NEXRAD grid cells within a TRMM grid cell of about 45-53 were averaged and the centroid of TRMM cell was used as raingauge station. TRMM data is satellite estimated precipitation data derived from TRMM Microwave Imager (TMI) and Precipitation Radar (PR), with fine spatial and temporal resolutions, but errors can be significant because satellite coverage is not continuous. They used the SWAT model to simulate streamflow using these three rainfall inputs, with the calibration period from July 2003 to December 2006 and validation period from January 2007 to December 2007. Both NEXRAD and TRMM data provided satisfactory results in streamflow simulations. In both watersheds, NEXRAD Stage III data obtained low mass balance errors (13%) between simulated and observed streamflow and E_{NS} greater than 0.60 for monthly results. The TRMM data greatly overestimated streamflow during August-December months in

one of the watersheds, with E_{NS} ranging from 0.38-0.94. They also observed mixed results with NEXRAD Stage III data.

The watershed modeling studies discussed above were summarized in table 2.1. They have assessed the quality of several types of NEXRAD data products and their performance in hydrologic modeling. These studies have averaged the NEXRAD grid cells on a larger subwatershed scale, the spatial distribution of rainfall was lost with the averaging of rainfall data. In this study, the watershed was delineated into 121 subwatersheds with an average area of subwatershed being 19 km^2, thereby reducing the number of grid cells to be averaged for a subwatershed. All the studies have used either NEXRAD Stage III or MPE product and this study was the first to evaluate the P3 product in watershed modeling.

Hydrologic models typically use the "nearest-neighbor" approach, which assigns each watershed or subwatershed rainfall data from the raingauge station closest to that watershed or subwatershed. NEXRAD rainfall data, however, are now available at the HRAP grid-cell resolution. Thus, watershed modeling studies that used NEXRAD data have adapted these data to the model using one of two methods: subwatershed rainfall data could be derived either from the average rainfall data of NEXRAD grid cells covering the subwatershed or from the individual NEXRAD grid cell closest to the subwatershed. Because of the additional processing required to develop area-weighted-average, subwatershed-specific NEXRAD rainfall amounts, most studies described above have applied the nearest-neighbor approach to assigning NEXRAD data to subwatersheds. Further study is needed to assess the hydrologic response to spatially averaged, subwatershed-specific, spatial rainfall estimates.

NEXRAD data for most RFCs have been developed using Stage III (1996-2001), MPE (2002-2006), and P3 (2006-present) bias adjustment algorithms. No studies were found that assessed the impact of the improved P3 bias adjustment procedures on hydrologic modeling. The availability of long-term P3 data for the ABRFC presents a unique opportunity to test the modeled hydrologic response to P3 data.

Table 2.1 Literature on watershed modeling studies using NEXRAD data

	Watershed Area	No. of Subwatersheds	Period of NEXRAD data	Method of rainfall input to model
Johnson et al. (1999)	3 watersheds – 1,646; 895; 285 km^2	-	Oct 1993 - July 1996	SAC-SMA model was used and they have not described the method of rainfall input to the model.
Guo et al. (2004)	1,645 km^2	-	May 1993 - Dec 1998	VIC-3L model was used and NEXRAD grids were aggregated to 1/8 degree (12 km) spatial resolution to match with UW data. The rainfall data input to model was not described.
Tuppad et al. (2010)	6,316 km^2	48	1995-2002	Areal average from grid cells covering the subwatershed was computed and used as precipitation input for subwatershed in SWAT.
Moon et al. (2004)	2,608 km^2	62 (average area of subbasin =40 km^2)	1999-2001	Rainfall data for each subbasin was estimated by computing the weighted average method from all the grid cells in a subbasin and used as input to SWAT.
Kalin and Hantush (2006)	120 km^2	29	July 2002 - April 2005	Centroid of NEXRAD grid cells were used as gauging stations in SWAT.
Tobin and Bennet (2009)	2 watersheds – 7,720 and 8,905 km^2	25 for each watershed	1998-2007	NEXRAD cells in a TRMM cell were averaged about 45-53 cells and used the centroid of TRMM cell as raingauge station.
This study	2,416 km^2	121	1996-2008	Rainfall data for each subwatershed was calculated by weighted average method for all the grid cells covering the subwatershed and used as input to SWAT.

2.5 Study Objectives

The goal of this study was to evaluate the performance of spatially averaged, subwatershed-specific NEXRAD P3 data on streamflow simulations by the SWAT hydrologic model. Specific objectives were

(1) to assess the agreement between NEXRAD P3 data and NCDC precipitation gauge data for precipitation gauge stations data within and around the North Fork Ninnescah Watershed,

(2) to assess the agreement of measured USGS streamflow data with SWAT-simulated streamflow using both spatially distributed NEXRAD P3 precipitation data and NCDC precipitation gauge data in North Fork Ninnescah Watershed, and

(3) to examine and describe the spatial and temporal characteristics of differences in modeled streamflow response to distributed P3 and point NCDC precipitation data.

CHAPTER 3 - Materials & Methods

3.1 Study Area

The North Fork Ninnescah Watershed above Cheney Reservoir (fig.3.1), located in south central Kansas, was defined by a USGS stream gauging station (07144780) and covers an area of 2400.17 km^2 (926.71 mi^2) within Reno, Kingman, Pratt, Stafford, Sedgwick counties in south-central Kansas. This watershed encompasses land in the North Fork Ninnescah (HUC 11030014) and South Fork Ninnescah (HUC 11030015) watersheds. The North Fork Ninnescah River, which is a tributary of the Arkansas River, generally flows eastward across south central Kansas into Cheney Reservoir. Cheney Reservoir was constructed in 1964 by the United States Bureau of Reclamation (USBOR). The reservoir was designed as a 100-year multipurpose project to supply water for the City of Wichita as well as to provide wildlife/recreation area and flood control. Cheney Lake currently supplies 60 to 70% of the Wichita's water supply (Cheney Lake Watershed, Inc. 2008).

Over 99% of the study area is used for agriculture. Landcover in the watershed is dominated by cropland (63%) and rangeland (24%). Major crops are winter wheat (26.33%), corn (8.47%), soybean (3.96%), grain sorghum (3.75%), alfalfa (2.24%) and other crops (20.02%) of the total watershed according to NASS 2007 landuse data (fig. 3.2).

Kansas receives most of its moisture from the Gulf of Mexico with an average annual precipitation of 735 mm (NCDC, 2008) and North Fork Ninnescah Watershed averages 695 mm (Bhuyan, 2001). The annual temperature extremes range from -15 °C to 41 °C in the watershed. According to the updated Koppen-Geiger climate classification (Kottek et al., 2006), the North Fork Ninnescah Watershed climate is categorized as Cfa: warm temperate, fully humid with hot summers.

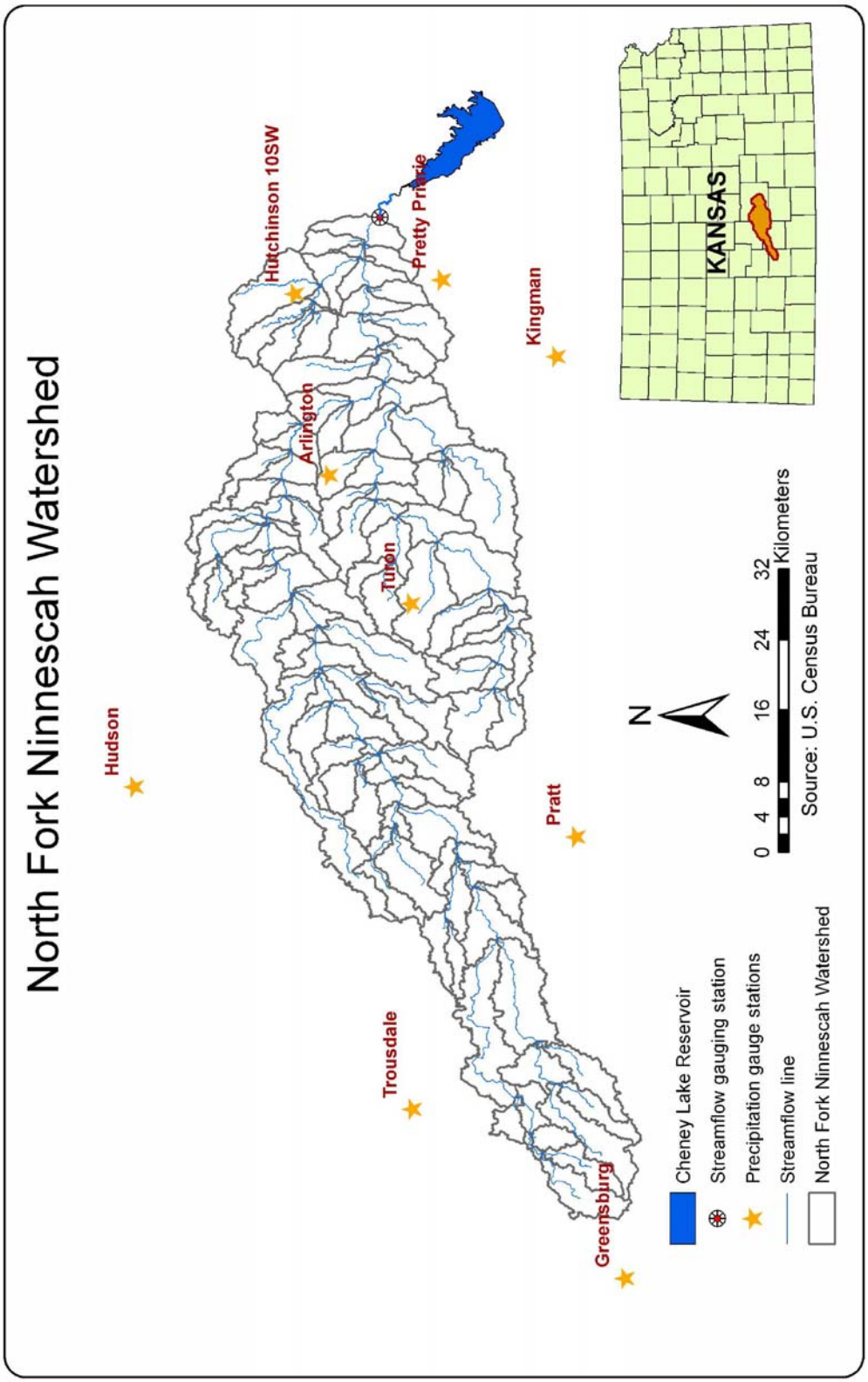

Figure 3.1 North Fork Ninnescah Watershed with stream network, NWS precipitation gauge stations and USGS stream gauging station.

3.2 SWAT Model

ArcGIS interface of the SWAT 2005 version (ArcSWAT-2005 Version 2.1.6) (Arnold et al., 1998; Neitsch et al., 2005a; 2005b) was used in this study. SWAT is a river basin or watershed scale model capable of predicting the impact of land management practices on water, sediment and chemical yields from large watersheds. The model is capable of simulating long periods for computing the effect of management changes. SWAT model is capable of handling both spatial and temporal data as input for estimating water yields (Arnold et al., 1998). SWAT model partitions the watershed into subwatersheds connected by a stream network and then into Hydrologic Response Units (HRU). HRUs are one or more unique combinations of soils, landuse and slope in each subwatershed. The delineation of sub watersheds and HRUs allows the SWAT to account for the spatial diversity of landuse, soils and slopes in the watershed. With HRU delineation, the computational costs of simulations can be minimized by lumping similar soil, landuse and slope areas into single unit (Neitsch et al., 2005a).

SWAT calculates surface runoff for each HRU based on USDA NRCS Curve Number (CN) method (USDA-SCS, 1972) or Green and Ampt infiltration method (Green and Ampt, 1911). The CN method was used for this study. The CN method assumes CN I at wilting point, CN III at field capacity and a CN of 100 at saturation point (Arnold et al., 2000), and CN is modified daily based on soil moisture. The surface runoff is calculated by

$$Q_{surf} = \frac{(R - 0.2S)^2}{(R + 0.8S)} \tag{3.1}$$

where,

Q_{surf} = surface runoff depth (mm),

R = total rainfall depth (mm), and

S = retention parameter (mm).

In this equation the initial abstraction is approximated as 0.2S, and the retention parameter is defined as

$$S = 25.4\,(\frac{1000}{CN} - 10) \tag{3.2}$$

where,

CN = daily curve number.

The CN is a function of hydrologic soil group, landuse, land management, and antecedent soil moisture conditions.

SWAT can calculate potential evapotranspiration by three methods: (1) the Penman-Monteith method; (2) the Priestly-Taylor method; and (3) the Hargreaves method (Neitsch et al., 2005a). Among the three methods, Penman-Monteith (Monteith, 1965) was used for this study at the suggestion of SWAT developers. The Penman-Monteith method requires climatic inputs of solar radiation, air temperature, relative humidity and wind speed (eq. 3.3).

$$ET_0 = \frac{0.408\Delta(R_n - G) + \gamma \frac{900}{T + 273.2} u_2 [e_s - e_a]}{\Delta + \gamma(1 + 0.34u_2)} \tag{3.3}$$

where,

ET_0 = reference evapotranspiration (mm/d),

R_n = net radiation ($MJ/m^2/d$),

G = soil heat flux density ($MJ/m^2/d$),

u_2 = wind speed at 2m height (m/s),

e_s = saturation vapor pressure at air temperature (kPa),

e_a = actual vapor pressure of air (kPa),

γ = the psychrometric constant ($kPa/^oC$),

T = Air temperature (^oC), and

Δ = slope of saturation vapor pressure curve at air temperature ($kPa/^oC$).

SWAT can apply either the variable storage method or the Muskingum routing method to route water through the watershed channel network to the outlet; both methods are variations of the kinematic wave model (Neitsch et al., 2005a). SWAT assumes that channels or reaches in the watersheds are of trapezoidal cross-section. SWAT accounts for the transmission losses, which reduce the runoff volume as water travels downstream. SWAT uses Manning's equation to calculate the rate and velocity of flow for every reach in the watershed at every time step.

$$Q = \frac{A\, r^{2/3}\, s^{1/2}}{n} \tag{3.4}$$

$$V = \frac{r^{2/3}\, s^{1/2}}{n} \tag{3.5}$$

where,

Q = the rate of flow in the channel (m^3/s),

A = the cross-sectional area of flow in the channel (m^2),

r = the hydraulic radius for a given depth of flow (m),

s = the slope of the channel length (m/m),

n = Manning's "n" coefficient for the channel, and

V = the velocity of flow in the channel (m/s).

3.3 Model Input Data

A 10-m resolution USGS digital elevation model (USGS-NED, 2008) was used in extracting stream network and delineating watershed and sub-watersheds. For this study the watershed was delineated into 121 sub-watersheds, using the ArcGIS interface developed for SWAT model (Neitsch et al., 2005a). The 121 subwatersheds delineation was selected so that average area of the subwatersheds was approximately equal to the area of a NEXRAD HRAP grid cell (16 km^2). The average area of subbasins was 1,983.61 ha (19.83 km^2), with a minimum of 1.28 ha and a maximum of 8786.54 ha. The slopes in the watershed ranged from 0.0% to 46.1%, with median slope of 0.9 %. Slopes in the watershed were classified into two categories: 89.18% of the watershed was in 0-3% classification and 10.82% of the watershed in 3-46.1% (fig. 3.2).

The USDA National Agricultural Statistics Service (NASS) (USDA-NASS, 2007) conducted an agricultural census in 2007 and developed a 1:100,000 scale landuse/landcover data for the whole US, which was used in this study. NASS landuse was produced from the Thematic Mapper (TM) instrument on Landsat 5 and Enhanced Thematic Mapper (ETM) on Landsat 7. Landcover in the watershed was dominated by cropland (63%) and rangeland (24%) (fig. 3.3). Major crops in watershed were winter wheat (41%), corn (13%), soybean (6%), grain sorghum (6%), alfalfa (3%) and other crops (31%) according to NASS 2007 landuse data.

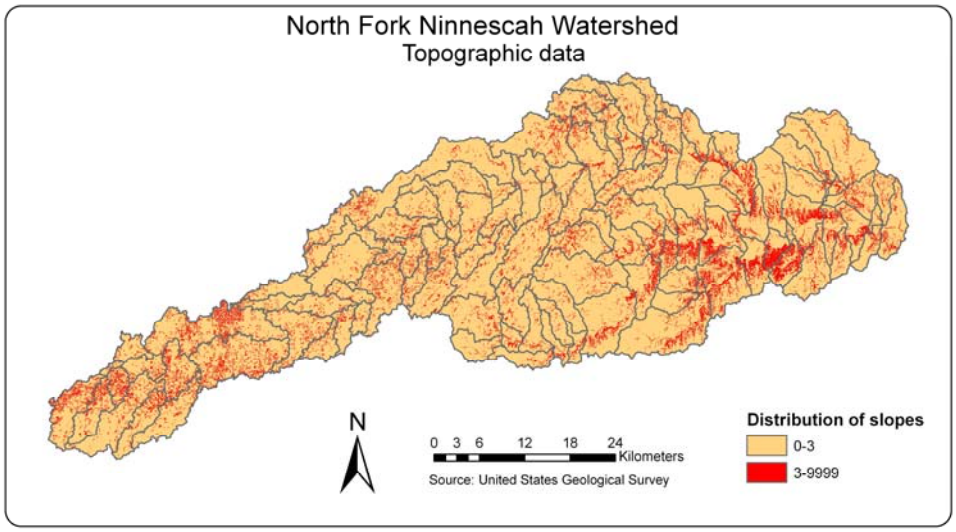

Figure 3.2 Spatial distribution of slopes for North Fork Ninnescah Watershed

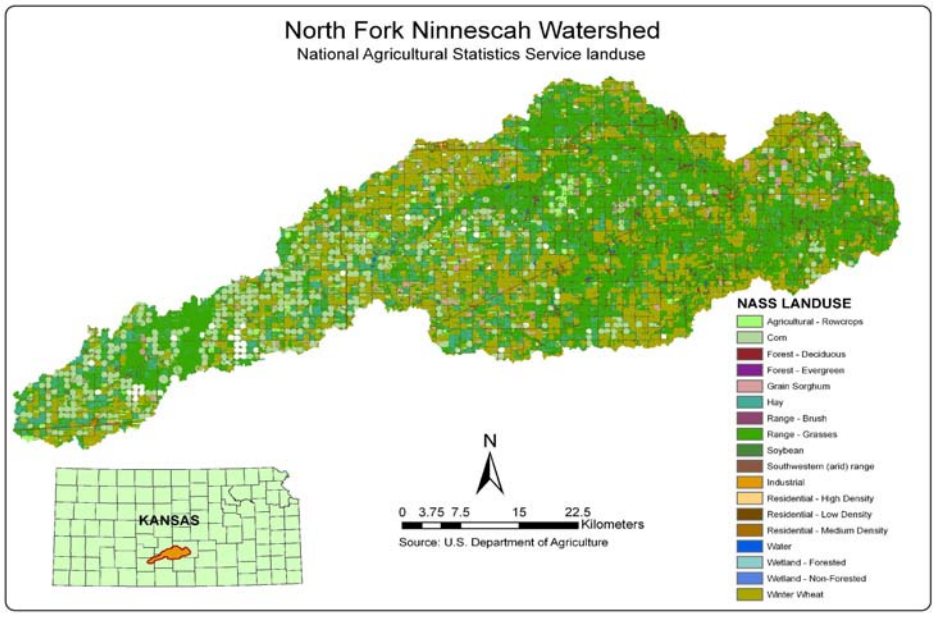

Figure 3.3 National Agricultural Statistics Service Landuse for North Fork Ninnescah Watershed

The USDA-NRCS Soil Survey Geographic database (USDA-NRCS, 2005), at a scale of 1:24000, was used as the soils input for the model. This dataset was developed by NRCS-National Cartography and Geospatial Center (NCGC) and is the most detailed county level data. The SSURGO data was prepared into SWAT format using ArcMap tool for preprocessing SSURGO soil database (Sheshukov et al., 2009). The soils in the watershed are mostly coarse-

loamy, fine-loamy and sandy soils; the soils are not concentrated at one place, but they are distributed throughout the watershed. The soils are classified into 4 groups: 20.8% of the watershed was in class A hydrologic soil group, 55.4% of the watershed was in class B, 13% of the watershed was in class C, and 10.8% of the watershed was in class D (fig. 3.4).

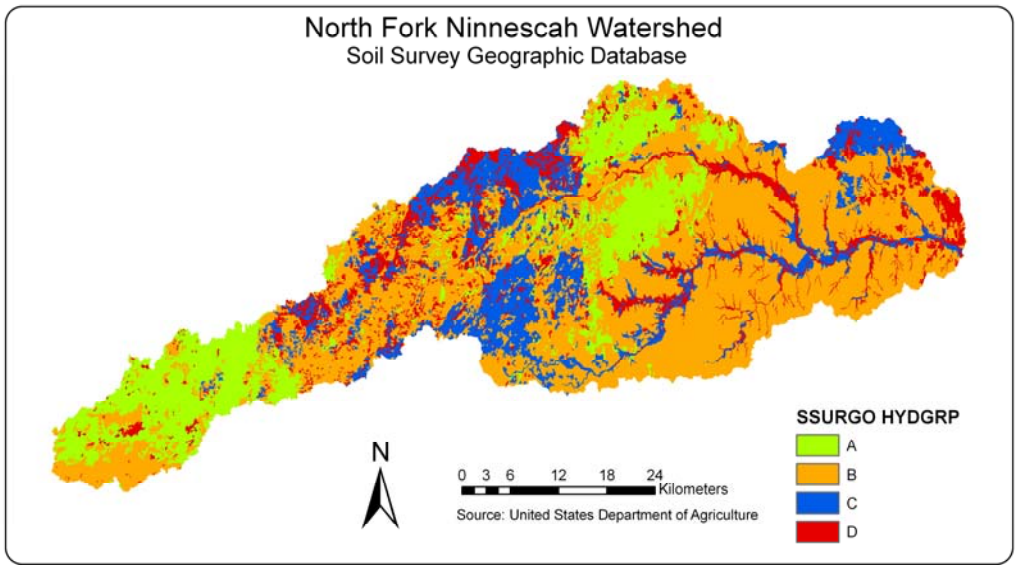

Figure 3.4 Spatial distribution of soils for North Fork Ninnescah Watershed

The daily maximum and minimum temperature data for the period of 1994 to 2008 was obtained from Mary Knapp (personal communication, 2009), Kansas State Climatologist at Kansas State University. The primary source of the data used in this study was from National Climatic Data Center Weather Data Library database (NCDC, 2008). Other Climatic data, including wind speed, solar radiation, and relative humidity, were obtained from SWAT weather generator database.

3.4 Precipitation data processing

3.4.1 Precipitation gauge data

Daily rainfall data was obtained from Mary Knapp (personal communication, 2009), Kansas State Climatologist at Kansas State University, Manhattan, KS. The primary source of this data used in this study was from National Climatic Data Center Weather Data Library database (NCDC, 2008). A total of 9 precipitation gauge stations within and around the North Fork Ninnescah Watershed were used for this study (fig. 3.1). The time period for this data

ranged from 1996 to 2008. This data was represented in 24-hr depths of rainfall recorded from 7:00 a.m. to 7:00 a.m. local time, for the day of observation. The total annual precipitation for each precipitation gauge used in this study was shown in table 3.1. Missing daily precipitation data at each station were replaced using data for the same day from the three nearest neighboring gauges weighted by distance using the inverse distance weighted (IDW) technique (see Appendix B for details). The number of days with missing data at each precipitation gauge station is reported in table 3.2.

3.4.2 NEXRAD data

The NEXRAD database of daily precipitation estimates was compiled from the NOAA-NWS database (NWS, 2009). North Fork Ninnescah Watershed is part of the Arkansas River Basin, and hence the NEXRAD data for this area were processed and maintained by ABRFC of the NWS. North Fork Ninnescah Watershed was covered by radars at Dodge City, KS and Wichita, KS (fig. 3.5). A total of 218 NEXRAD grid cells (4 km × 4 km) covered the study area (fig. 3.6). The precipitation data used for this study was from 1 January 1996 to 31 December 2008. Daily NEXRAD data for each HRAP grid were obtained by summing hourly data from the 7:00 a.m. to 7:00 a.m. period each day, and assigning the precipitation sum to the ending date, in order to correspond with daily precipitation gauge data. NEXRAD data were compiled into SWAT format with NEXRAD Tool (see Appendix A for details) developed by Dr. Xingong Li and Tingting Xu (University of Kansas).

SWAT accepts one gauge station for each subwatershed. The default SWAT procedure assigns to each subwatershed the precipitation gauge station nearest to the subwatershed centroid. The NEXRAD Tool was used to create the equivalent of a precipitation gauge station at the centroid of each subwatershed. Daily precipitation data for each subwatershed was estimated using an area-weighted average of all NEXRAD grid cells that covered the subwatershed (fig. 3.6, fig. 3.7) (see Appendix A for details). This method enabled SWAT to access precipitation data from a precipitation gauge station placed at the centroid of each subwatershed.

Table 3.1 Total annual precipitation (mm) for precipitation gauge stations used in this study

Station	1996	1997	1998	1999	2000	2001	2002	2003	2004	2005	2006	2007	2008
Arlington	-	-	-	-	-	-	822.9	584.2	795.0	741.7	647.7	995.7	782.3
Greensburg	856.0	934.7	622.3	629.9	962.6	589.3	607.1	523.2	632.4	718.8	571.5	985.5	668
Hudson	670.6	825.5	708.6	756.9	756.9	645.2	762.0	614.7	845.8	731.5	685.8	1074.4	871.2
Hutchinson 10SW	660.4	820.4	830.6	779.8	856.7	627.4	797.5	759.4	843.3	822.9	591.8	1008.3	965.2
Kingman	995.7	944.8	838.2	800.1	883.9	584.2	861.1	820.4	965.2	789.9	789.9	883.9	660.4
Pratt	838.2	899.2	614.7	744.2	883.9	386.1	840.7	637.5	850.9	647.7	701.1	967.7	602.0
Pretty Priarie	-	-	-	-	-	-	911.8	741.7	947.4	904.2	566.4	927.1	873.7
Trousdale	960.1	988.1	553.7	690.9	858.5	530.8	520.7	449.5	662.9	632.4	563.8	927.1	688.3
Turon	-	-	-	-	-	-	728.9	642.6	919.5	792.5	675.6	955.1	744.2

Table 3.2 Number of days missing precipitation data for each station

Station	1996	1997	1998	1999	2000	2001	2002	2003	2004	2005	2006	2007	2008
No. of days in year	366	365	365	365	366	365	365	365	366	365	365	365	366
Arlington	366	365	365	365	366	365	13	39	31	10	35	2	2
Greensburg	67	68	51	31	34	34	41	45	45	45	19	260	116
Hudson	2	0	1	2	0	0	0	0	0	0	0	0	2
Hutchinson 10SW	27	28	28	17	21	16	26	26	12	26	10	10	20
Kingman	36	37	33	16	2	4	4	4	7	125	1	33	96
Pratt	5	9	4	7	0	67	38	16	15	17	9	12	65
Pretty Priarie	366	365	365	365	366	365	9	15	15	20	6	11	10
Trousdale	7	10	7	5	3	7	4	5	6	4	4	8	10
Turon	366	365	365	365	366	365	16	20	14	16	14	18	8

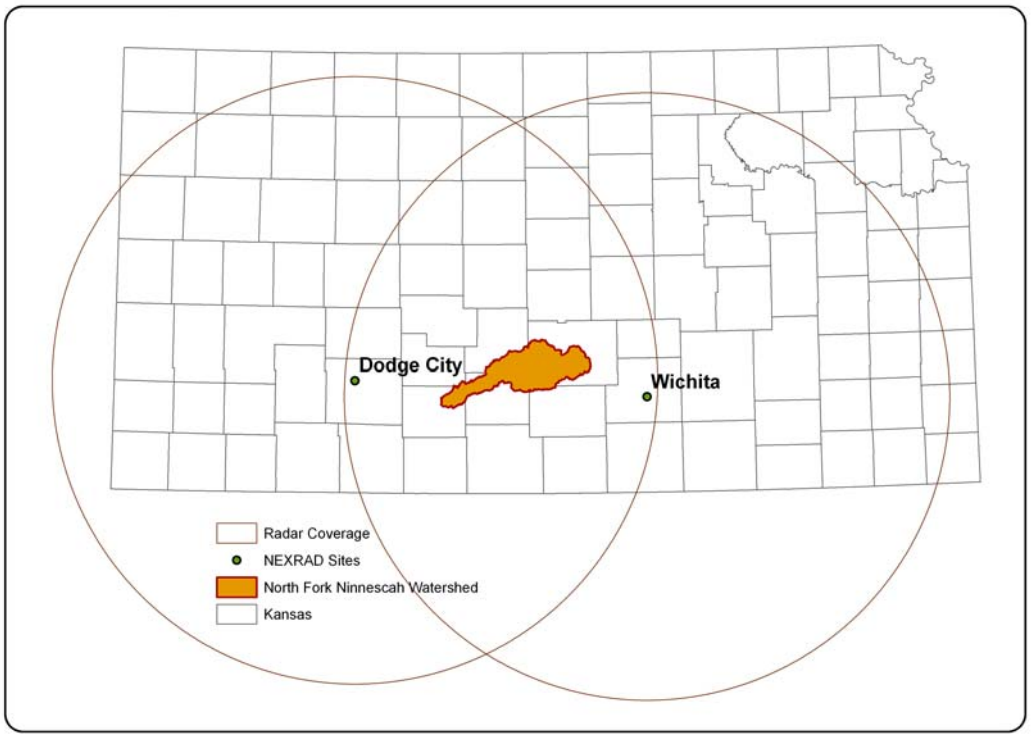

Figure 3.5 North Fork Ninnescah Watershed covered by two nearest radars with 143-nautical mile (230-km) radius coverage area

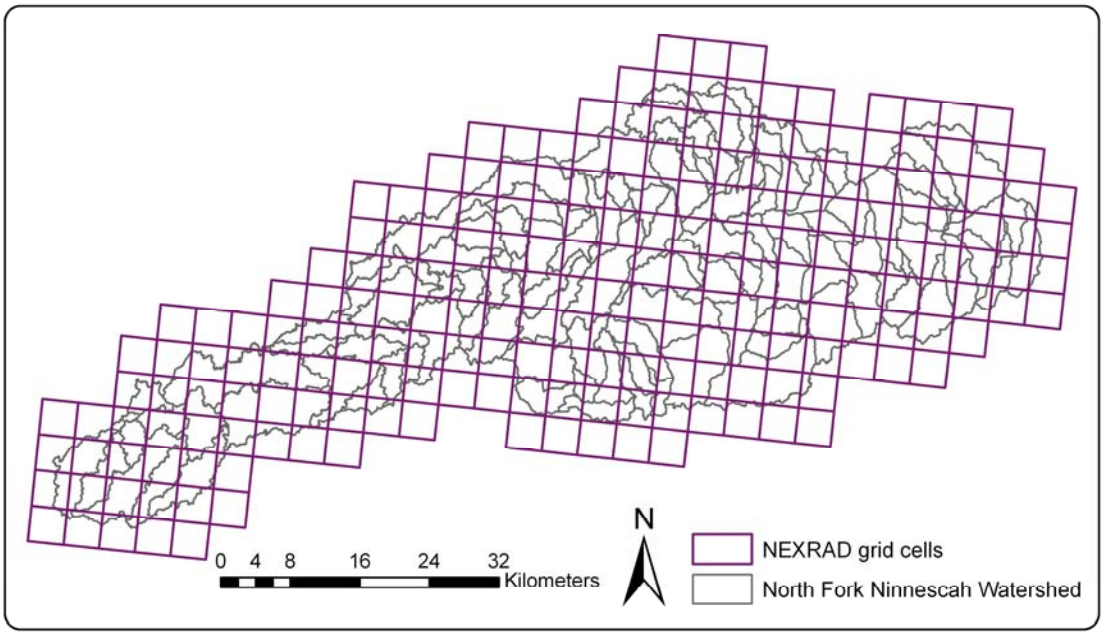

Figure 3.6 NEXRAD grid coverage on North Fork Ninnescah Watershed

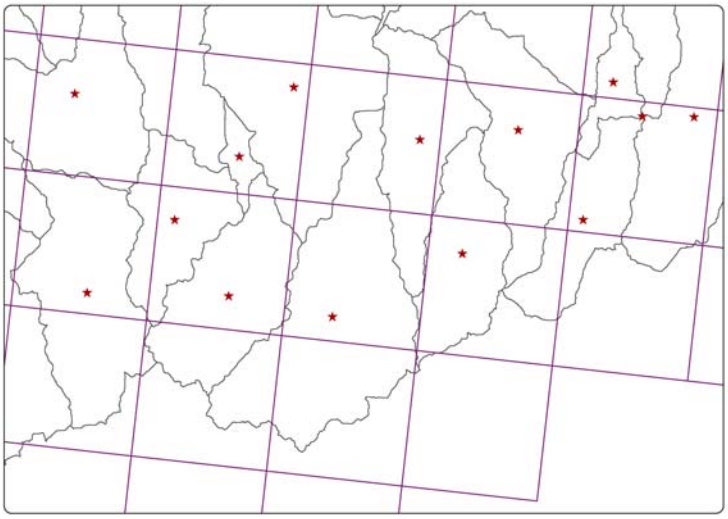

Figure 3.7 Example enlargement of a portion of the watershed showing subwatersheds and NEXRAD grid overlay

3.5 Management data

3.5.1 Terraces

Terraces are earthen embankments constructed across the field slope to reduce the speed of runoff and allow soil particles to settle down. Terraced land data (fig. 3.8) were obtained from a Cheney Lake Watershed, Inc. database, which included all terraces installed in the watershed using a cost-share fund program as well as from supplemental ground surveys (Devlin et al., 2008). A total of 1369 conservation practices were implemented from 1994 through 2006, and terrace installation was top ranked among the conservation practices (Devlin et al., 2008). Before 1994, there were approximately 17806.16 ha (44,000 ac) or 12.7% of cropland with terraces and from 1994 to 2006 new terraces were installed on 7742.44 ha (19,132 ac) in the watershed (Devlin et al., 2008). Majority of these terraces were installed in the eastern part of the watershed due to the steeper slopes in that region. The simulation of terraced land data for North Fork Ninnescah Watershed in the SWAT model was done by changing the CN_{II} and USLE support practice (P) factor for HRUs that were covered by the terraced lands. The CN_{II} values for terraces with different tillage practices and different soils were obtained from National Engineering Handbook (USDA-SCS, 1972). The P factor 0.2 for terraces was used based on values reported by Wischmeier and Smith (1978).

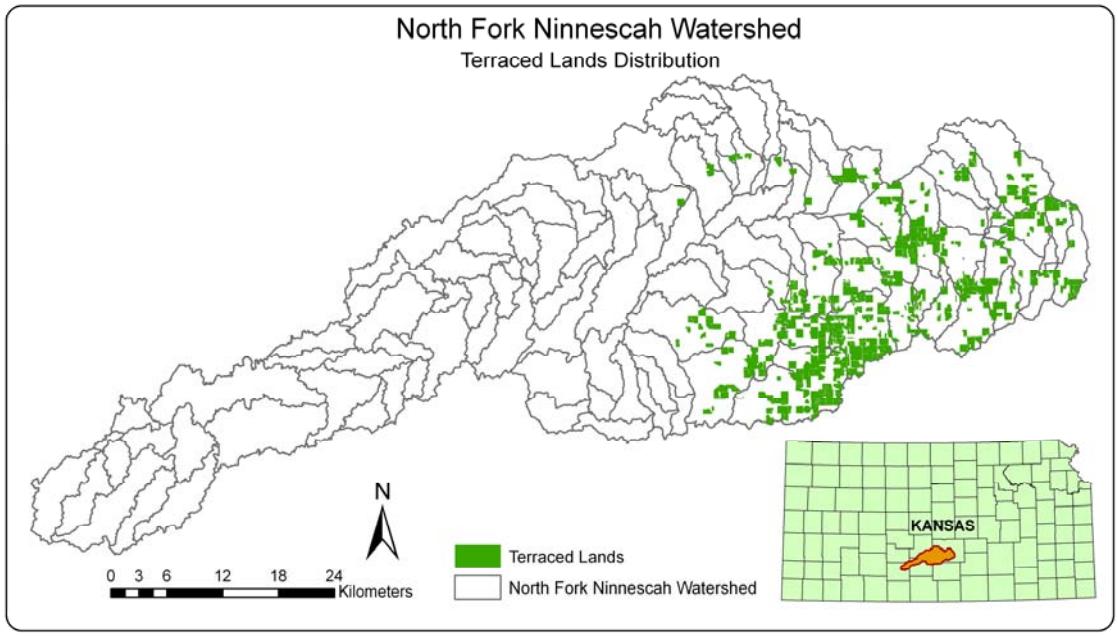

Figure 3.8 Terraced lands distribution in North Fork Ninnescah Watershed

3.5.2 Tillage

Spatial and temporal distribution of tillage data used in the simulation of SWAT was prepared by using multiple data sources. The primary source of this data was Cheney Lake Watershed Inc, a non profit watershed management organization, and the other sources were field surveys and farmer surveys. All the survey data and field data were combined into a single dataset. In order to account for spatial variability within the combined dataset, the watershed was divided into 5 tillage regions based on areas with similar soils, tillage patterns and sub-basin boundaries (fig. 3.9). Overall the tillage distribution in North Fork Ninnescah Watershed was 70% conservation till and 30% no-till (table 3.3). The total distributions of crop percentages in each region were shown in table 3.4.

In order to match the above tillage practices, all winter wheat in the watershed was assumed to be conventional till, and all other crops were no till. In North Fork Ninnesach Watershed, winter wheat was mostly a continuous crop and conventional till (Philip L. Barnes, personal communication, 2009). The modeled tillage practices in the SWAT were 63% of

conventional till and 37% of no-till in the watershed, which were similar to the actual conditions in North Fork Ninnescah Watershed.

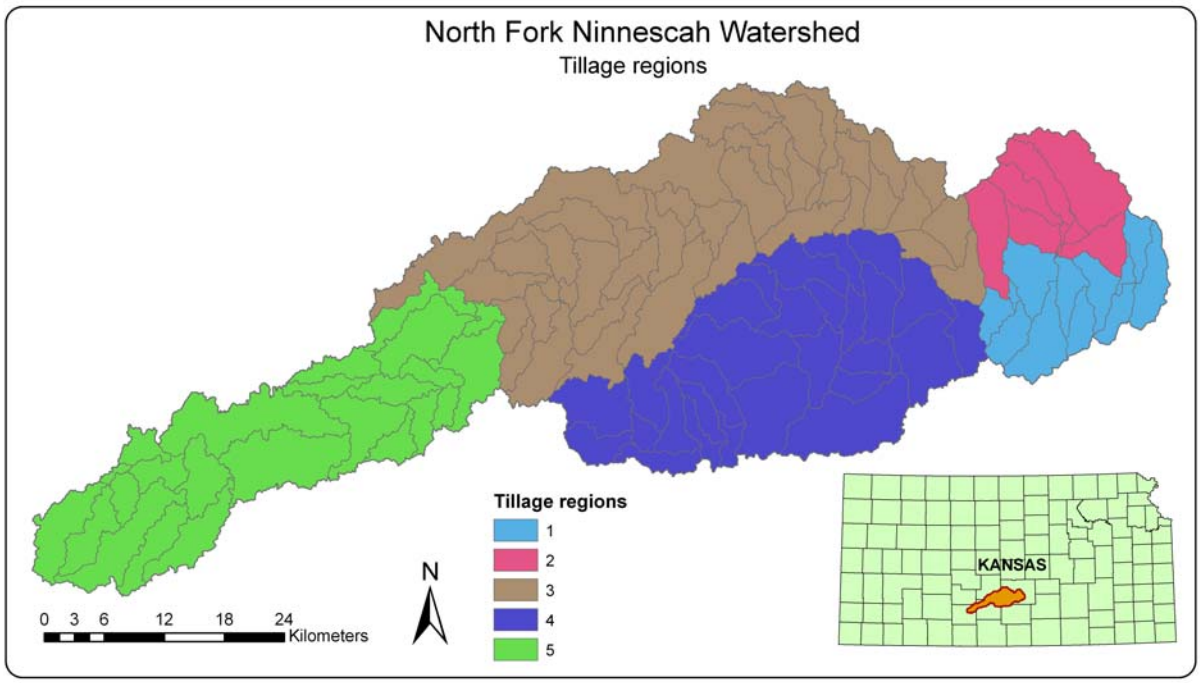

Figure 3.9 Tillage regions in North Fork Ninnescah Watershed

Table 3.3 Distribution of tillage practice in five regions

Tillage Region	Cropland Surveyed		Tillage Practice (%)		Modeled Practice (%)	
	(ha)	(%)	CT	NT	CT	NT
Region 1	12,690	78	70	30	71	29
Region 2	10,420	99	55	45	68	32
Region 3	20,620	46	80	20	67	33
Region 4	27,080	82	80	20	78	22
Region 5	7,880	28	25	75	39	61
Total	78,690	59	70	30	63	37

Table 3.4 Distribution of crop land percentages in five regions

Region	Total area (km^2)	% of cropland					Total % of cropland in region
		WWHT	CORN	SOYB	GRSG	AGRR	
1	180.64	20.98	4.17	3.50	1.25	16.14	46.04
2	169.11	35.68	7.10	6.62	5.34	9.28	64.02
3	835.66	26.21	5.51	3.09	4.91	21.10	60.82
4	642.51	32.97	3.63	2.52	3.56	18.09	60.77
5	572.25	17.98	20.00	6.22	2.63	25.01	71.84
Total area	2400.17	26.33	8.47	3.96	3.75	20.02	62.53

3.6 Model Setup and Calibration

3.6.1 Model Setup

The watershed was classified into two regions based on slope values. The first region had a slope range from 0-3 % and the second region had a slope range from 3-46.1 %. SWAT model classified the watershed into a total of more than 25,000 HRUs, because of detailed NASS landuse, SSURGO soils data and slope classifications. Since SWAT cannot handle too many HRUs, a threshold of 5% for landuse over sub-basin area, threshold of 10% for soils class over landuse area, and threshold of 5% for slope class over soil area was given to reduce the number of HRUs to 2,841. The baseline Base flow Alpha Factor (ALPHA_BF) was calculated from Base flow filter program (see Appendix C for details) recommended by Arnold et al. (1995). The average separated baseflow was between 37-74% of the total annual streamflow for NF Ninnescah above Cheney Reservoir gauging station (Bhuyan, 2001). Terraced land data were input based on year-2006 and tillage management operations data were input based on year-2007 (Parajuli et al., 2009).

A series of six SWAT simulations for the North Fork Ninnescah Watershed were conducted with calibrating the SWAT model using NEXRAD P3 data and NCDC Precipitation gauge (PG) data from 1 January 2002 to 31 December 2008. Precipitation data from the 1 January 1996 to 31 December 2001 period were used as a warm-up period in each case, but

NEXRAD data were used for the NEXRAD model runs, and NCDC data were used for the NCDC runs. The P3-calibrated model was validated using PG data for the same simulation period (2002-2008), and vice versa. Both P3 and PG calibrated models were also validated for the 1 January 1996 to 31 December 2001 period. For the 1996 to 2001 validation runs, the 1 January 2003 to 31 December 2008 period was used a warm-up period. Again, data source (NEXRAD or NCDC) was kept consistent between validation and warm-up periods. NEXRAD precipitation data were not available for the period before 1996, therefore we selected a hydrologic period (2003-2008) with reasonably similar characteristics. In particular, the average annual streamflow at USGS gauging station (07144780) for 2007 to 2008 period most closely matched the average annual streamflow pattern of 1994 to 1995 period: years 1994 and 2007 were wet years followed by a moderate annual flow in 1995 and 2008, respectively.

3.6.2 Model Calibration

Calibration of the SWAT model was done to represent the hydrologic processes in the study area more realistically. The SWAT model was calibrated with measured streamflow from the USGS gauging station at North Fork Ninnescah above Cheney Reservoir (07144780). Calibration procedure used in this study is shown in figure 3.10. Runoff events in the streamflow record were calibrated first, and then the base flow from the watershed was calibrated. Flow parameter values were adjusted only within the ranges shown in table 3.5. The baseline flow parameters used in the calibration process were selected based on the preliminary results of the SWAT model. Flow parameters were either increased or decreased from their respective baseline values depending on the nature of the flow hydrograph and modeling efficiency. Fine-tuning for each parameter was done up to their highest decimal point level to get maximum Nash-Sutcliffe Efficiency (E_{NS}) between observed and simulated streamflow. After maximum E_{NS} was attained, each calibrated parameter value was again increased and decreased from the calibrated value to assure no further improvements in modeling efficiency were possible. Parameters Sol_K and REVAPMN did not show any effect on flow prediction and model efficiency in this watershed.

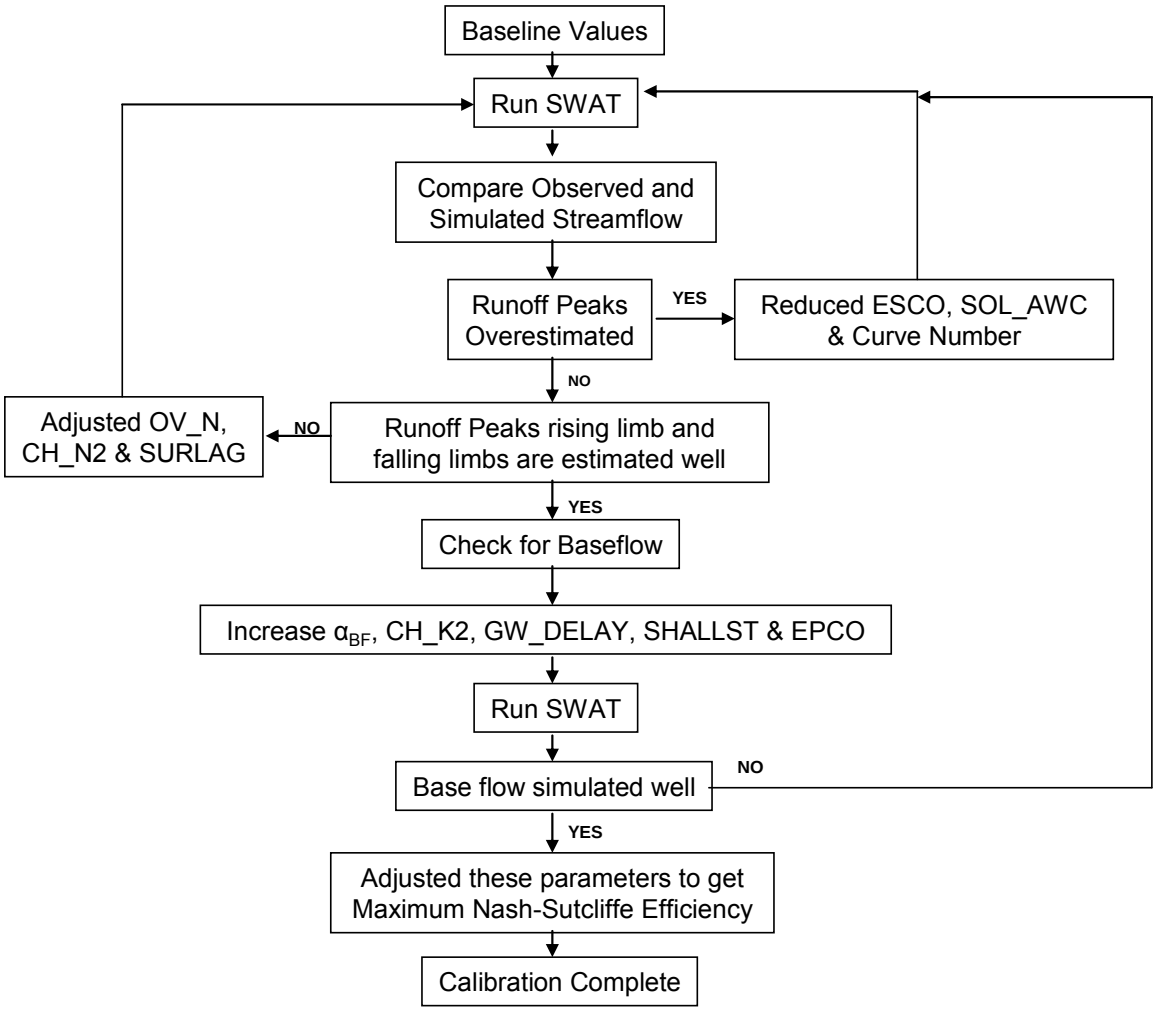

Figure 3.10 Calibration procedure used in this study

Table 3.5 SWAT Model Calibration Parameters

Variable	Description	Initial value	Baseline value	Model range	Unit
CN	Curve Number	.mgt file	.mgt file	±20%	-
ESCO	Soil Evaporation Compensation Factor	0.95	0.01	0 to 1	-
ALPHA_BF	Base Flow Recession Constant	0.048	0.024	0 to 1	Days
SOL_AWC	Soil Available Water Content	.sol file	.sol file	0 to 1	mm/mm
EPCO	Plant Uptake Compensation Factor	1.0	1.0	0 to 1	-
GW_Revap	Groundwater Revaporation Coefficient	0.02	0.02	0.02 to 0.2	-
GW_DELAY	Groundwater Delay time	31	91	0 to 500	Days
Ch_K2	Channel Hydraulic Conductivity	0	0	-0.01 to 500	mm/hr
Ch_N2	Channel Roughness Coefficient	0.014	0.014	-0.01 to 0.3	-
SURLAG	Surface Runoff Lag Coefficient	4	4	1 to 24	-
SMTMP	Snow Melt Base Temperature	0	0	-5 to 5	°C
Sol_K	Saturated Hydraulic Conductivity	.sol file	.sol file	0 to 2000	mm/hr
REVAPMN	Threshold depth of water in the shallow aquifer for revaporation to occur	0	0	0 to 500	mm
SHALLST	Initial Depth of Shallow Aquifer	0.5	990	0 to 1000	mm

3.7 Statistical Analysis

SWAT model responses for streamflow were evaluated based on measured flow data at North Fork Ninnescah Cheney Reservoir (07144780). Statistical parameters used to evaluate the relationship between measured and simulated streamflow are Estimation Bias, Nash-Sutcliffe efficiency (E_{NS}), ratio of Root Mean Square Error (RMSE) to Standard Deviation (RSR), and

PBIAS. The performance ratings for the above statistics recommended by Moriasi et al. (2007) were listed in table 3.6.

3.7.1 Nash Sutcliffe Efficiency

Nash-Sutcliffe modeling efficiency (eq. 3.6) has been widely used to evaluate the performance of hydrologic models (Wilcox et al., 1990). Nash-Sutcliffe modeling efficiency indicates the consistency of predicted flow with measured flow. The value of Nash-Sutcliffe efficiency range from 1 to -∞, where a value of one indicates perfect model fit and a value of zero indicates that observed streamflow is better than the simulated streamflow (Nash and Sutcliffe, 1970). Nash-Sutcliffe Coefficient of Efficiency using observed median is used for this analysis based on the suggestion by Coffey et al. (2004) that the median is a better estimator of central tendency for log-normal data.

$$E_{NS} = 1 - \frac{\Sigma_{i=1}^{n}(O_i - P_i)^2}{\Sigma_{i=1}^{n}(O_i - \overline{O})^2} \tag{3.6}$$

where,

E_{NS}: Nash-Sutcliffe Coefficient of Efficiency using observed mean,

P_i: Predicted daily value (streamflow, m^3/s),

O_i: observed daily value (streamflow, m^3/s),

$\overline{O}$: median of observed daily value (streamflow, m^3/s), and

n: number of observations

3.7.2 RMSE to standard deviation ratio (RSR)

The RMSE to Standard Deviation ratio (RSR) of observed data (eq. 3.7) standardizes RMSE using the standard deviation of the observations. It combines both an error index and the additional information recommended by Legates and McCabe (1999). RSR varies from the optimal value of 0, which indicates zero RMSE or residual variation and therefore perfect model simulation, to a large positive value. The lower RSR, the lower the RMSE and better the model simulation performance (Moriasi et al., 2007).

$$RSR = \frac{\left[\sqrt{\sum_{i=1}^{n}(Y_i^{obs} - Y_i^{sim})^2}\right]}{\left[\sqrt{\sum_{i=1}^{n}(Y_i^{obs} - Y^{mean})^2}\right]} \quad (3.7)$$

where,

RSR = RMSE to standard deviation ratio,

Y_i^{obs} = observed value for event i,

Y_i^{sim} = predicted value for event i,

Y^{mean} = mean of observed values, and

n = number of observations

3.7.3 Percent Bias (PBIAS)

Percent bias (eq. 3.8) measures the average tendency of the simulated data to be larger or smaller than their observed counterparts. The optimal value of PBIAS is 0.0, with low-magnitude values indicating accurate model simulations. Positive values indicate model underestimation bias, and negative values indicate model overestimation bias (Gupta et al., 1999). PBIAS is the deviation of data values being evaluated, expressed as a percentage and is calculated from

$$PBIAS = \left[\frac{\sum_{i=1}^{n}(Y_i^{obs} - Y_i^{sim})\,100}{\sum_{i=1}^{n}Y_i^{obs}}\right] \quad (3.8)$$

where,

PBIAS = percent bias

Y_i^{obs} = observed value for event i,

Y_i^{sim} = predicted value for event i, and

n = number of observations

Table 3.6 Classification of model efficiencies for flow parameters (Moriasi et al., 2007)

Class	E_{NS}	RSR	PBIAS
Very good	1.00 – 0.75	0.00 – 0.50	< ±25
Good	0.75 – 0.65	0.50 – 0.60	±25 - ±30
Satisfactory	0.65 – 0.50	0.60 – 0.70	±30 - ±55
Unsatisfactory	≤ 0.50	> 0.70	> ±55

CHAPTER 4 - Results & Discussions

4.1 Comparing precipitation gauge and weighted average NEXRAD precipitation data

SWAT assigned precipitation gauge stations to subwatersheds based on the distance between precipitation gauge station and the centroid of the subwatershed; precipitation data from the nearest precipitation gauge station to the subwatershed was used in simulating hydrologic processes of the watershed. The North Fork Ninnescah Watershed was divided into 8 regions based on SWAT-assigned precipitation gauge stations to subwatersheds (fig. 4.1).

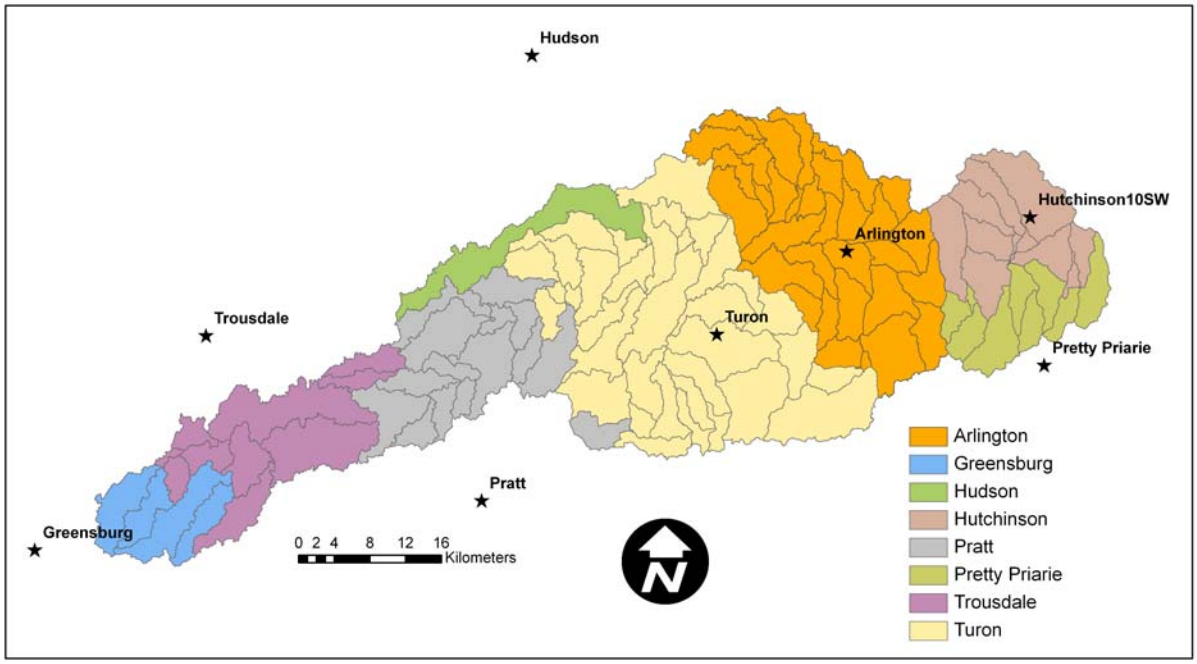

Figure 4.1 Subwatersheds assigned to each precipitation gauge by SWAT based on nearest gauging station

Precipitation data from the ground-based precipitation gauge stations and the corresponding weighted-average NEXRAD data for each subwatershed were compared. NEXRAD data for each subwatershed were calculated by using area-weighted average of all NEXRAD grid cells covering the subwatershed. The statistic used to find the consistency between NEXRAD and precipitation gauge data was estimation efficiency, which is the same as Nash-Sutcliffe efficiency (E_{NS}). The calculated statistics were attached to the watershed polygon layer file to show the spatial variation of E_{NS} throughout the watershed. The areal distribution of

E_{NS} between NEXRAD P3 data and PG data during 1996-2001 period over the North Fork Ninnescah Watershed is shown in figure 4.2.

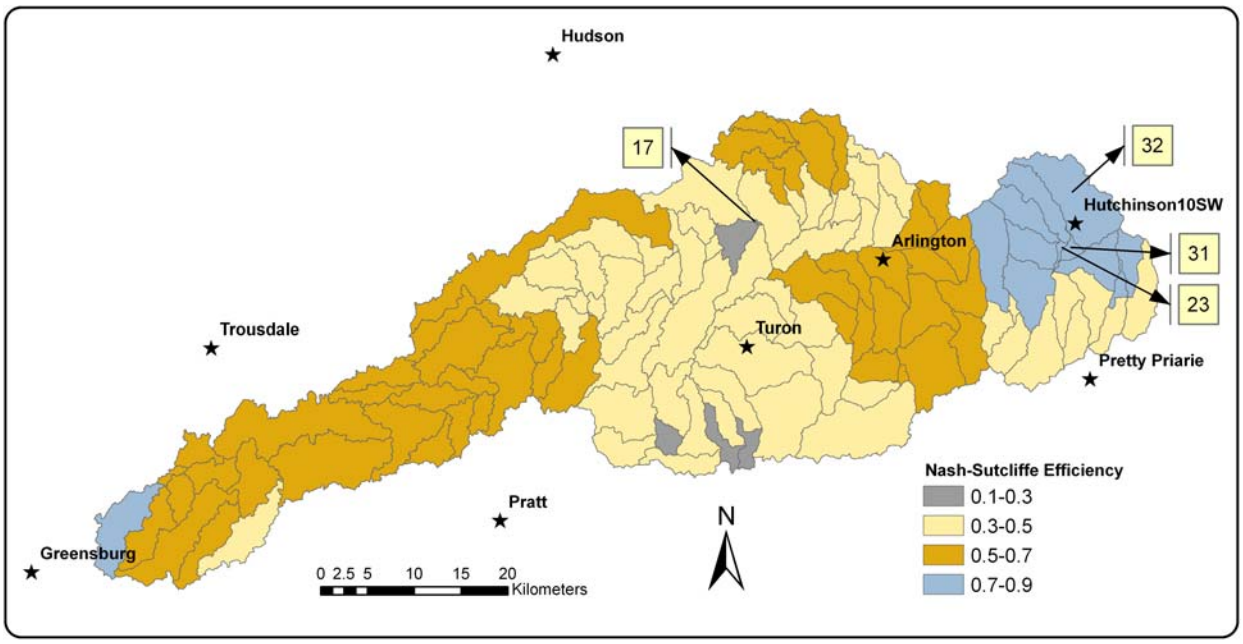

Figure 4.2 Spatial distribution of model estimation efficiency (E_{NS}) between P3 and PG data during 1996-2001

The agreement of raingage data compared to NEXRAD P3 precipitation data for subwatersheds in the Hutchinson10SW region was ranked 'very good' (E_{NS} of 0.75 – 1.00) according to table 3.6. Highest E_{NS} was found between subwatersheds 23, 31, 32 and Hutchinson10SW (0.86), and the lowest E_{NS} was between subwatershed 17 and Turon (0.16). NEXRAD P3 data was in good agreement with stations Greensburg, Trousdale, Hudson, and some subwatersheds covered by Arlington. The least agreement was for stations Turon, Pretty Priarie and Arlington, which did not collect data during the 1996-2001 period. Precipitation data for the 1996 to 2001 period for these stations were calculated by Inverse Distance Weighted method (see Appendix B for details) using nearby stations.

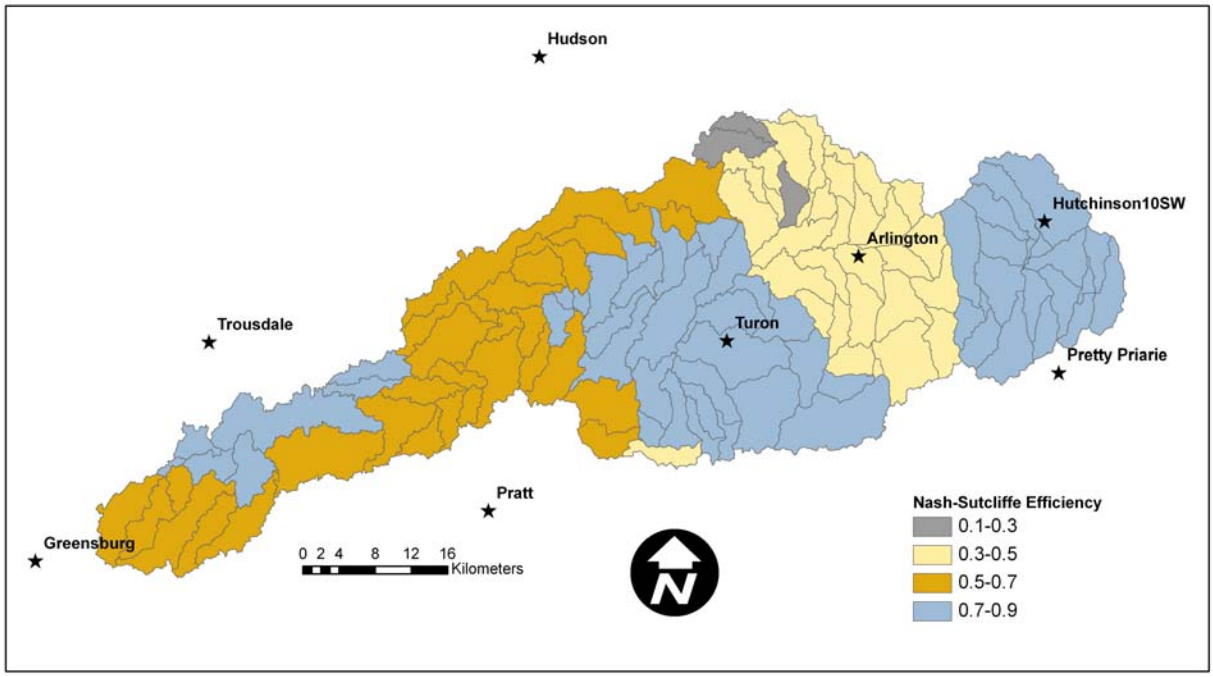

Figure 4.3 Spatial distribution of model estimation efficiency (E_{NS}) between P3 and PG data during 2002-2008

The agreement between P3 data and PG data during 2002-2008 period over the North Fork Ninnescah Watershed is shown in figure 4.3. Overall E_{NS} between precipitation gauge stations and their corresponding P3 data has increased during 2002-2008, and the number of subwatersheds having 'very good' efficiency also increased. In the P3 vs. PG comparison during 1996-2001 period, there were only 12 subwatersheds having 'very good' efficiency, but the number of subwatersheds increased to 58 in the P3 Vs PG comparison during 2002-2008 period. Also, 72% of the subwatersheds had $E_{NS} > 0.50$. Arlington station has the lowest E_{NS} with P3 data during 2002-2008 period, but the efficiency has increased if Arlington-subwatersheds P3 data was compared to either Hutchinson10SW or Turon station. The P3 precipitation data was in very good agreement within Arlington subwatersheds P3 data, the coefficient of determination (r^2) within the subwatersheds weighted average P3 data was above 0.85. The estimation efficiency of 'Pretty Priarie' increased from 'fair' to 'very good' when compared to P3 data during 1996-2001 period. The greatest E_{NS} was found for stations Pretty Priarie (0.88) and Hutchinson (0.84) with P3 data.

The weighted average P3 data has high E_{NS} for the subwatersheds that were close to the precipitation gauge stations except for Arlington. NCDC precipitation gauge stations Turon,

Arlington and Pretty Priarie have started collecting precipitation data from 2002 and with the addition of new precipitation gauge stations the E_{NS} has increased from 2002. P3 data after 2002 has better agreement with PG data compared to P3 data before 2002.

4.2 Model calibration with P3 (2002-2008)

Initial analysis of the observed streamflow at North Fork Ninnescah above Cheney Reservoir showed that the watershed had an average daily streamflow of 3.47 m^3/s during the calibration period. The dry year (2006) had an average daily streamflow of 1.62 m^3/s, indicating substantial base flow contribution to streamflow in this watershed. Similarly, a previous study found average separated baseflow was between 37-74% of the total annual streamflow for North Fork Ninnescah above Cheney Reservoir gauging station (Bhuyan, 2001). The calibration period covered distinct climate periods with dry and wet years. The calibrated parameter values are shown in table 4.1

Table 4.1 SWAT calibrated parameter values for North Fork Ninnescah Watershed using P3 (2002-2008) data.

Parameter	Baseline value	Calibrated value
CN	.mgt file	-15% from baseline
ESCO	0.01	0.25
EPCO	1.0	0.8
ALPHA_BF	0.024	0.62
SOL_AWC	.sol file	-15% from baseline
GW_DELAY	91	235
SMTMP	0	-3
CH_K2	0	15
CH_N2	0.014	0.05
SURLAG	4	2

The SWAT simulated flow and observed flow at the USGS gauging station (07144780) for the calibration period (2002-2008) was compared. The model calibration performance statistics were shown in table 4.2. The statistics used in the comparison were E_{NS}, RSR and PBIAS.

Table 4.2 Statistical performance of SWAT model calibrated using P3 (2002-2008) data

Time period	E_{NS}	RSR	PBIAS (%)
Daily	0.35	0.80	0.94
Monthly	0.52	0.69	1.19
Yearly	0.80	0.40	0.93

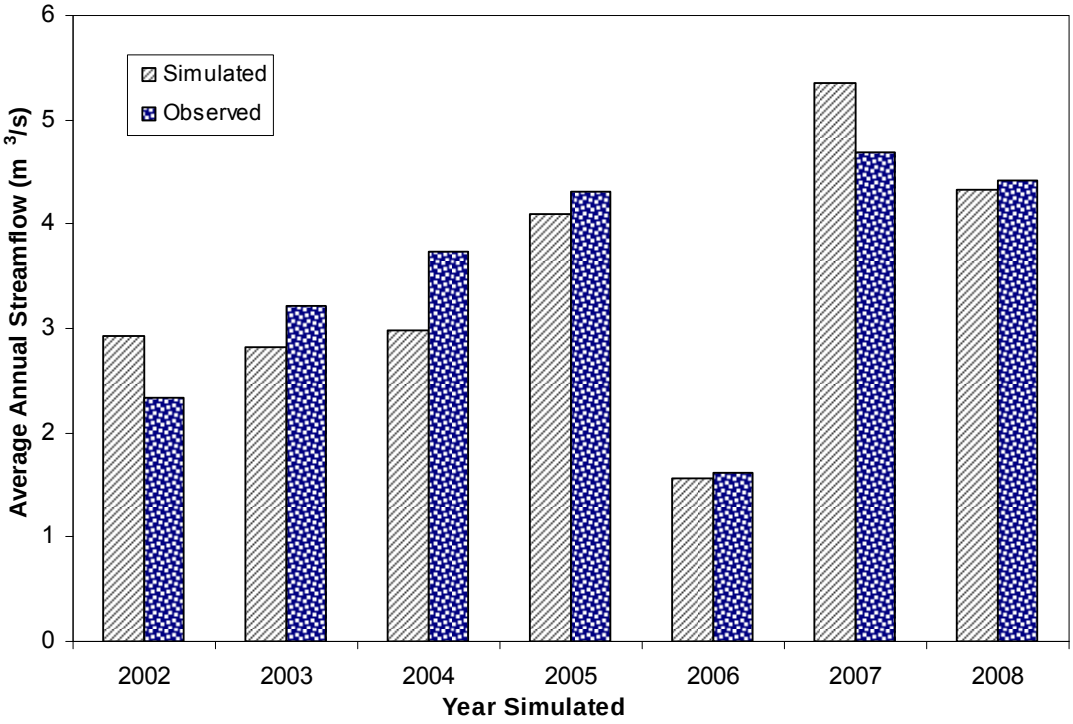

Figure 4.4 Plot of annual average observed and SWAT-simulated streamflow (m^3/s) calibrated using P3 (2002-2008) data.

The guidelines in table 3.6 show that the calibrated SWAT model with P3 data yielded 'very good' E_{NS}, 'very good' RSR and 'excellent' PBIAS values for annual streamflow. The E_{NS} indicated that simulated average annual streamflow was consistent with observed average annual streamflow. The lower RSR value proved that model performance was better at simulating average annual streamflow than shorter temporal scales, and a positive PBIAS value indicated model slightly underestimates the observed streamflow. These statistics showed that SWAT estimated average annual streamflow trends corresponded well to the observed average annual streamflow trends.

The plot of average annual streamflow (fig. 4.4) showed that SWAT overestimated the annual average streamflow during wet years (2002 and 2007) and underestimated the annual

average streamflow the years. Overall, SWAT slightly underestimated the annual average streamflow with P3 data.

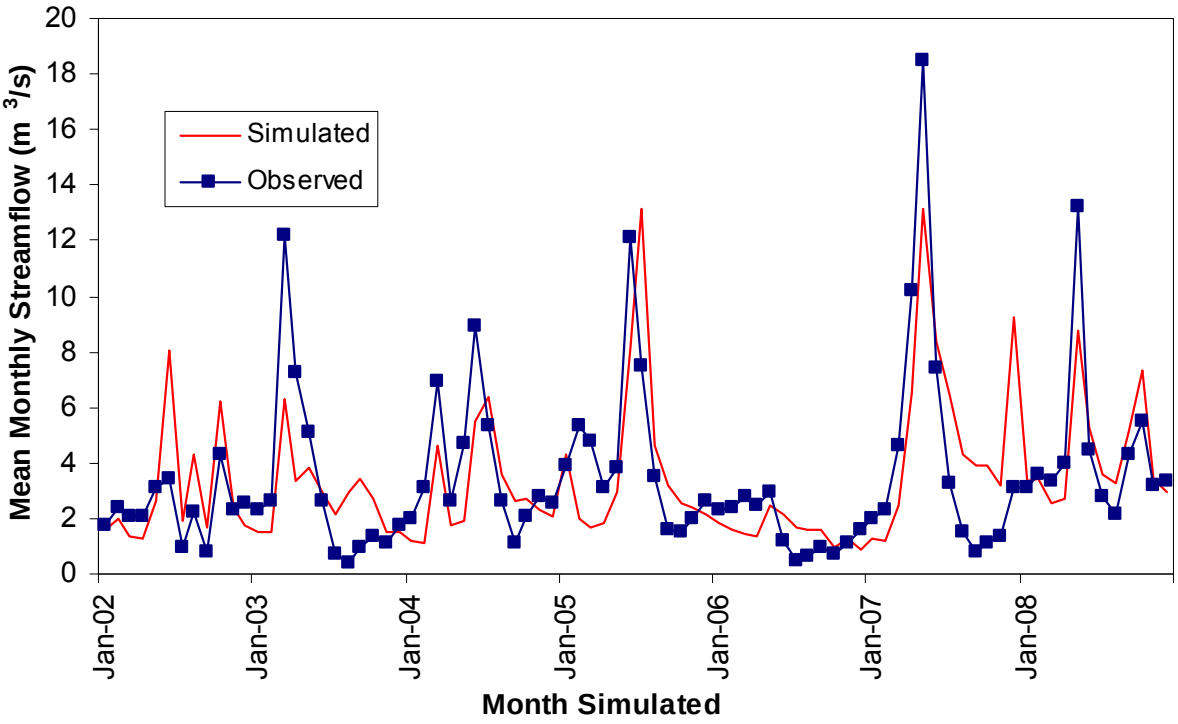

Figure 4.5 Plot of mean monthly observed and SWAT-simulated streamflow (m^3/s) calibrated using P3 (2002-2008) data.

The statistical performance at the monthly time step was E_{NS} of 0.52, RSR of 0.69 and PBIAS of 1.18%. The E_{NS} of simulated and observed mean monthly streamflow value was slightly above the satisfactory range, and model performance at monthly scale decreased compared to annual streamflow efficiencies. The PBIAS of simulated and observed mean monthly streamflow value was in the excellent class, a positive PBIAS value indicated underestimation of simulated mean monthly streamflow compared to observed flow.

The plot of mean monthly streamflow (fig. 4.5) showed that SWAT continuously overestimated the mean monthly streamflow during June-November for all years and generally underestimated the mean monthly streamflow during winter months (December-February). Arnold et al. (2000) observed a similar trend in their study, with underpredicted flow during spring and overestimated flow in fall. They attributed this trend to snow-melt simulation, seasonal variation in evapotranspiration (ET), and soil moisture conditions. In this agricultural study area, ET could have contributed to a similar seasonal trend in SWAT simulated flows. However, monthly flow during December-2007 did not follow the seasonal trend of

underpredicting flow; SWAT has overpredicted the freezing precipitation that occurred in December-2007 with substantial amount of 109 mm of precipitation.

The calibration performance statistics decreased for daily streamflow values compared to monthly and annual values. The E_{NS} for daily streamflow was 0.35, which suggests a fair consistency between observed and simulated daily streamflow. RSR for daily streamflow was 0.89, indicating poor model performance at daily simulation. Overall, SWAT model underestimated the daily streamflow values indicated by a positive PBIAS value of 0.94%. The simulated daily streamflow mostly follows the observed streamflow except in some situations where the streamflow was either overestimated or underestimated (fig. 4.6).

For some rising limbs in simulated surface runoff events (hydrographs) did not match the observed streamflow; the rising limbs were simulated before the observed event, but the falling limbs followed the streamflow well. Snow storms in January-2005 and December-2007 were completely overestimated by SWAT-P3 simulation. The simulated runoff volumes of snow storms were much higher before adjusting snow melt temperature (SMTMP) to -3 °C. The median of simulated flow was 2.37 m^3/s and median of observed was 2.30 m^3/s for the calibration period, indicating very good estimation of base flow from the watershed. The calibrated SWAT model yielded some unusual streamflow results for some rainfall events, for which flow was overestimated by a factor of 3 or more, these overestimated runoff events were among the top 10 largest events. The overestimation of some runoff events by SWAT decreased the overall modeling efficiency at daily scale. Model efficiency was tested again after removing the 5 peak events both in observed and simulated streamflow, the daily E_{NS} increased to 0.61 from 0.35, monthly E_{NS} increased to 0.58 from 0.52, and yearly E_{NS} remained the same.

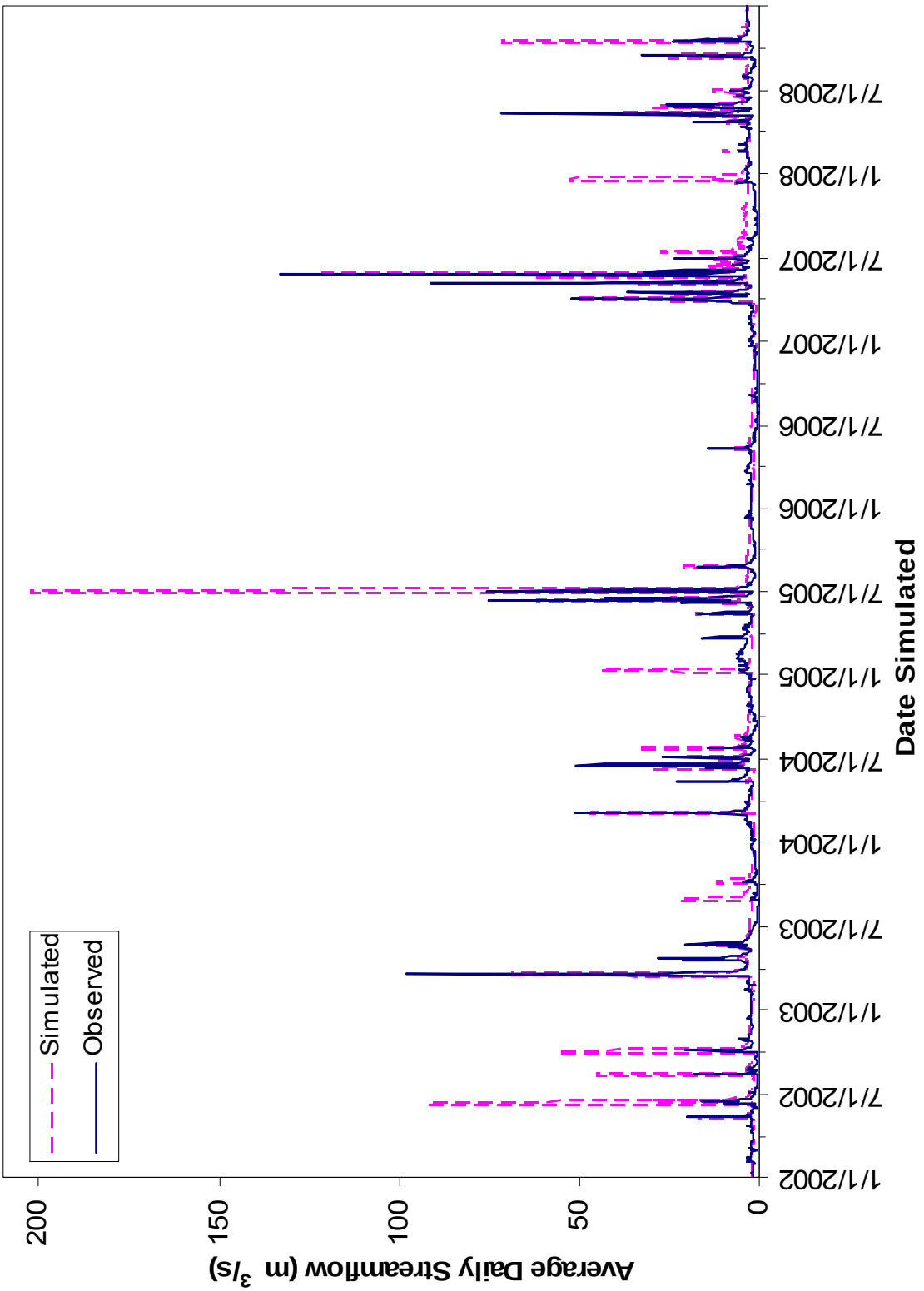

Figure 4.6 Plot of average daily observed and SWAT-simulated streamflow (m^3/s) calibrated using NEXRAD P3 (2002-2008) data.

4.2.1 Validation of P3 (2002-08) with PG (2002-08)

The SWAT model was validated with PG data to check performance of calibrated model with PG data. Model validation involves running a model using input parameters measured or determined during the calibration process (Moriasi et al., 2007), to check the model performance. The SWAT model was run with PG data using the calibrated parameters and remaining parameters were kept constant as used in calibrated SWAT model. SWAT-PG simulation performance statistics were shown in table 4.3.

Table 4.3 Statistical performance of SWAT model validation using PG (2002-2008) data based on P3 (2002-2008) calibration parameters.

Time period	E_{NS}	RSR	PBIAS (%)
Daily	0.27	0.85	-7.95
Monthly	0.53	0.68	-7.65
Yearly	-0.01	0.93	-7.97

SWAT model validation statistics with precipitation gauge data from 2002-2008 period at yearly time step were E_{NS} of -0.01, RSR of 0.93 and PBIAS of -7.97%. A negative E_{NS} indicated the model was unsatisfactory and negative PBIAS value indicated the model overestimated the yearly flow. SWAT-PG simulation estimated yearly flow 'very well' with slight underestimations and overestimations compared to USGS observed streamflow, except in year 2007, annual flow in 2007 was overestimated (fig. 4.7). The observed average annual flow in 2007 was 4.69 m^3/s whereas the observed flow was 7.35 m^3/s, annual flow in 2007 was overestimated by 56.7%. Modeling efficiency was calculated again after removing the 2007 annual flow, E_{NS} increased to 0.83 from -0.01. The overestimation of annual flow in 2007 by SWAT has decreased the overall modeling efficiency.

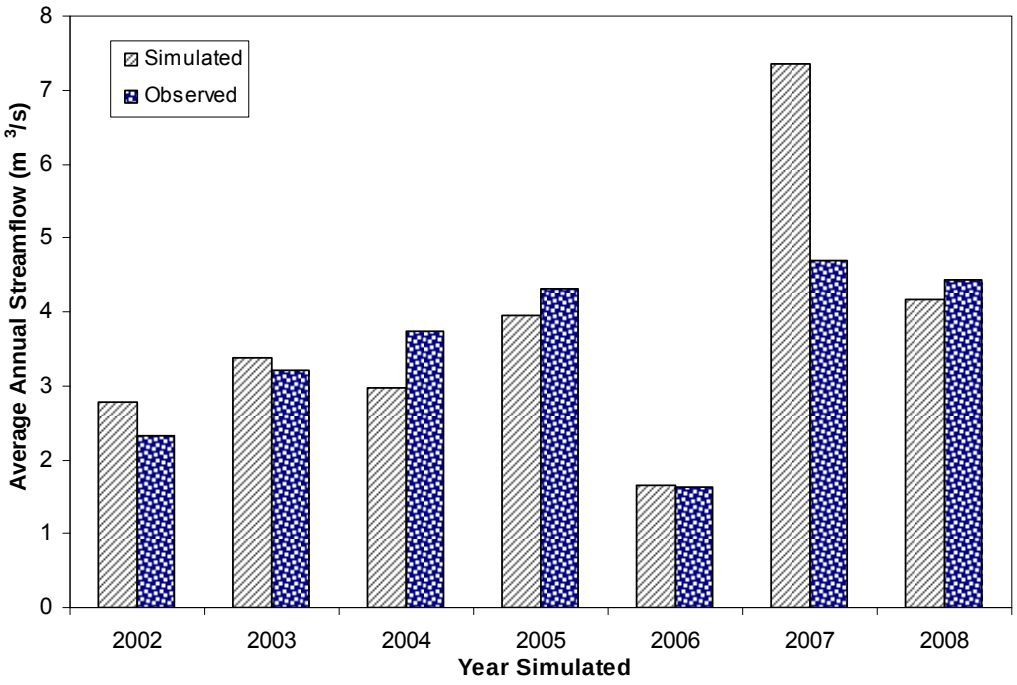

Figure 4.7 Plot of average annual observed and SWAT-simulated streamflow (m^3/s) for SWAT-PG simulation

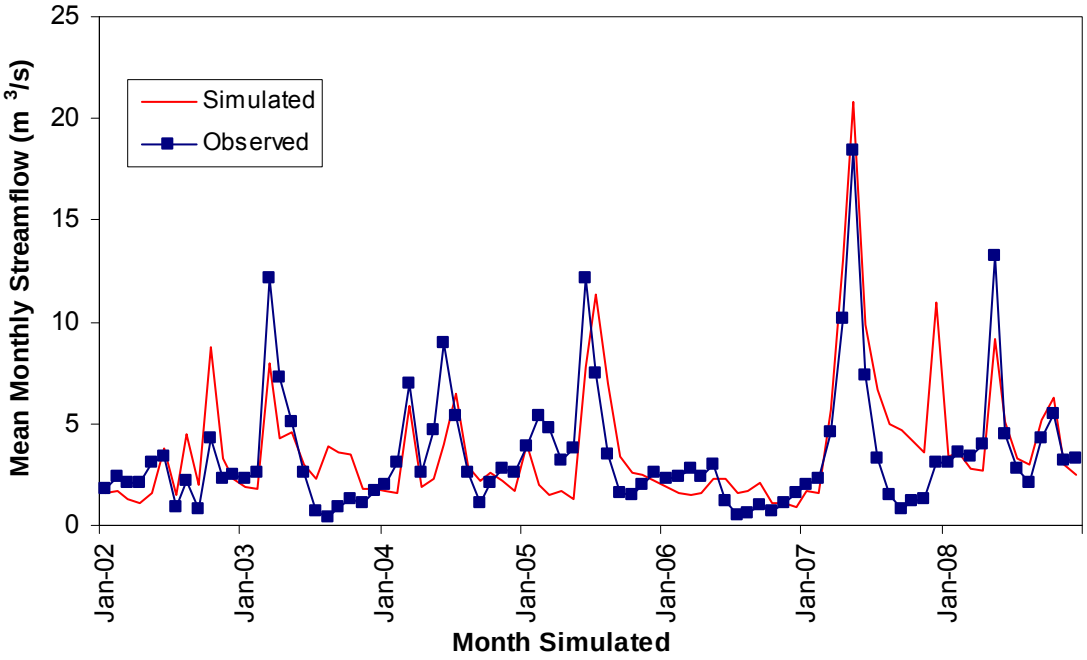

Figure 4.8 Plot of mean monthly observed and simulated streamflow (m^3/s) for SWAT-PG simulation

SWAT-PG simulation performance at monthly time step showed that efficiency of model was in satisfactory range with E_{NS} of 0.53 and RSR of 0.68. The monthly E_{NS} was high compared to annual E_{NS}, but the PBIAS value remained same as -7.65%, negative PBIAS value indicated the monthly flow was overestimated. SWAT-PG simulation followed the seasonal trend discussed in section 4.2, overestimating the monthly streamflow during June-November and underestimated the flow during winter months (November-February). The seasonal trend was not observed during December-2007 (fig. 4.8), mean monthly was overestimated, a similar overestimation was observed in December-2007 P3 data.

The SWAT model validation statistics with precipitation gauge data at daily time step were with E_{NS} of 0.27 and RSR of 0.85. The E_{NS} for daily streamflow of 0.27 suggesting a fair consistency between observed and simulated streamflow, and RSR of 0.87 indicated poor model performance at daily simulation. SWAT model overestimated the daily streamflow indicated by a negative PBIAS value of -7.95%. The simulated daily streamflow mostly matched the observed streamflow, except for some runoff events with overestimations and underestimations (fig. 4.9). SWAT model overestimated some runoff events by a factor of 3 or more especially during fall months (July and October), the high-intensity and short-duration rainfall events over the precipitation gauge station might have caused the overestimation of runoff events.

The overestimation of runoff events were observed with P3 data too, but the amount of runoff estimated with PG data was high compared to P3 data. SWAT overestimated some runoff events with both P3 and PG data, one or more small rainfall events followed by a big rainfall event during the overestimated runoff events might have filled up all the soil pores and caused more runoff than observed flow.

The median of streamflow indicates the baseflow of the watershed and median of observed streamflow during 2002-2008 period was 2.30 m^3/s, whereas the median of simulated streamflow was 2.36 m^3/s. The baseflow was simulated very well with precipitation gauge data by SWAT.

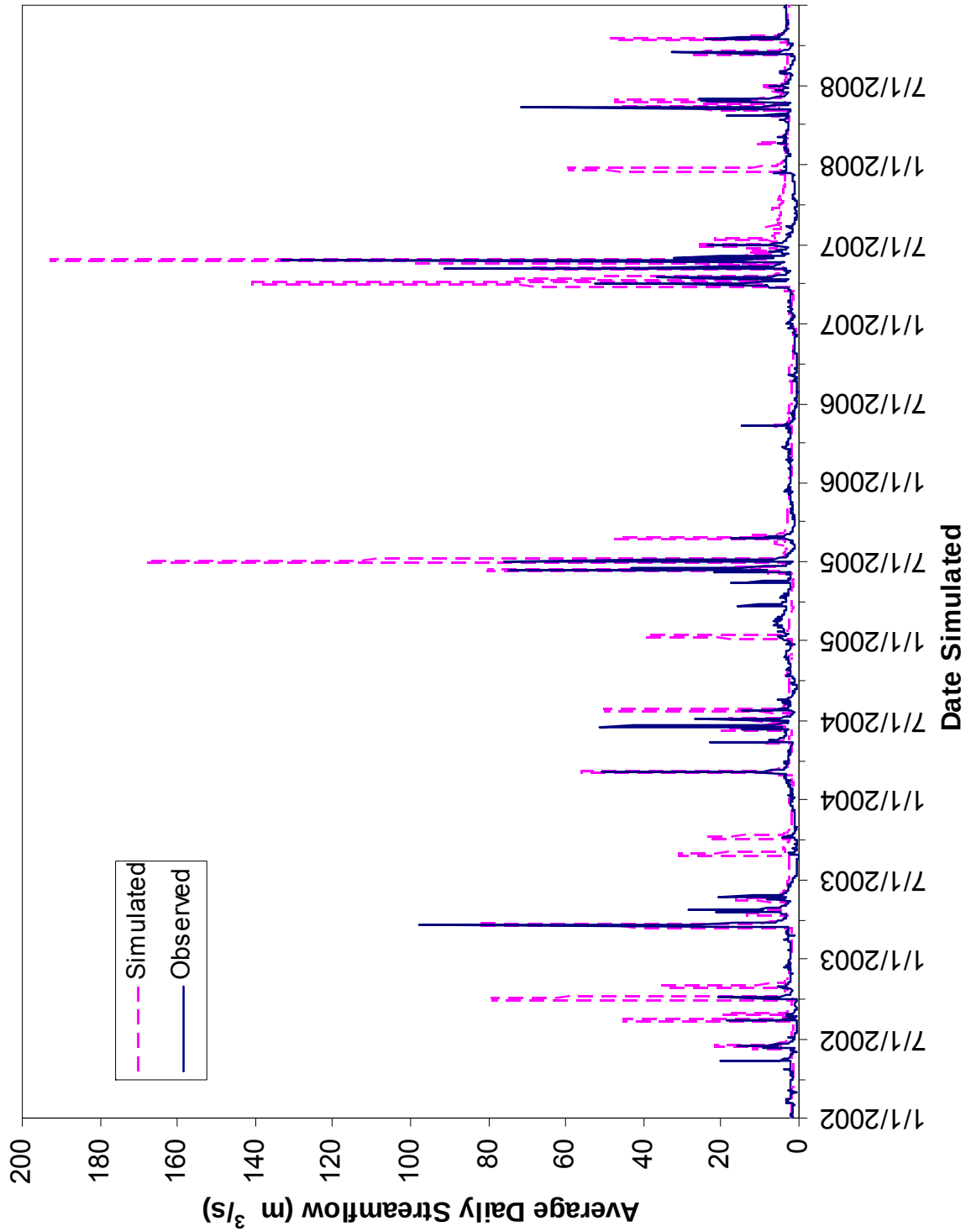

Figure 4.9 Plot of average daily observed and simulated streamflow (m^3/s) for SWAT-PG simulation

4.2.2 Validation P3 (2002-08) with P3 (1996-2001)

The SWAT model was validated with P3 data from 1996 - 2001, using the same calibrated parameter values to check the accuracy of model. SWAT model was run with P3 data using calibrated parameters. SWAT performance statistics during the validation period were presented in table 4.4.

Table 4.4 Statistical performance of SWAT model validation using P3 (1996-2001) data based on P3 (2002-2008) calibration parameters.

Time period	E_{NS}	RSR	PBIAS (%)
Daily	-0.03	1.01	1.78
Monthly	0.19	0.89	2.05
Yearly	-0.80	1.22	1.80

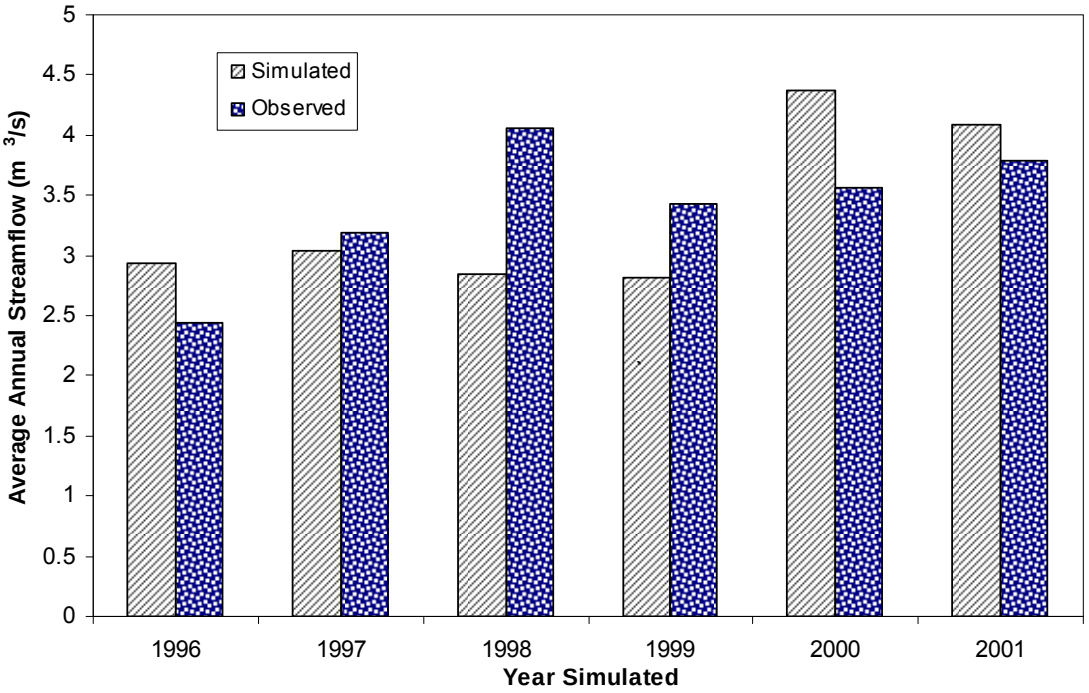

Figure 4.10 Average annual observed and SWAT-simulated streamflow (m^3/s) for validation using P3 (1996-2001) data based on P3 (2002-2008) calibration parameters.

The statistics for SWAT-P3 simulation showed that E_{NS} of -0.80 and RSR of 1.22 at yearly time step were unsatisfactory. A positive PBIAS value of 1.80% indicated, model underestimated the flow using P3 data. SWAT underestimated the streamflow in 1998, 1999 and overestimated the streamflow in 1996, 2000 (fig. 4.10). SWAT underestimated the streamflow in

1998 by 42% and overestimated the streamflow in 2000 by 18%. Overall, SWAT model slightly underestimated the streamflow with P3 data from 1996-2001.

The statistical performance at monthly time step for SWAT-P3 simulation was E_{NS} of 0.19, RSR of 0.89 and PBIAS of 2.05%. The model efficiency at monthly time step increased compared to yearly time step and RSR indicated the model was in unsatisfactory class. A PBIAS value of 2.05% indicated the model underestimated the mean monthly streamflow. SWAT model followed the seasonal pattern of overestimating the flow during June-November and underestimated the flow during December-April for all the years (fig. 4.11). The SWAT-P3 simulation underestimated the streamflow during winter months, but this underestimation was extreme in particular months and the streamflow was listed in table 4.5 below. The underestimation of simulated streamflow during the specified months was from 103% to 320% with observed streamflow.

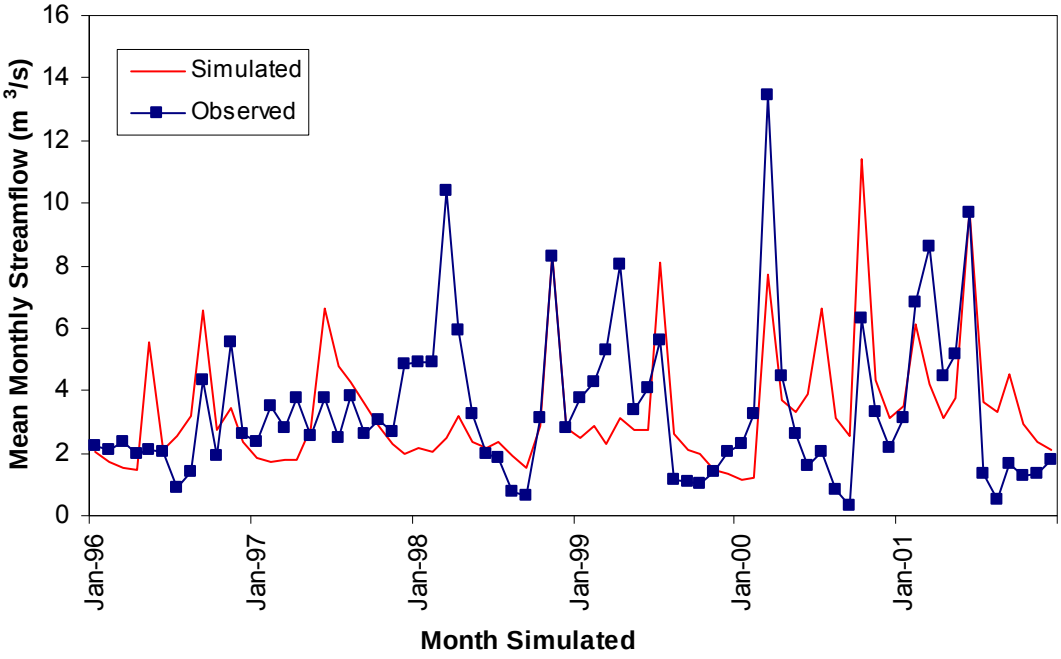

Figure 4.11 Mean monthly observed and SWAT-simulated streamflow (m^3/s) for validation using P3 (1996-2001) data based on P3 (2002-2008) calibration parameters.

Table 4.5 Observed and simulated mean monthly streamflow (m^3/s) during overestimated months

Month	Observed mean monthly flow (m^3/s)	Simulated mean monthly flow (m^3/s)
March-1998	10.40	2.48
April-1999	8.00	3.10
March-2000	13.44	7.69
March-2001	8.60	4.22

The model performance at daily time step was unsatisfactory with E_{NS} of -0.03 and RSR of 1.01 with Stage III data. The positive PBIAS value was 1.78% indicated that model underestimated the flow. SWAT-P3 simulation estimated runoff events well throughout the simulation period, except for some runoff events during May-October months throughout the simulation period (fig. 4.12). For some runoff events, SWAT overestimated runoff events by a factor of 3 or more and for a one rainfall event on 25 September 2000, the average daily observed streamflow was 38.22 m^3/s and the SWAT simulated streamflow was 173.5 m^3/s, streamflow was overestimated by 353%. The statistical performance of SWAT-P3 simulation at daily time step was unsatisfactory with a negative E_{NS} of -0.03 and RSR of 1.01. A positive PBIAS value of 1.78% indicated the SWAT-P3 simulation underestimated the streamflow, even though there were some extremely overestimated runoff events during the simulation period, overall the SWAT model slightly underestimated the streamflow. SWAT-P3 simulation has several overestimated and underestimated runoff events, only a small number of runoff events were simulated well. For example, a rainfall event on 5/10/1996 for precipitation gauge station Turon was 7.50 mm and the weighted average P3 data for subwatersheds around the Turon station was between 11.21 -141.21 mm. SWAT overestimated the simulated flow on 5/10/1996 which was 74.42 m^3/s and whereas the observed flow was 1.70 m^3/s. Precipitation data for the Turon station before 2002 was calculated by using IDW method from 3 nearest gauging stations. The median of observed streamflow which indicates the base flow of the watershed was 2.40

m^3/s and the median of simulated streamflow was 2.48 m^3/s, the model simulated base flow well with P3.

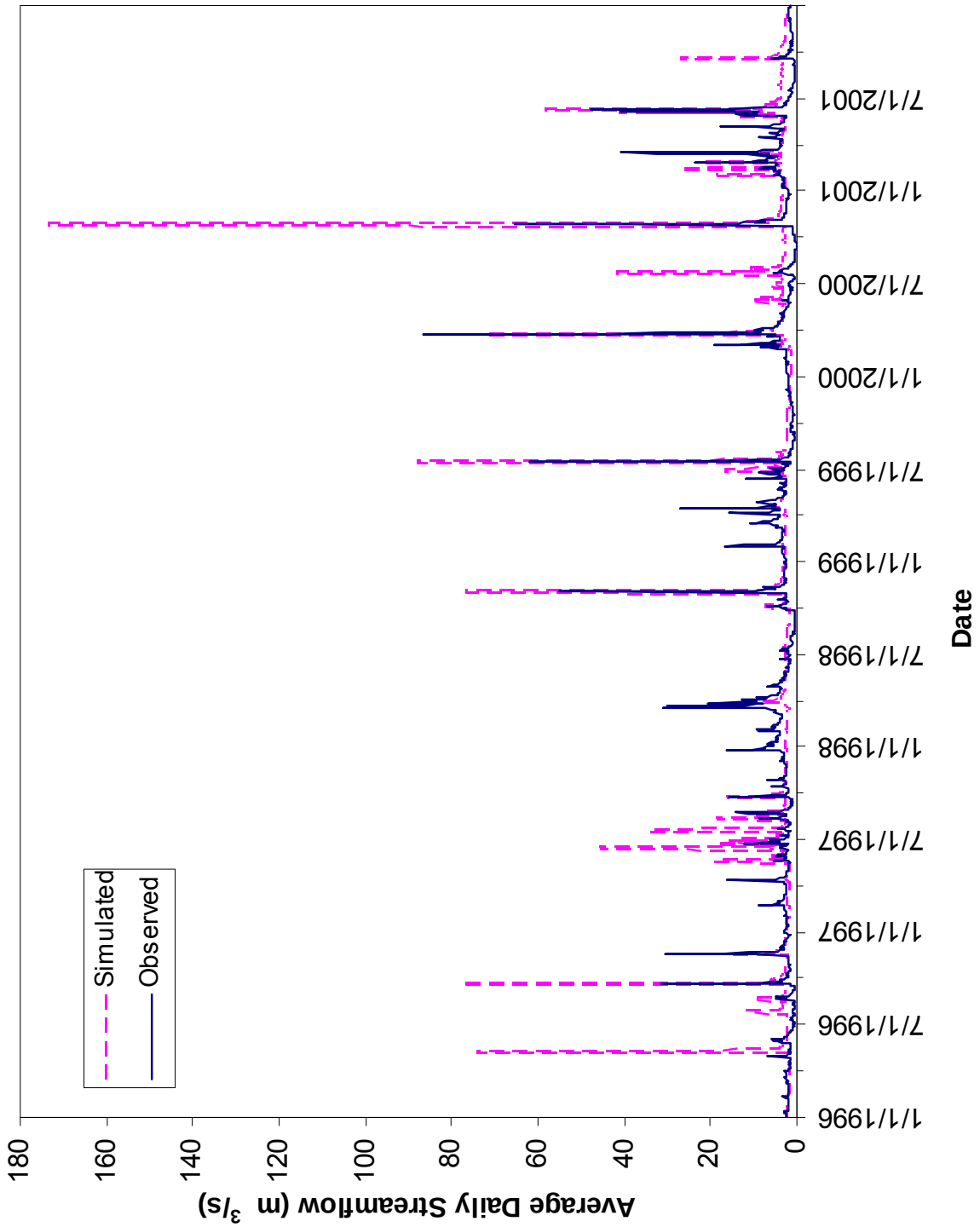

Figure 4.12 Average daily observed and SWAT-simulated flow (m^3/s) for validation using P3 (1996-2001) data based on P3 (2002-2008) calibration parameters.

4.3 Model calibration with precipitation gauge (PG) (2002-2008)

The SWAT model was again calibrated with precipitation gauge data from 1 January 2002 to 31 December 2008 period. The calibrated SWAT model was validated with P3 data to evaluate the performance of P3 data with a PG calibrated model. The calibrated model parameters were listed in the table 4.6.

Table 4.6 SWAT calibrated parameter values for North Fork Ninnescah Watershed using PG (2002-2008) data.

Parameter	Baseline value	Calibrated value
CN	.mgt file	-15% from baseline
ESCO	0.01	0.10
EPCO	1.0	0.95
ALPHA_BF	0.024	0.62
SOL_AWC	.sol file	-15% from baseline
GW_DELAY	91	380
SMTMP	0	-3
CH_K2	0	15
CH_N2	0.014	0.05
SURLAG	4	2

The SWAT simulated streamflow and observed streamflow at the USGS gauging station (07144780) for the calibration period (2002-2008) was compared. The model calibration performance statistics were shown in table 4.7. The statistics used in the comparison were E_{NS}, RSR and PBIAS.

Table 4.7 Statistical performance of SWAT model calibrated using PG (2002-2008) data.

Time period	E_{NS}	RSR	PBIAS (%)
Daily	0.40	0.77	1.47
Monthly	0.60	0.62	1.72
Yearly	0.43	0.69	1.45

The statistical performance of calibrated SWAT model with precipitation gauge data at yearly time step were E_{NS} of 0.43, RSR of 0.69 and PBIAS of 1.45%. A positive PBIAS value represents slight underestimation of the overall average annual streamflow, but the figure 4.13 shows that flow during 2007 was overestimated which has compensated the underestimations of flow in other years. SWAT-PG simulation performance at monthly time step showed that efficiency of the model was in satisfactory range with E_{NS} of 0.60 and RSR of 0.62. The monthly E_{NS} was high compared to annual and daily E_{NS}, and the PBIAS value was 1.72% with slight overestimation of streamflow. SWAT-PG simulation followed the seasonal trend discussed in section 4.2, overestimating the monthly streamflow during June-November and underestimated the streamflow during winter months (November-February). The seasonal trend was not observed during the year 2004; streamflow was underestimated throughout the year in 2004 (fig. 4.14). SWAT simulated monthly streamflow from January-2007 to June-2007 was estimated very well with observed streamflow.

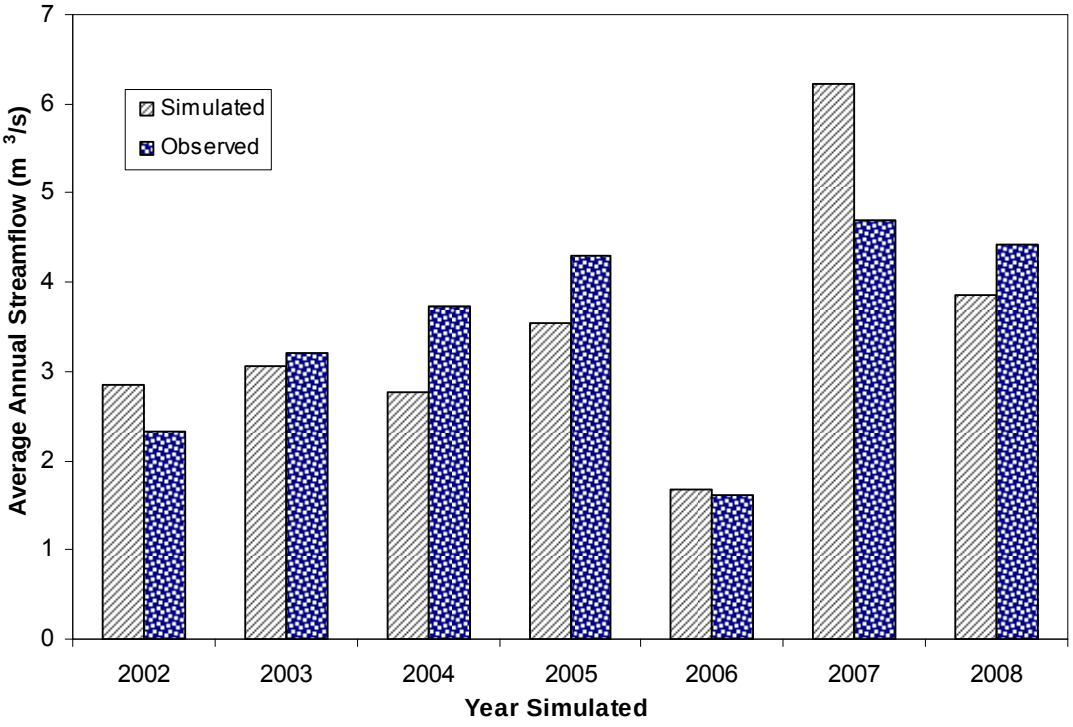

Figure 4.13 Average annual observed and SWAT-simulated streamflow (m^3/s) calibrated using PG (2002-2008) data.

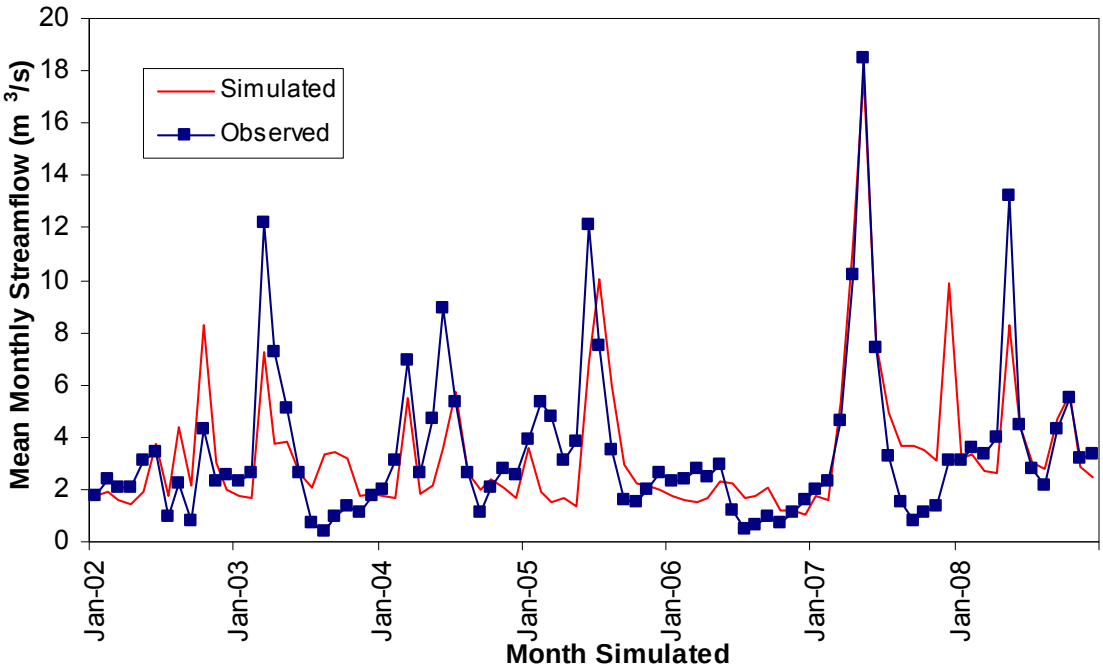

Figure 4.14 Mean monthly observed and SWAT-simulated streamflow (m^3/s) calibrated using PG (2002-2008) data.

The calibration performance statistics for daily streamflow values were low compared to monthly and annual values. The E_{NS} for daily streamflow was 0.40, which suggests a fair consistency between observed and simulated daily streamflow. Overall, SWAT model underestimated the daily streamflow values indicated by a positive PBIAS value of 1.47%. The streamflow was overestimated some runoff events especially during fall months throughout the simulation period (fig. 4.15). The median of the observed streamflow represents the base flow of the watershed which was 2.29 m^3/s and the median of the simulated streamflow was 2.22 m^3/s, this shows that base flow was estimated well by the model.

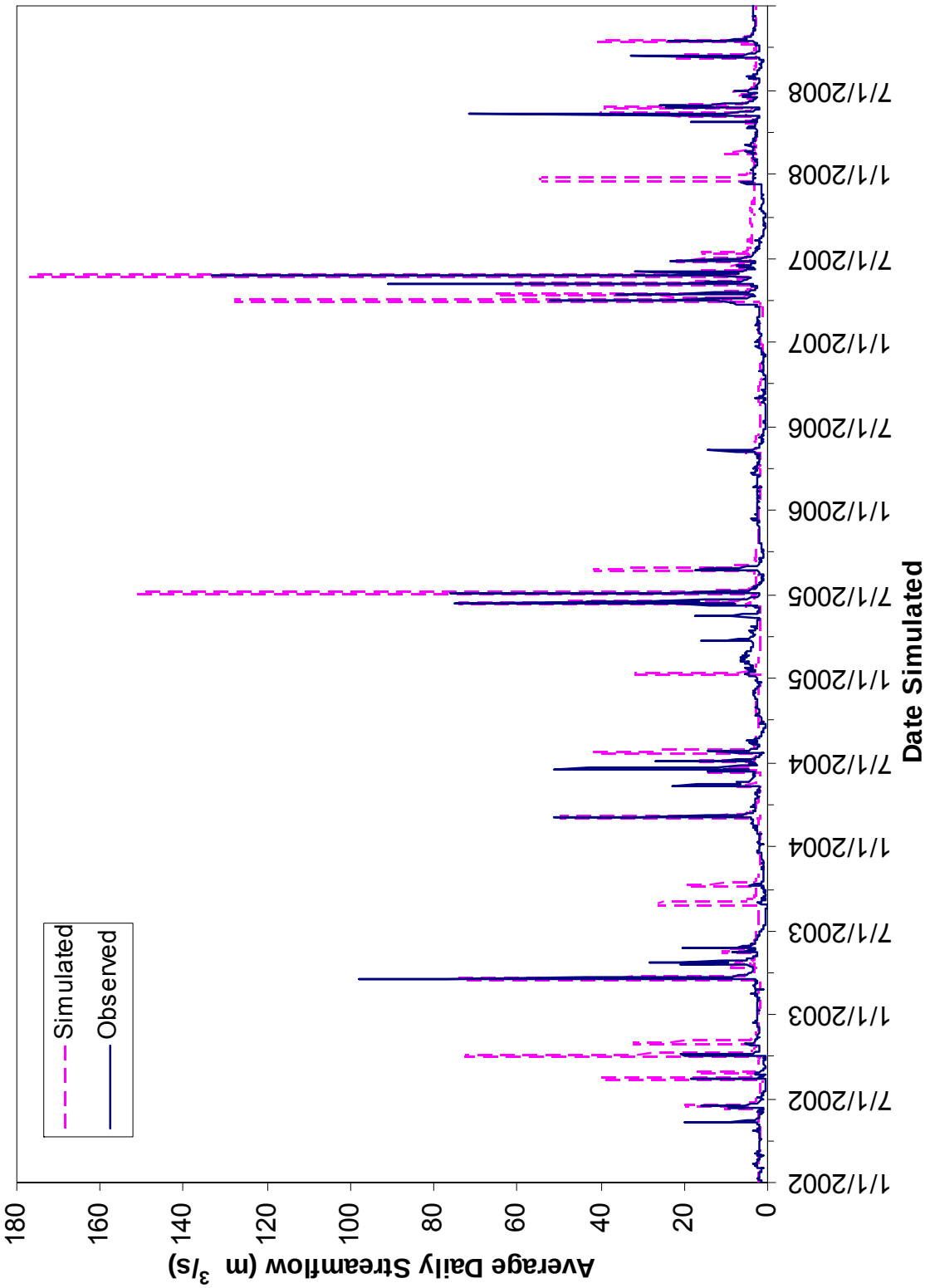

Figure 4.15 Average daily observed and SWAT-simulated streamflow (m^3/s) calibrated using PG (2002-2008) data.

4.3.1 Validation of PG (2002-08) with P3 (2002-08)

The calibrated SWAT model with precipitation gauge data was validated with P3 data to check the performance of calibrated model with P3 data. SWAT-P3 performance statistics were shown in table 4.8.

Table 4.8 Statistical performance of SWAT model validation using P3 (2002-2008) data based on PG (2002-2008) calibration parameters.

Time period	E_{NS}	RSR	PBIAS (%)
Daily	0.40	0.77	9.90
Monthly	0.52	0.68	10.10
Yearly	0.70	0.50	9.90

SWAT- P3 simulation statistics showed that model performance was good with E_{NS} of 0.70 and RSR of 0.50. A positive PBIAS value of 9.90% indicated the model underestimated the annual streamflow. Annual streamflow was simulated well throughout the simulation period with underestimations in most of the period (fig. 4.16). Overall, the SWAT simulated the annual streamflow well with P3 data than PG data.

SWAT model performance statistics at monthly time step with P3 data was satisfactory with E_{NS} of 0.52 and RSR of 0.68. The PBIAS value of 10.10% indicated the model underestimated the monthly streamflow. SWAT model followed the seasonal pattern of overestimating the streamflow during June-November and underestimated the streamflow during December-April, except in December-2007 which was overestimated (fig. 4.17).

The statistics at daily time step showed that model performance was satisfactory with E_{NS} of 0.40 and RSR of 0.77. A positive PBIAS value of 9.90% indicated the model underestimated the daily streamflow compared to observed streamflow. SWAT model yielded equal daily E_{NS} with both P3 and PG data. The plot of observed and SWAT-P3 simulated streamflow was shown in figure 4.18. The median of the observed streamflow represents the base flow of the watershed which was 2.29 m^3/s and the median of the simulated streamflow was 2.22 m^3/s, this shows that base flow was estimated very well by the model with P3 data.

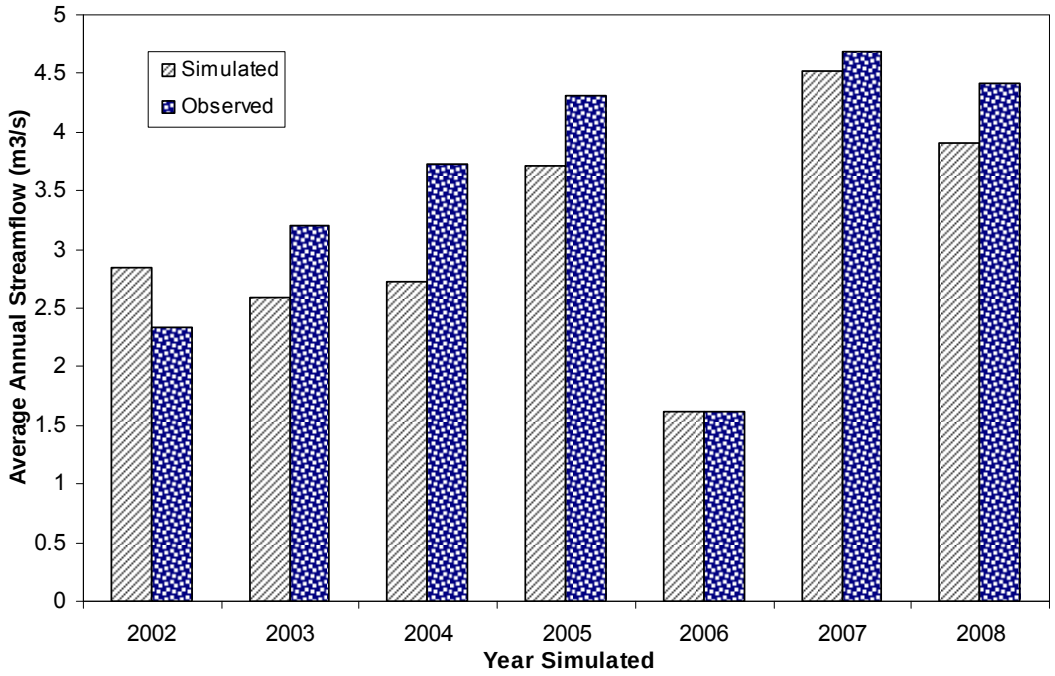

Figure 4.16 Annual average observed and SWAT-simulated streamflow (m^3/s) for validation using P3 (2002-2008) data based on PG (2002-2008) calibration parameters.

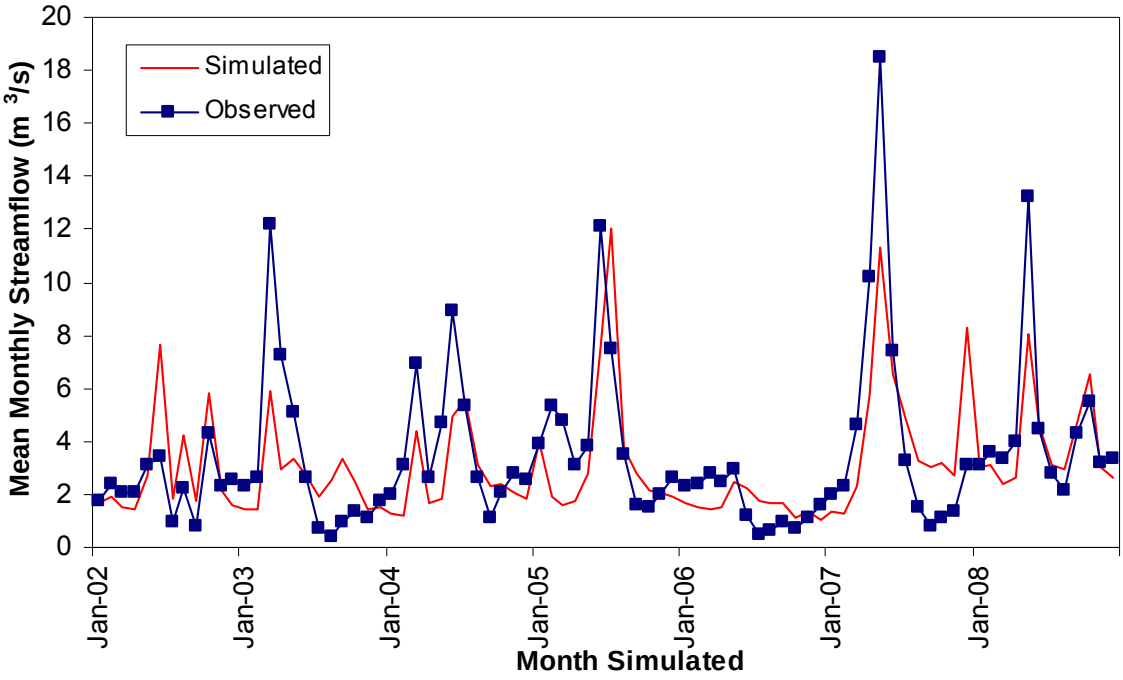

Figure 4.17 Mean monthly observed and SWAT-simulated streamflow (m^3/s) for validation using P3 (2002-2008) data based on PG (2002-2008) calibration parameters.

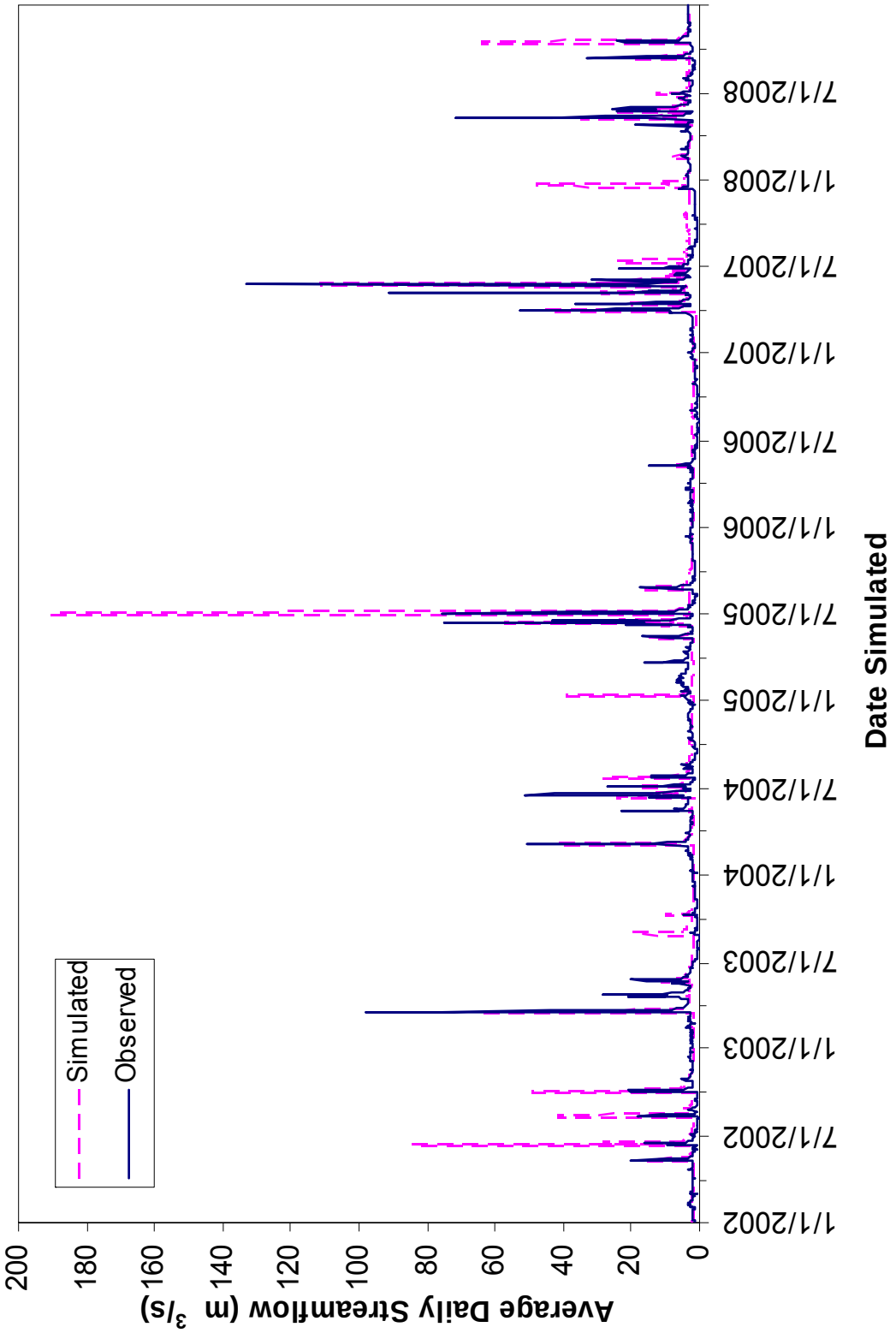

Figure 4.18 Average daily observed and SWAT-simulated streamflow (m^3/s) for validation using P3 (2002-2008) data based on PG (2002-2008) calibration parameters.

4.3.2 Validation of PG (2002-08) with PG (1996-2001)

The SWAT model was again validated with ground-based precipitation gauge data to check performance of calibrated model with PG data and to analyze the P3 data. SWAT-PG performance statistics were shown in table 4.9.

Table 4.9 Statistical performance of SWAT model validation using PG (1996-2001) data based on PG (2002-2008) calibration parameters.

Time period	E_{NS}	RSR	PBIAS (%)
Daily	0.36	0.79	2.84
Monthly	0.30	0.83	3.05
Yearly	-0.73	1.20	2.85

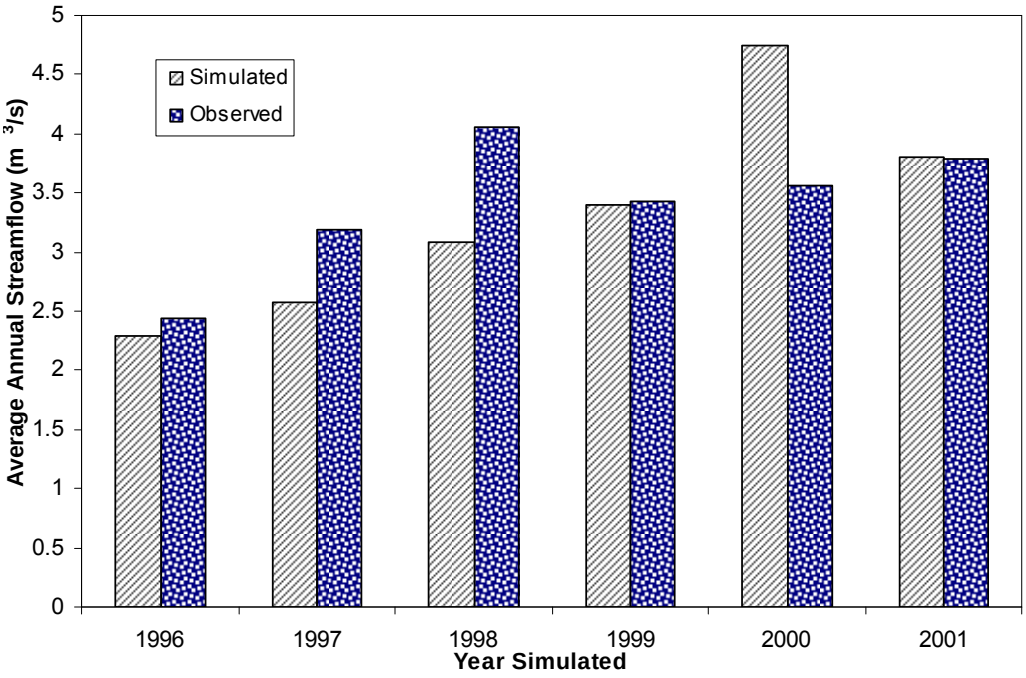

Figure 4.19 Average annual observed and SWAT-simulated streamflow (m^3/s) for validation using PG (1996-2001) data based on PG (2002-2008) calibration parameters.

SWAT-PG simulation statistics at yearly time step showed that model performance was unsatisfactory with E_{NS} of -0.73 and RSR of 1.20. A positive PBIAS value indicated the model underestimated the annual streamflow. Annual streamflow in year 1998 was underestimated and streamflow in 2000 was overestimated (fig. 4.19). The overestimation of streamflow in 2000 was compensated by the underestimation of streamflow in remaining years. SWAT model

performance statistics at monthly time step with precipitation gauge data were E_{NS} of 0.30, RSR of 0.83 and PBIAS of 3.05%. A positive PBIAS value indicated the model underestimated the monthly streamflow with precipitation gauge data. The underestimation of streamflow was extreme during December-1997 to April-1998 (fig. 4.20) with precipitation gauge data and similar underestimation of streamflow was observed with P3 data during the same period.

The modeling efficiency at daily time step (E_{NS} = 0.36) was better compared to monthly and annual efficiencies. Streamflow simulation with precipitation gauge data has completely missed estimating a series of rainfall events in March-1998 (fig. 4.21). The daily streamflow was estimated well with precipitation gauge data than P3 data. The median of the observed streamflow represents the base flow of the watershed was 2.40 m^3/s and the median of the simulated streamflow was 2.67 m^3/s, indicating the model has slightly overestimated the base flow.

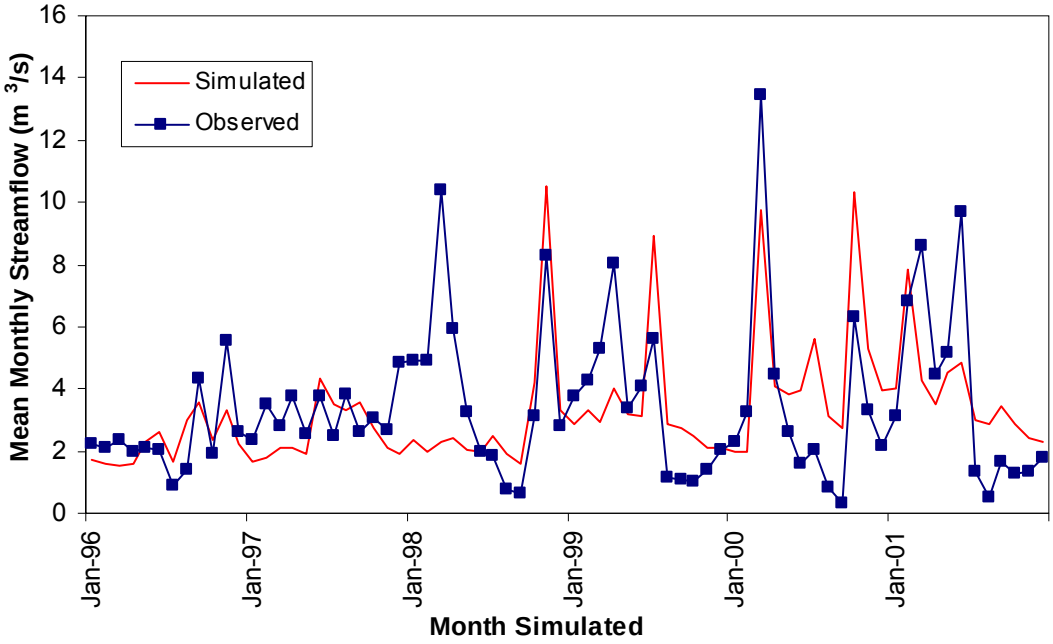

Figure 4.20 Mean monthly observed and SWAT-simulated streamflow (m^3/s) for validation using PG (1996-2001) data based on PG (2002-2008) calibration parameters.

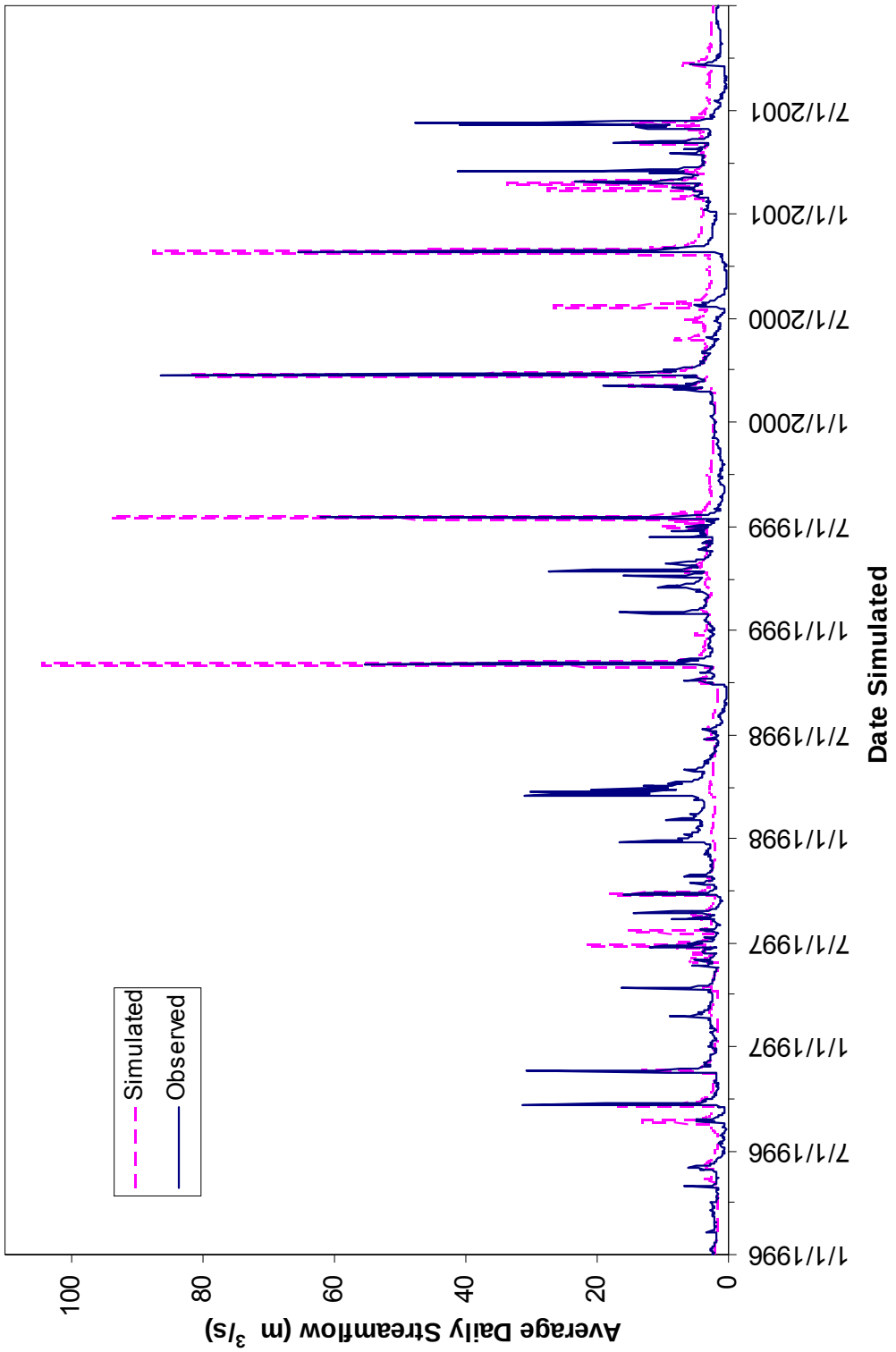

Figure 4.21 Average daily observed and SWAT-simulated streamflow (m^3/s) for validation using PG (1996-2001) data based on PG (2002-2008) calibration parameters.

4.4 Discussion

This study compared the precipitation estimates between P3 and PG stations, it was observed that P3 data has more agreement with PG data during 2002-2008 than for P3 and PG data in 1996-2001. With the addition of new NCDC precipitation gauge stations from 2002 to process the P3 rainfall product has reduced the biases that were present in the P3 data before 2002. Of all the precipitation gauge stations, Arlington station and its corresponding subwatersheds P3 data had low E_{NS}, but the E_{NS} has increased when the Arlington-subwatersheds P3 data was compared to Hutchinson10SW station. There can be several reasons for low E_{NS} between Arlington and subwatersheds P3 data, NWS might not have used the Arlington station to calculate the bias correction factor, which will be applied to P3 data. SWAT streamflow response was calibrated with P3 and PG data separately and their statistics were listed in table 4.10.

Table 4.10 Comparison of statistics between calibrated and validated models

Time period	Calibration		Validation	
	P3[1]		PG[2]	
	E_{NS}	PBIAS(%)	E_{NS}	PBIAS(%)
Daily	0.35	0.94	0.27	-7.95
Monthly	0.52	1.19	0.52	-7.65
Yearly	0.80	0.93	-0.01	-7.97
	PG[3]		P3[4]	
	E_{NS}	PBIAS(%)	E_{NS}	PBIAS(%)
Daily	0.40	1.47	0.40	9.90
Monthly	0.60	1.72	0.52	10.10
Yearly	0.43	1.45	0.70	9.90

1 = SWAT model calibrated with P3 data

2 = SWAT model validated with PG data (P3 calibration)

3 = SWAT model calibrated with PG data

4 = SWAT model validated with P3 data (PG calibration)

The statistics showed that the daily and monthly E_{NS} of the SWAT-PG calibrated model were slightly better than the SWAT-P3 calibrated model, but the yearly E_{NS} for the SWAT-P3 simulation (0.80) was much better than the SWAT-PG simulation (0.43). At the same time the

PBIAS values at all time scales for SWAT-PG simulation were higher than SWAT-P3 simulation. The SWAT-PG calibrated model was validated with P3 data and the statistics for SWAT-P3 validated model had slightly higher daily E_{NS} than the SWAT-P3 calibrated model, but the yearly E_{NS} and PBIAS values was comparatively high for the SWAT-P3 calibrated model.

SWAT model calibration with PG data has improved the overall E_{NS} and PBIAS compared to SWAT-PG validation (P3 calibrated model). The calibrated SWAT model with PG data produced better E_{NS} with P3 data. SWAT was calibrated with P3 and PG data and their performances were evaluated throughout the simulation period for each year. The simulated average annual streamflow with both calibrated models and observed flow were shown in figure 4.22 and their daily E_{NS} and PBIAS for each year during 2002-2008 period were listed in table 4.11. Precipitation gauge data shown in the graph was from Hutchinson10SW station and the P3 precipitation data was from weighted average subwatershed data nearby the gauging station. Hutchinson 10SW precipitation gauge station was mostly overpredicting the precipitation from year 2005 to 2008 compared to P3 data and P3 has overpredicted the precipitation in 2002. The daily E_{NS} for both calibrated models was mostly close to each other except in 2002 and 2005. In 2005, Hutchinson 10SW station was overpredicting the precipitation than P3, but the SWAT has underestimated the streamflow with PG data compared to SWAT-P3 estimated flow. The overestimations of streamflow in 2002 and 2007 were compensated by the streamflow underestimations in the remaining years which resulted in excellent overall PBIAS values for both simulations. The SWAT-P3 calibrated model performed well in both dry (2006) and wet (2007) years compared to SWAT-PG calibrated model. SWAT streamflow response was overestimated with PG data in 2007 compared to P3 data.

Table 4.11 Daily E_{NS} and PBIAS values for both the calibrated model runs

		2002	2003	2004	2005	2006	2007	2008	Overall
P3	E_{NS}	-4.16	0.65	0.45	-0.22	0.03	0.58	0.45	0.35
	PBIAS (%)	-25.62	11.81	20.00	4.80	3.33	-14.13	2.29	0.94
PG	E_{NS}	-2.35	0.70	0.37	0.34	0.02	0.33	0.59	0.40
	PBIAS (%)	-21.67	4.69	25.90	17.99	-3.21	-32.83	12.80	1.47

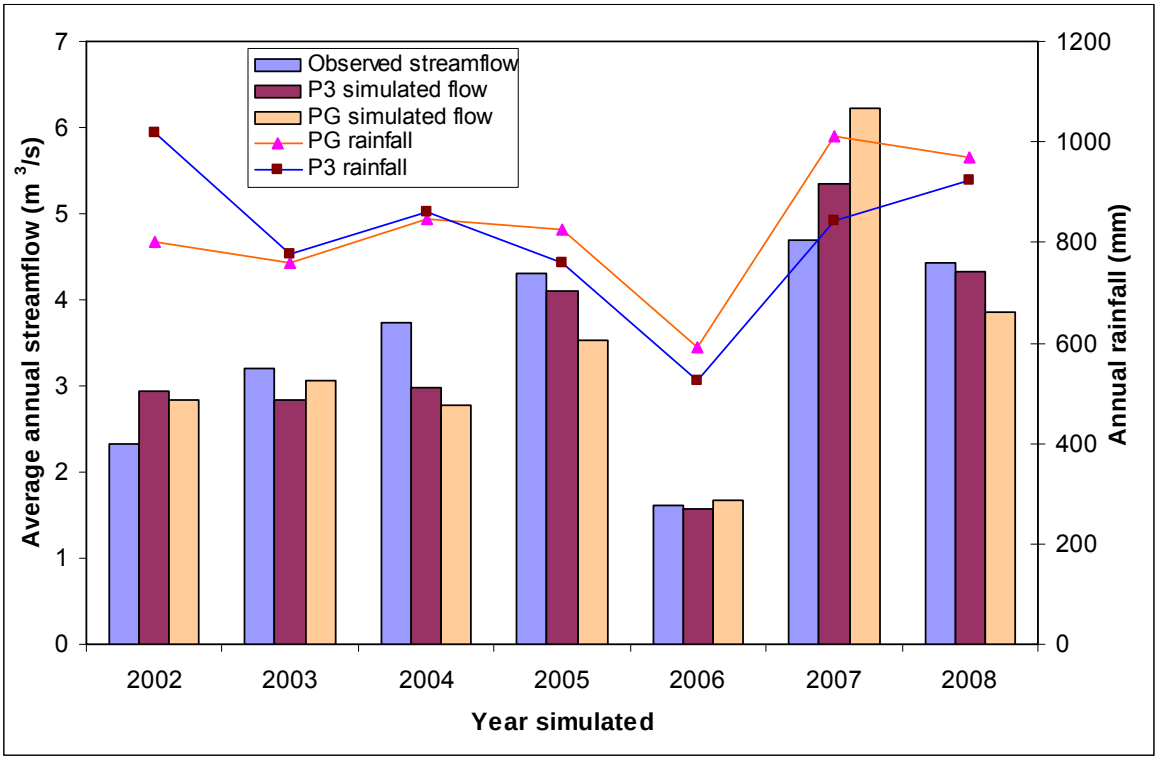

Figure 4.22 Average annual streamflow comparison between observed flow and simulated flow with P3 and PG data

Calibrating the model with two different precipitation data sets will yield different model parameters. The flow parameters were adjusted to make up with limitations in the precipitation data. SWAT model was calibrated with P3 and PG data for a period from 2002-2008 and the calibrated parameters were shown in table 4.12. Most of the flow parameters were same for both of the calibrated models, except ESCO, EPCO and GW_DELAY.

Table 4.12 Comparison of calibrated parameters with P3 and PG data

Parameter	P3 Calibration	PG Calibration
ESCO	0.25	0.1
EPCO	0.80	0.95
GW_DELAY	235	380

The SWAT-P3 calibration had high evaporation coefficients and low GW_DELAY compared to SWAT-PG calibration. The evaporation from soil will be maximum when ESCO reaches 0.0; the transpiration from plants will be high if EPCO reaches 1.0 and the GW_DELAY parameter is the time taken for the water from soil profile to exit into the shallow aquifer, if

GW_DELAY is high, the model releases water slowly into the aquifer which helps in releasing base flow during longer dry periods. Comparison between P3 and PG rainfall data showed that P3 has underestimated the precipitation data in most of the subwatersheds compared to PG data in 2002-2008 period. With the overestimation of precipitation data by PG stations, the PG-calibrated SWAT model generated high evaporative coefficients in order to match the observed streamflow. Even though the SWAT-PG calibrated model had high evaporation coefficients, some runoff events during the simulation period were overestimated. The ESCO value of 0.1 in SWAT-PG calibration shows that the model was evaporating the moisture from top soil layers and GW_DELAY was increased to obtain streamflow during dry periods (winter months) at the outlet of the watershed. The most sensitive parameters in calibrating the SWAT model were ESCO, CN, SOL_AWC, EPCO, CH_K2, and GW_DELAY in North Fork Ninnescah Watershed.

SWAT streamflow response from a subwatershed varies with its location and precipitation product in the watershed. The North Fork Ninnescah Watershed was divided into four parts: Western part, Red Rock Creek, Goose Creek, and Central part, as shown in figure 4.23. The annual streamflow from these subwatersheds were extracted for SWAT-P3 calibrated simulation and SWAT-PG calibrated simulation. The average annual streamflow for both the calibrated simulations in selected subwatersheds were show in table 4.13.

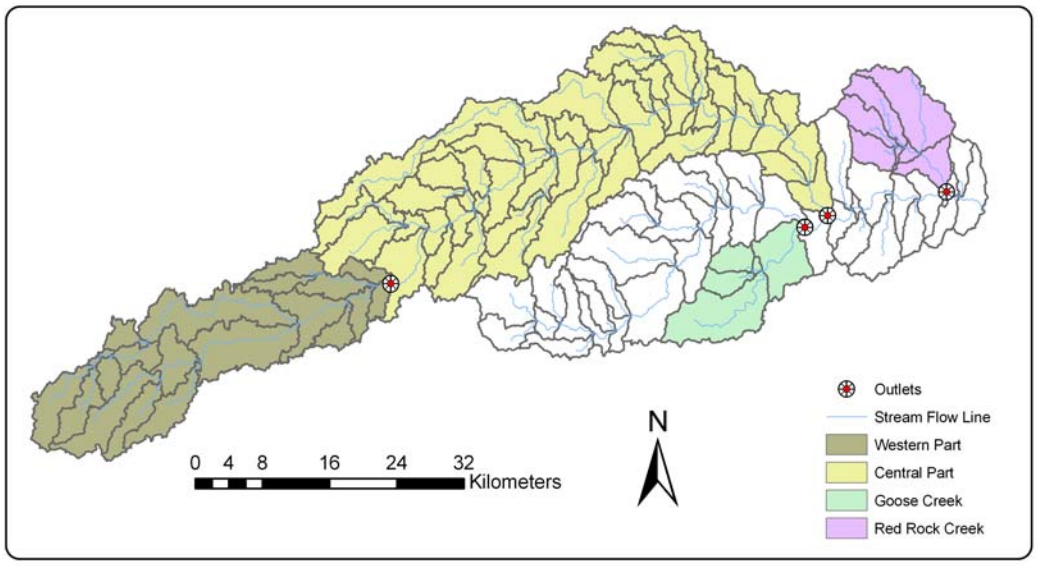

Figure 4.23 Map of North Fork Ninnescah Watershed showing the four regions inside the watershed

Table 4.13 Simulated average annual streamflow per unit area (m^3/day/km^2) within the North Fork Ninnescah Watershed

Region	Red Rock Creek (39)		Goose Creek (87)		Central Part (63)		Western Part (94)	
Area (km^2)	136.04		133.84		941.40		466.21	
	P3	PG	P3	PG	P3	PG	P3	PG
2002	235.8	79.54	69.0	45.9	101.1	125.9	37.7	74.7
2003	149.9	68.23	47.3	32.7	112.3	147.1	32.7	64.6
2004	91.5	70.05	44.3	30.7	120.5	124.3	49.5	60.9
2005	149.6	175.11	103.1	59.7	150.3	141.5	62.3	41.9
2006	30.4	42.32	31.2	21.5	58.2	75.2	47.0	31.9
2007	170.9	305.40	67.5	136.4	183.6	241.7	342.8	198.5
2008	158.6	199.06	56.0	62.4	156.1	140.6	196.8	135.9
Median	149.9	79.5	56.0	45.9	120.5	140.6	49.5	64.6

(_) = Subwatershed ID for aggregating streamflow

The Central Part and Red Rock Creek were having relatively high streamflow from their respective outlets throughout the simulation period when compared to other regions in the watershed. The Goose Creek and Western part had fairly low flows from their respective subwatersheds. The low streamflow response from the western part of the watershed might be due to the presence of A group soils which are dominant in this region and relatively low slopes. The majority of C and D group soils were present in the central part of the watershed (fig. 3.4), and all the streamflow from the western part of the watershed flows into central part which had high streamflow response compared to other regions. The Goose Creek has land slopes of above 3 % and soil groups C and D were mostly concentrated at the outlet, which was a good condition to produce high runoff, but the low streamflow response from this watershed might be due to the presence of terraced lands in this part of the watershed. The simulated streamflow with P3 data was overestimated in Western Part during the initial years of the simulation period, simulated streamflow with P3 data was underestimated in Red Rock Creek for the same simulation period. The streamflow was overestimated with PG data in Red Rock Creek from 2005-2008 simulation period, whereas streamflow was underestimated with PG data for the same period in Western part. Mixed results were observed with the simulated streamflow using different sources of

precipitation data and in different parts of the watershed. The accuracy of the spatially distributed NEXRAD P3 data can be explained better if the streamflow simulations were made at the above specified locations of the subwatersheds, further analysis was not made due to the lack of availability of streamflow measurements inside the watershed.

The E_{NS} between the SWAT-P3 simulated streamflow and SWAT-PG simulated streamflow was calculated for each year in different parts of the watershed to test the agreement within the simulated streamflow. The statistics were listed in table 4.14. The Central part of the watershed was found to be the best agreement and lower PBIAS values between the simulated streamflow with two precipitation products. The wet year 2007 had better E_{NS} between the simulated streamflow in all parts of the watershed. The P3 data mostly overestimated the streamflow in Goose Creek compared to precipitation gauge data. The P3 data overestimated the streamflow in Red Rock Creek in 2002 and 2003 compared to precipitation gauge data, which resulted in unsatisfactory PBIAS values. SWAT streamflow response during 2002 and 2006 had poor E_{NS} throughout the watershed. Parts of the watershed that had low streamflow response had poor agreement between simulated streamflow compared to the Central part, which had high streamflow response.

Table 4.14 Daily E_{NS} and PBIAS values between P3 simulated flow and PG simulated flow

		2002	2003	2004	2005	2006	2007	2008
Red Rock Creek	E_{NS}	-4.41	-0.97	0.33	0.46	0.06	0.52	0.74
	PBIAS (%)	-196.45	-119.62	-30.60	14.56	28.12	44.03	20.32
Goose Creek	E_{NS}	-1.32	0.54	-0.28	0.52	-1.25	0.55	0.03
	PBIAS (%)	-50.4	-44.71	-44.51	-72.77	-44.98	50.55	10.22
Central Part	E_{NS}	0.44	0.60	0.72	0.56	0.51	0.78	0.46
	PBIAS (%)	26.48	28.27	6.07	-11.68	10.51	-3.94	-21.98
Western Part	E_{NS}	0.11	0.11	0.55	-0.92	-0.23	0.56	0.50
	PBIAS (%)	49.62	49.35	18.65	-48.70	-47.38	-72.70	-44.78

Both the calibrated SWAT models (P3 and PG) were validated with P3 data and PG data from 1996-2001 period. The statistical performance was listed in the table 4.15. The performance of P3 data during 1996-2001 with both the calibrated models were approximately the same, except the PBIAS values with precipitation gauge calibrated model were high. In the calibration process, the model parameters were adjusted accordingly to the limitations with the precipitation product and match the observed streamflow with simulated streamflow. Lower PBIAS values were observed when the model was validated with same precipitation product. Overall, precipitation gauge data simulated streamflow well compared to P3 data during 1996-2001 period with both model validations.

Table 4.15 Comparison of statistics between validated models

Time period	P3[1]		P3[2]		PG[3]		PG[4]	
	E_{NS}	PBIAS (%)	E_{NS}	PBIAS (%)	E_{NS}	PBIAS (%)	E_{NS}	PBIAS (%)
Daily	-0.03	1.78	0.14	11.15	0.31	-8.33	0.36	2.84
Monthly	0.19	2.05	0.20	11.39	0.24	-8.11	0.30	3.05
Yearly	-0.80	1.80	-1.26	11.17	-1.45	-8.31	-0.73	2.85

1 = SWAT model validated with P3 data (P3 calibration)

2 = SWAT model validated with P3 data (PG calibration)

3 = SWAT model validated with PG data (P3 calibration)

4 = SWAT model validated with PG data (PG calibration)

CHAPTER 5 - Conclusions and Recommendations

5.1 Conclusions

This study was the first of its kind to evaluate the NEXRAD P3 product with a SWAT model. Before using the NEXRAD P3 data in hydrologic modeling we tested the agreement between P3 data and the PG data. It was found that P3 data has good agreement with PG data after 2002, the addition of new precipitation gauge stations data into the P3 radar precipitation processing reduced the biases that were present before 2002. The quality of NEXRAD P3 precipitation estimates could be improved if the biases were computed with better ground-based precipitation gauge densities.

The SWAT model was first calibrated with P3 data and PG data from 2002-2008 period to the measured USGS streamflow in North Fork Ninnescah Watershed and then the P3-calibrated model was validated with PG data for the same simulation period and vice versa. The PG-calibrated model produced slightly better daily and monthly E_{NS} values compared to P3-calibrated model, but the overall E_{NS} and PBIAS values were higher for P3-calibrated model. Even though the SWAT model was calibrated at daily time step, E_{NS} and PBIAS values at monthly and yearly time steps were also assessed to observe the overall modeling efficiency. In both the calibrated model simulations, the overestimations of streamflow in 2002 and 2007 were compensated by the streamflow underestimations in remaining years which resulted in excellent overall PBIAS values for both simulations. Both the calibrated models were also validated with P3 and PG data from 1996-2001 period and the model validation from 1996-2001 has produced greater E_{NS} with PG data compared to P3 data. We have observed that PBIAS values were better when the calibrated model was validated with same precipitation product.

The spatial and temporal characteristics of SWAT streamflow response in North Fork Ninnescah Watershed were examined for the calibrated models (P3 and PG). The SWAT streamflow response from the subwatershed varied with its location and year of simulation in the watershed. The Central Part and Red Rock Creek were having high streamflow response than the other regions of the watershed. The agreement between the simulated flows with P3 and PG data was high in wet years compared to dry years. The spatial variation of streamflow response in the watershed was greater compared to the temporal variation in both the calibrated models. The quality of the NEXRAD P3 product can be better estimated if the SWAT simulations were

performed within the watershed, further analysis was not made due to the lack of availability of flow measurements inside the watershed.

The results of this study showed that the spatial representation of precipitation data by NEXRAD P3 data has improved the modeling performance, similar to initial hypothesis that use of improved spatial precipitation resolution from NEXRAD data should improve hydrologic modeling relative to the use of point precipitation gauge data. The spatial variation of streamflow response within the watershed was greater compared to the temporal variation in the watershed. Streamflow simulations were overestimated by precipitation gauge data in wet years which were well estimated by NEXRAD P3 data, this concludes that precipitation data collected at a point may not be the same over an area. Hydrologic models use precipitation data from a precipitation gauge station and the method of converting the spatially distributed NEXRAD data into a precipitation gauge station was crucial to model output. Streamflow simulations have to be performed in large watersheds that could have spatial variation in precipitation and distinct climates, in order to estimate the quality of NEXRAD data. The performance of spatially distributed NEXRAD data could be better estimated when the area of subwatershed was less than area of NEXRAD grid cell, so that each subwatershed have their own unique precipitation data and the model could use the spatial variability of precipitation data provided by NEXRAD. The agreement between precipitation gauge data and the NEXRAD data has to be estimated, before using the NEXRAD data in models.

5.2 Recommendations

- The bias adjustment procedures used in estimating NEXRAD data were different for P3 and MPE or Stage III. The P3 data uses unique bias for each HRAP grid cell whereas MPE or Stage III data uses a single bias for a radar site. The influence of P3 bias processing methods on the quality of NEXRAD data can be estimated by evaluating the MPE and P3 data for the same period.
- The quality of NEXRAD P3 data can be better understood if the data were tested with other watersheds in ABRFC basin. This could help us in understanding how the magnitude and distribution of precipitation varies in ABRFC basin. The NEXRAD P3 data were available for long-term period of record and the performance of P3 data could be tested throughout the ABRFC basin.

- The spatial distribution of precipitation data can also be obtained from satellites and the satellite data could be used to evaluate the performances of NEXRAD P3, MPE and Stage III data spatially.
- The bias adjustment factor depends heavily on the density of precipitation gauge stations used in estimating NEXRAD P3 data. Increasing the precipitation gauge density could improve the quality of P3 estimates, the impacts of precipitation gauge density on NEXRAD P3 data performance could be studied.
- Models use precipitation data from a precipitation gauge station, and in this study NEXRAD spatial data was area-weighted average to the HRAP grid cells covering the subwatershed to convert spatial data into point data. Each NEXRAD grid cell could also be used as a precipitation gauge station and allow the model to pick the nearest grid cell to the subwatershed. The impacts of different methods of NEXRAD precipitation input to the model could be studied to evaluate the uncertainty associated with averaging of grid cells.
- In this study precipitation data for a subwatershed was derived from the area-weighted average of the NEXRAD grid cells covering the subwatershed, and depending on the size of the subwatershed the number of HRAP grid cells used in estimating precipitation data will vary. As the number of grid cell used to averaging increases, the spatial variability of precipitation and uncertainty in streamflow simulations might increase. Different subwatershed scales could be tested to evaluate the effect of decreasing spatial variation in precipitation over a subwatershed and to find the optimum subwatershed scale for streamflow simulations.

CHAPTER 6 - References

Arnold, J. G., P. M. Allen, R. Muttiah, and G. Bernhardt. 1995. Automated baseflow separation and recession analysis techniques. *Ground Water* 33(6): 1010-1018.

Arnold, J. G., R. Srinivasan, R. S. Muttiah, and J. R. Williams. 1998. Large area hydrologic modeling and assessment Part I: Model development. *J. American Water Resources Assoc.* 34(1): 73-89.

Arnold, J. G., R. S. Muttiah, R. Srinivasan, and P. M. Allen. 2000. Regional estimation of base flow and groundwater recharge in the Upper Mississippi River Basin. *J. Hydrology* 227: 21-40.

Barnes, P. L. 2009. Personal communication (Email: lbarnes@ksu.edu or Phone: 785-532-2921). Manhattan, Kans.: Kansas State University.

Beasley, D. B., L. F. Huggins, and E. J. Monke. 1980. ANSWERS: A model for watershed planning. *Trans. ASAE* 23(4): 938-944.

Bhuyan, S. 2001. An integrated modeling process to assess water quality for watersheds. PhD diss. Manhattan, Kans.: Kansas State University, Department of Biological and Agricultural Engineering.

Bicknell, B. R., J. C. Imhoff, J. L. Kittle, A. S. Donigian, and R. C. Johanson. 1993. Hydrologic Simulation Program-FORTRAN (HSPF). User's Manual for Release 10. Athens, Geor.: U.S. EPA-600/R-93/174.

Bingner, R. L. 1996. Runoff simulated from Goodwin Creek Watershed using SWAT. *Trans. ASAE* 39(1): 85-90.

Bingner, R. L., J. Garbrecht, J. G. Arnold, and R. Srinivasan. 1997. Effect of watershed subdivision on simulation runoff and fine sediment yield. *Trans. ASAE* 40(5): 1329-1335.

Bosch, D. D., R. Bingner, F. G. Theurer, G. Felton, and I. Chaubey. 1998. Evaluation of AnnAGNPS water quality model. ASAE Paper No. 98-2195. St. Joseph, Mich.: ASAE.

Chaubey, I., C. T. Haan, J. M. Salisbury, and S. Grunwald. 1999. Quantifying model output uncertainty due to spatial variability of rainfall. *J. American Water Resources Assoc.* 35(5): 1113-1123.

Cheney Lake Watershed, Inc. 2008. Information about Cheney Lake Watershed available at http://www.cheneylakewatershed.org/. Accessed on July 2008.

Coffey, M. E., S. R. Workman, J. L. Taraba, and A.W. Fogle. 2004. Statistical procedures for evaluating daily and monthly hydrologic model predictions. *Trans. ASAE* 47(1): 59-68.

Cotter, A. S., I. Chaubey, T. A. Costello, T. S. Sorens, and M. A. Nelson. 2003. Water quality model output uncertainty as affected by spatial resolution of input data. *J. American Water Resources Assoc.* 39(4): 977-986.

Daggupati, P., A. Y. Sheshukov, K. R. Doulgas-Mankin, P. L. Barnes, and D. L. Devlin. 2009. Field-scale targeting of cropland sediment yields using ArcSWAT. Proceedings of the 5th International SWAT Conference, Boulder, CO. Aug 5-7, 2009. College Station, Tex.: Texas A&M University.

Devlin, D., N. Nelson, L. French, H. Miller, P. L. Barnes, and L. Frees. 2008. Cheney Lake Watershed: Conservation practice implementation history and trends. Manhattan, Kans.: Kansas State University. EP-157.

Di Luzio, M., J. G. Arnold, and R. Srinivasan. 2005. Effect of GIS data quality on small watershed streamflow and sediment simulations. *Hydrol. Proc.* 19: 629-650.

Faures, J.-M., D. C. Goodrich, D. A. Woolhiser, and S. Sorooshian. 1995. Impact of small-scale spatial variability on runoff modeling. *J. Hydrol.* 173:309-326.

Fulton, R. A., J. P. Breidenbach, D. J. Seo, and D. A. Miller. 1998. WSR-88D rainfall algorithm. *Weather Forecasting* 37: 377-395.

Gilley, J. E., S. C. Finkner, and G. E. Varvel. 1986. Runoff and erosion as affected by sorghum and soybean residue. *Trans. ASAE* 29(6): 1605-1622.

Green, W. H. and G. A. Ampt. 1911. Studies on soil physics, 1. The flow of air and water through soils. *J. Agricultural Sciences* 4: 11-24.

Guo, J., X. Liang, and L. R. Leung. 2004. Impacts of different precipitation data sources on water budgets. *J. Hydrology* 298: 311-334.

Gupta, H. V., S. Sorooshian, and P. O. Yapo. 1999. Status of automatic calibration for hydrologic models: Comparison with multilevel expert calibration. *J. Hydrologic Eng.* 4(2): 135-143.

Harrison, D. L., S. J. Driscoll, and M. Kitchen. 2000. Improving precipitation estimates from weather radar using quality control and correction techniques. *Meteorological Applications* 7(2): 135-144.

Heathman, G. C., D. C. Flanagan, M. Larose, and B. W. Zuercher. 2008. Application of Soil and Water Assessment Tool and Annualized Agricultural Non-Point Source models in the St. Joseph River Watershed. *J. Soil Water Cons.* 63(6): 552-568.

Hernandez, M., S. C. Miller, D. C. Goodrich, B. F. Goff, W. G. Kepner, C. M. Edmonds, and K. B. Jones. 2000. Modeling runoff response to land cover and rainfall spatial variability in semi-arid watersheds. *Environ. Monitoring and Assessment* 64: 285-298.

Jayakrishnan, R., R. Srinivasan, and J. G. Arnold. 2004. Comparison of raingage and WSR-88D Stage III precipitation data over the Texas-Gulf basin. *J. Hydrology* 292: 135-152.

Johnson, D., M. Smith, V. Koren, and B. Finnerty. 1999. Comparing mean areal precipitation estimates from NEXRAD and rain gauge networks. *J. Hydrologic Eng.* 4(2): 117-124.

Kalin, L., and M. M. Hantush. 2006. Hydrologic modeling of Eastern Pennsylvania Watershed with NEXRAD and rain gauge data. *J. Hydrologic Eng.* 11(6): 555-569.

Knapp, M. 2009. Personal communication (Email: mknapp@k-state.edu or Phone: 785-532-7019). Manhattan, Kans.: Kansas State University.

Kottek, M., J. Grieser, C. Beck, B. Rudolf, and F. Rubel. 2006. World Map of the Koppen-Geiger climate classification updated. *Meterologische Zeitschrift* 15(3): 259-263.

Lawrence, B. 2010. Personal communication (Email: Bill.Lawrence@noaa.gov, Phone: 918-832-4110). Tulsa, Okla.: National Oceanic and Atmospheric Administration.

Leavesley, G. H., R. W. Lichty, B. M. Troutman, and L. G. Saindon. 1983. Precipitation-Runoff Modeling System-User's manual. Lakewood, Col.: U.S. Geological Survey Water Resources Division. Report: 83-4238.

Legates, D. R., and G. J. McCabe. 1999. Evaluating the use of "goodness-of-fit" measures in hydrologic and hydroclimatic model validation. *Water Resources Res.* 35(1): 233-241.

McCuen, R. H. 1998. *Hydrologic analysis and design*. Upper Saddle River, N.J.: Prentice-Hall, Inc.

Metcalf and Eddy, Inc. 1971. Storm Water Management Model Final Report-11024DOC 07/71. Washington. D.C.: U.S. Environmental Protection Agency. Water Quality Office.

Monteith, J. L. 1965. Evaporation and Environment. In the state and movement of water in living organisms, XIXth Symposium Soc. Swansea. Cambridge University Press.

Moon, J., R. Srinivasan, and J. H. Jacobs. 2004. Streamflow estimation using spatially distributed rainfall in the Trinity River Basin, TEXAS. *Trans. ASAE* 47(5): 1445-1451.

Moriasi, D. N., J. G. Arnold, M. W. Van Liew, R. L. Binger, R. D. Harmel and T. L. Veith. 2007. Model evaluation guidelines for systematic quantification of accuracy in watershed simulations. *Trans. ASABE* 50(3): 885-900.

Nash, J. E., and J. V. Sutcliffe. 1970. River flow forecasting through conceptual models. Part I: A discussion of principles. *J. Hydrology* 10(3): 282-290.

NCDC. 2008. National Climatic Data Center, National Weather Service. Available at http://www.ncdc.noaa.gov/oa/climate/stationlocator.html. Accessed June 2008.

Neitsch, S. L., J. G. Arnold, J. R. Kiniry, and J. R. Williams. 2005a. Soil and Water Assessment Tool Theoretical Documentation, Version 2005. Temple, Tex.: Grassland, Soil and Water Research Laboratory. Agricultural Research Service. Blackland Research Center. Texas Agricultural Experiment Station.

Neitsch, S. L., J. G. Arnold, J. R. Kiniry, R. Srinivasan and J. R. Williams. 2005b. Soil and Water Assessment Tool Input/Output file Documentation, Version 2005. Temple, Tex.: Grassland, Soil and Water Research Laboratory. Agricultural Research Service. Blackland Research Center. Texas Agricultural Experiment Station.

NWS. 2006. MPE Editor User's Guide, Build 7.1 (June 26, 2006). Silver Spring, M.D.: National Weather Service, Office of Hydrologic Development.

NWS. 2009. National Weather Service NEXRAD data. Available at http://dipper.nws.noaa.gov/hdsb/data/nexrad/nexrad.html. Accessed January 2009.

NWS-ABRFC. 2010. National Weather Service Arkansas Red Basin River Forecast Center. http://www.srh.noaa.gov/abrfc/?n=pcpn_methods. Accessed 10 April 2010.

Parajuli, P. B., N. O. Nelson, L. D. Frees, and K. R. Mankin. 2009. Comparison of AnnAGNPS and SWAT model simulation results in USDA-CEAP agricultural watersheds in south-central Kansas. *Hydrological Processes* 23(5): 748-763.

Saleh, A., J. G. Arnold, P. W. Gassman, L. M. Hauck, W. D. Rosenthal, J. R. Williams, and A. M. S. McFarland. 2000. Application of SWAT for the Upper North Bosque River Watershed. *Trans. ASAE* 43(5): 1077-1087.

Seo, D. J. 2003. Multi-sensor precipitation estimation. National Weather Service, River Forecast System (NWSRFS) International Workshop, Kansas City. Silver Spring, M.D.: .National Weather Service, Office of Hydrologic Development.

Sheshukov, A. Y., P. Daggupati, M. C. Lee, and K. R. Douglas-Mankin. 2009. ArcMap tool for pre-processing SSURGO soil database for ArcSWAT. Proceedings of the 5th International SWAT Conference, Boulder, CO. Aug 5-7, 2009. College Station, Tex.: Texas A&M University.

Shirmohammadi, A., K. S. Yoon, W. J. Rawls, and O. H. Smith. 1997. Evaluation of curve number procedures to predict runoff in GLEAMS. *J. American Water Resources Assoc.* 45(3): 1069-1076.

Singh, J., H. V. Knapp, J. G. Arnold, and M. Demissie. 2005. Hydrological modeling of the Iroquois River Watershed using HSPF and SWAT. *J. American Water Resources Assoc.* 41(2): 343-360.

Singh, V. P., and D. K. Frevert. 2006. Watershed Models. Boca Raton, Fl.: CRC Press, Taylor & Francis Group.

Srinivasan, R. 2005. Advanced SWAT BASINS training manual. Blackland Research Center. Temple, Tex.: Texas A&M University.

Tobin, J. K and M. E. Bennet. 2009. Using SWAT to model streamflow in two river basins with ground and satellite precipitation data. *J. American Water Resources Assoc.* 45(1): 253-271.

Tuppad, P., K. R. Douglas-Mankin, J. K. Koelliker, and J. M. S. Hutchinson. 2010. SWAT discharge response to spatial rainfall variability in a Kansas watershed. *Trans. ASABE* 53(1): 65-74.

USDA-NASS. 2007. U.S. Department of Agriculture National Agricultural Statistics Survey. Available at http://www.nass.usda.gov/research/Cropland/SARS1a.htm. Accessed October 2008.

USGS-NED. 2008. U.S. Geological Survey National Elevation Dataset. Available at http://seamless.usgs.gov/ as of 26 August 2008.

USDA-NRCS. 2005. U.S. Department of Agriculture Soil Survey Geographic database. Available at http://soildatamart.nrcs.usda.gov. Accessed November 2008.

USDA-SCS. 1972. National Engineering Handbook, Hydrology Chapter 4. Washington, D.C.: U.S. Department of Agriculture, Soil Conservation Service.

USDA-SCS. 1986. Urban Hydrology for Small Watersheds. Technical Release 55. Washington, D.C.: U.S. Department of Agriculture, Soil Conservation Service.

Van Rompaey, A. J. J., and G. Govers. 2002. Data quality and model complexity for regional scale soil erosion prediction. *International J. Geographical Information Science* 16(7): 663-680.

Wang, X., X. Hongjie, S. Hatim, and Z. Jon. 2008. Validating NEXRAD MPE and Stage III precipitation products for uniform rainfall on the Upper Guadalupe River Basin of the Texas Hill Country. *J. Hydrology* 348: 73-86.

Wilcox, B. P., W. J. Rawls, D. L. Brakensiek, and J. R. Wight. 1990. Predicting runoff from rangeland catchments: A comparison of two models. *Water Resources Res.* 26: 2401-2410.

Wischmeier, W. H., and D. D. Smith. 1978. Predicting rainfall erosion losses: A guide to conservation planning, Agriculture Handbook No. 537, U.S. Department of Agriculture: Washington D.C. 58 pp.

Xie, H., Z. Xiaobing, M. H. H. Jan, R. V. Enrique, G. Huade, Q. T. Yong, and E. S. Eric. 2006. Evaluation of NEXRAD Stage III precipitation data over a semiarid region. *J. American Water Resources Assoc.* 42(1): 237-256.

Young, C. B., and N.A. Brunsell. 2008. Evaluating NEXRAD estimates for the Missouri River Basin: Analysis using daily raingauge data. *J. Hydrologic Eng.* 13(7): 549-553.

Appendix A - NEXRAD Tool

NEXRAD, an entire system of WSR-88D radars and associated processing equipment, were used to generate precipitation data with spatial & temporal distribution over large areas. Radar system collects the data by sending microwave signals (long wavelengths are not susceptible to atmospheric scatterings and can easily pass through clouds) into the atmosphere and the signals get scattered when they collide with target (clouds), and the radar receptor collects the bounced signals. A reflectivity-rainfall relationship (also known as Z-R relationship), $Z = a R^b$ is used to calculate the rainfall using the reflectivity of returned signals (Harrison, et al., 2000). The raw radar products undergo processing and bias corrections made by Hydrometeorological Analysis and Support (HAS) forecaster at the River Forecast Center (RFC) (Johnson et al., 1999).The data is stored in XMRG format, which contains rainfall data in form of grid cells and the area of this pixel is approximately equal to 16 km^2. Each pixel has its own precipitation data. The original grid data was stored in Hydrologic Rainfall Analysis Project (HRAP) or secant polar stereographic projection in compressed XMRG files. NEXRAD grid coverage over the study area projected into NAD 83 UTM-14 projection is shown in figure A.1.

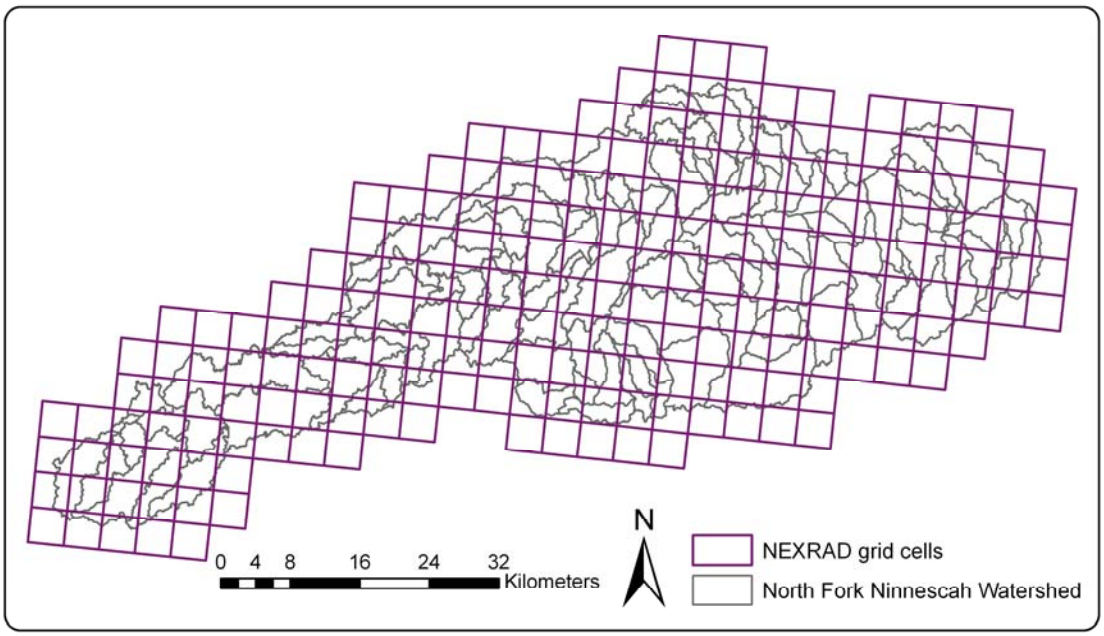

Figure A.1 NEXRAD grid cell coverage over North Fork Ninnescah Watershed

A.1 Developing precipitation gauge station for each subwatershed

SWAT uses weather data from the nearest station to the centroid of the subwatershed and assigns only one gauging station per subwatershed. Centroid of each subwatershed was calculated and a point file generated by NEXRAD tool, was used as precipitation gauge station for the corresponding subwatershed. Precipitation gauge station developed by NEXRAD tool for North Fork Ninnescah Watershed is shown in figure A.2.

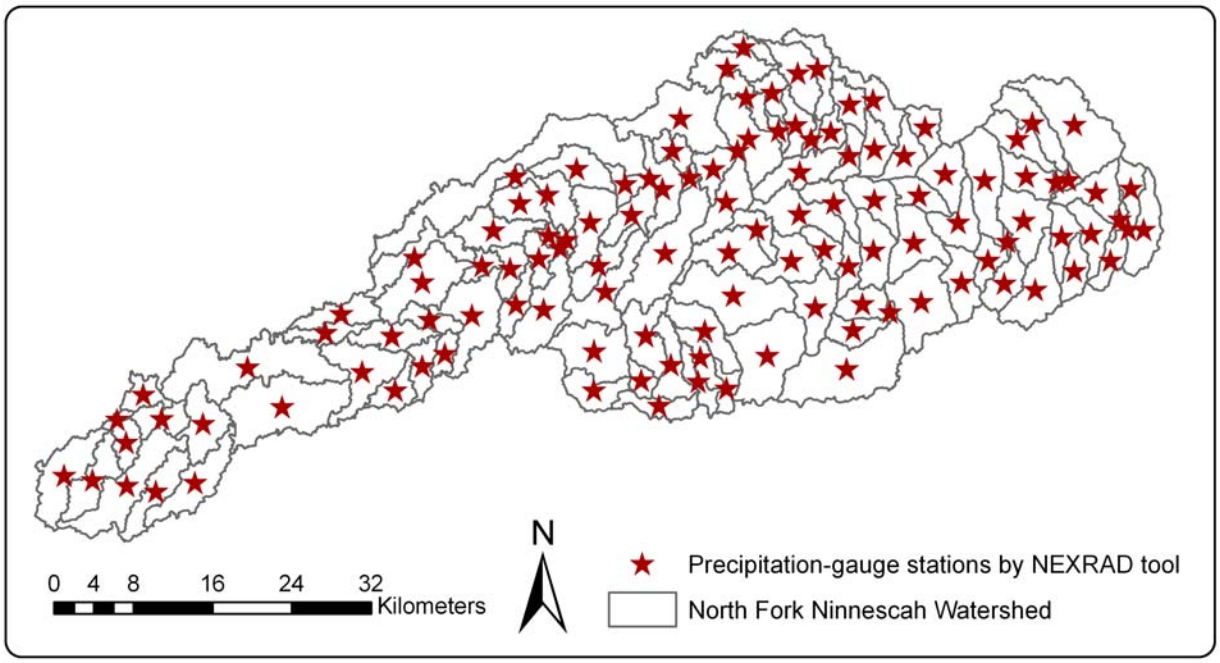

Figure A.2 Precipitation gauge stations developed by NEXRAD tool for North Fork Ninnescah Watershed

A.2 Extracting precipitation data for each precipitation gauge stations

NEXRAD grid cells covering a subwatershed were identified for each subwatershed. NEXRAD tool determines how each grid cell cuts the subwatershed into pieces and the percentage of each piece in the subwatershed. Grid cell covering a Subwatershed was shown in figure A.3. ArcObjects, VBA and Matlab programs were used in developing NEXRAD tool.

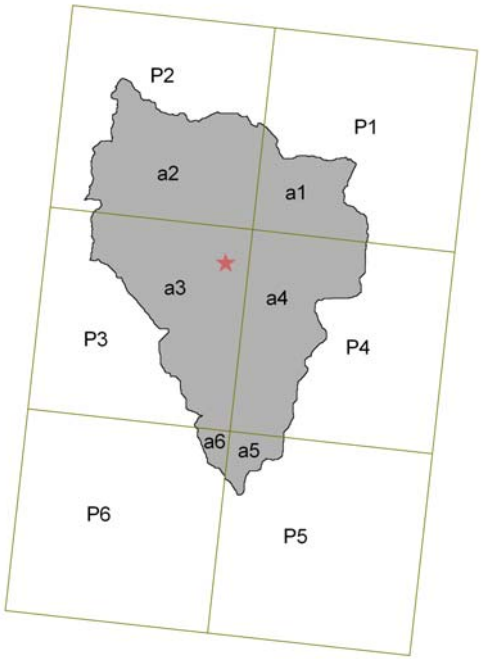

Figure A.3 NEXRAD grid cell coverage over a subwatershed

Rainfall data on a specific day for a specific subwatershed was calculated by using weighted average method. The above process is repeated to obtain NEXRAD data for each subwatershed.

$$R = \frac{a1\ P1 + a2\ P2 + a3\ P3 + a4\ P4 + a5\ P5 + a6\ P6}{a1 + a2 + a3 + a4 + a5 + a6} \quad \text{(A.1)}$$

where,

R = rainfall data for a subwatershed on a specific day, (mm)

a = area of subwatershed piece, (km^2) and

P = precipitation data of NEXRAD grid cell, (mm)

References

Harrison, D. L., S. J. Driscoll, and M. Kitchen. 2000. Improving precipitation estimates from weather radar using quality control and correction techniques. *Meteorological Applications* 7(2): 135-144.

Johnson, D., M. Smith, V. Koren, and B. Finnerty. 1999. Comparing mean areal precipitation estimates from NEXRAD and rain gauge networks. *J. Hydrologic Eng.* 4(2): 117-124.

Appendix B - Inverse Distance Weighting Method

Inverse Distance Weighted method is a deterministic interpolation method, a process of predicting the unknown data at a gauging station by using data from multiple neighboring gauges weighted by distance. Inverse Distance Weighted (IDW) method is one of the most frequently-used methods for estimating missing rainfall amounts at a gauging station (Teegavarapua and Chandramoulia. 2005; Keckler, 1995). IDW method is based on the assumption that rainfall data from rain gauge stations that are closer to one another are more similar than those that are farther apart. The closest gauging station to the gauging station being estimated will have more influence or weight on the predicted value than those that are farther away. IDW assigns weights to neighboring observed values based on distance to the interpolation location and the interpolated value is the weighted average of the observations (Ahrens, 2005). The IDW results depend on the distance between the gauging stations and the data from stations near one another in space are more likely to be similar than the data from locations remote from one another (Sullivan and Unwin, 2003). IDW method calculates the rainfall data without results exceeding the range of input data. The equation of IDW method is

$$P_c = \frac{\sum_i P_i \, d^{-k}}{\sum_i d^{-k}} \tag{B.1}$$

where,

P_c = rainfall for the gauging station to be predicted, (mm)

P_i = rainfall data from one of the neighboring gauge station, (mm)

d = distance between the predicted and measured gauging stations, (m) and

k = weight known as the friction distance that ranges from 1.0 to 6.0.

The most commonly used value for k is 2 which is used for this study (Teegavarapua and Chandramoulia. 2005). As the weighting power increases, the lesser will be the effect of farther stations data on the station data being estimated. The value of rainfall data being estimated at gauging stations will be closer to the nearest gauging station as the weighting power increases and with smaller power, weighting is more evenly distributed among the neighboring stations.

References

Ahrens, B. 2005. Distance in spatial interpolation of daily rain gauge data. *Hydrology and Earth System Sciences Discussion* 2: 1893-1923.

Teegavarapua, R., and V. Chandramoulia. 2005. Improved weighting methods, deterministic and stochastic data-driven models for estimation of missing precipitation records. *J. Hydrology* 312: 191-206.

Keckler, P. K. 1995. Surfer to Windows. Golden, Col.: Golden Software, Inc.

O'Sullivan, D., and D. J. Unwin. 2003. Geographic Information Analysis. Hoboken, N.J.: John Wiley & Sons, Inc.

Appendix C – Base Flow Alpha Factor

Base flow is considered as the groundwater contribution to streamflow and there are several automated techniques and manual methods to separate base flow from streamflow. The base flow was separated from streamflow by an automated recursive digital filter program or base flow filter program (Arnold et al., 1995). The base flow filter program uses streamflow records to estimate fraction of base flow contribution to streamflow, base flow recession constant and base flow days. The base flow recession constant or base flow alpha factor is a direct index of groundwater flow response to changes in recharge (Smedema and Rycroft, 1983). The base flow recession constant values vary with land responses to recharge, values from 0.1-0.3 for lands with slow response to recharge and values from 0.9-1.0 for lands with rapid response to recharge (Neitsch et al., 2005). The equation of the filter is

$$q_t = \beta\, q_{t-1} + (1+\beta)/2\,(Q_t - Q_{t-1}) \tag{C.1}$$

where,

q_t= filtered surface runoff at the time step t,

Q_t = the original streamflow, and

β = filter parameter,

Base flow, b_t at a time step is

$$b_t = Q_t - q_t \tag{C.2}$$

The base flow alpha factor can be calculated, if the number of base flow days was known.

$$\alpha_{gw} = 2.3/BFD \tag{C.3}$$

where,

α_{gw} = the base flow recession constant, and

BFD = the number of base flow days for the watershed.

Base flow was calculated by using traditional hydrograph separation for different parts of Cheney Lake Watershed and the separated baseflow was between 37-74% of the total annual streamflow by manual separation (Bhuyan, 2001). The baseflow contribution in Cheney Lake Watershed was between 46-65% of the daily streamflow calculated by Base flow Filter Program. Alpha factor or base flow recession constant was 0.024 and base flow days were 95.91.

References

Arnold, J. G., P. M. Allen, R. Muttiah, and G. Bernhardt. 1995. Automated base flow separation and recession analysis techniques. *Ground Water* 33(6): 1010-1018.

Bhuyan, S. 2001. An integrated modeling process to assess water quality for watersheds. PhD diss. Manhattan, Kans.: Kansas State University, Department of Biological and Agricultural Engineering.

Neitsch, S.L., J.G. Arnold, J.R. Kiniry, R. Srinivasan and J.R. Williams. 2005. Soil and Water Assessment Tool Input/Output File Documentation, Version 2005. Temple, Tex.: Grassland, Soil and Water Research Laboratory, Agricultural Research Service, Blackland Research Center, Texas Agricultural Experiment Station.

Smedema, L. K. and D. W. Rycroft. 1983. Land drainage-planning and design of agricultural drainage systems. Ithica, N.Y.: Cornell University Press.